NSIDE TRACK with Noel Heiks, Nuvotronics | 33



Broadband Amps Hold Gain And Power Steady | 97





Confidence on the Cutting Edge.

In the Lab | On the Manufacturing Floor | In the Field



World's first portfolio of VNAs that bring Non-linear Transmission Line (NLTL) technology to every measurement scenario from on-wafer device characterization to R&D testing to manufacturing and field operations.

Learn more: www.anritsu.com





Amplifiers

Attenuators - Variable

DLVA & ERDLVA & SDLVA's

DTO's & Frequency Synthesizers

Filters

Form, Fit & Function Products

IFM's & Frequency Discriminators

Integrated MIC/MMIC Modules

I/Q Vector Modulators

Limiters & Detectors

Log Amplifiers

Pulse & Bi-Phase Modulators

Phase Shifters

Rack & Chassis Mount
Products

Receiver Front Ends & Transceivers

Single Sideband Modulators

SMT & QFN Products

Solid-State Switches

Switch Matrices

Switch Filter Banks

Threshold Detectors

USB Products

Planar Monolithics Industries, Inc.

Offering State-Of-The-Art RF and Microwave Components
& Integrated Assemblies From DC to 40GHz

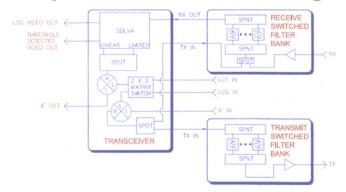
100MHz to 18GHz Transceiver 3U Open VPX Architecture

- 0.1 to 18.0 GHz Transceiver
- 3U Open VPX Architecture
- VITA 67 RF Interface
- Up to 4GHz Instantaneous Bandwidth
- Customizable Switched Filter Banks



- BIT Test Mode for Closed Loop Testing
- Linear & Limited RF, SDLVA Output Channels
- Log & Threshold Video SDLVA Output Channels
- Time Gated SDLVA's for Pulse Blanking
- CW Immunity
- Input Selection for Two Independent LO
- frequencies (4 to 20GHz)
- -80 to +10dBm Input Power Range
- IF Frequency of 100MHz to 4.0GHz
- LVDS Control Logic
- Ruggedized Construction for Military Applications
- 160mm x 100mm x 12HP per VITA 46 Standards (6.299" x 3.937" x 2.388")

Simplified Functional Block Diagram



West Coast Operation:

4921 Robert J. Mathews Pkwy, Suite 1 El Dorado Hills, CA 95762 USA Tel: 916-542-1401 Fax: 916-265-2597

Email: sales@pmi-rf.com

East Coast Operation:

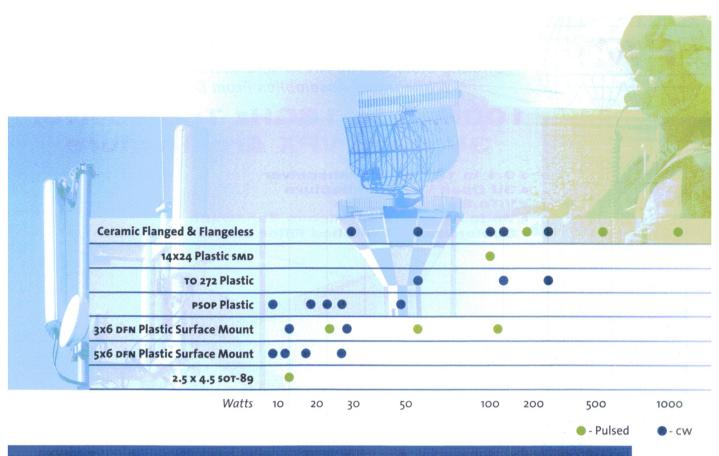
7311-F Grove Road Frederick, MD 21704 USA Tel: 301-662-5019 Fax: 301-662-1731

Website: www.pmi-rf.com

Hermetic Sealing, High Reliability to Mil-Std-883, Small Quantity Requirements accepted.

We offer Custom Designs

ISO9001:2008 REGISTERED



Shattering the Barriers to Mainstream GaN Adoption

MACOM revolutionizes RF applications by securing the supply of the industry's only proven, performance-driven GaN portfolio

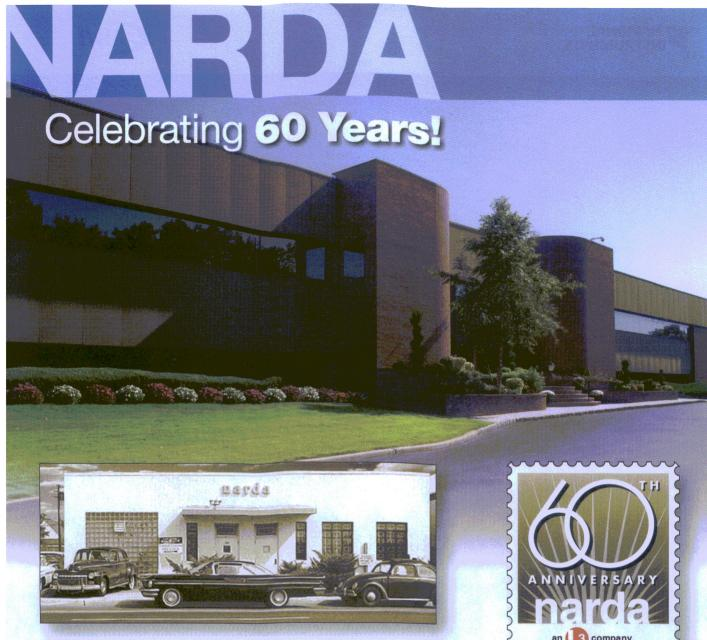
MACOM GaN transistors improve upon the high-power handling and voltage operation of LDMOS with the high-frequency performance of GaAs. Improved bandwidth, efficiency and power density give your applications greater power in a variety of packages.

Leveraging deep experience in RF, MACOM engineers are expanding our power transistor family to fuel the future of military and commercial radar as well as other commercial applications. These rugged devices deliver greater flexibility and multi-function capability in your radar communications.

Our growing pulsed power GaN portfolio includes 5w-9ow Pk transistors in DFN and SOT-89 plastic packaging, up to 1000w ceramic packages and L-, S-band fully matched modules. Our new cw GaN portfolio includes ceramic package transistors up to 200w, DFN packages from 5w to 25w and TO-272 plastic packages from 5ow to 200w.

Only MACOM shatters the final barriers to mainstream GaN adoption by offering dual sourcing for surety of supply.





Narda started in 1954 as a small group of engineers on Long Island offering new and innovative technology to a growing RF and microwave industry. Sixty years later, Narda has become the global standard for quality and durability by continually producing the industry's most reliable RF and microwave components. We thank you for sixty years of loyalty to Narda Microwave, and look forward to serving you in the years to come.



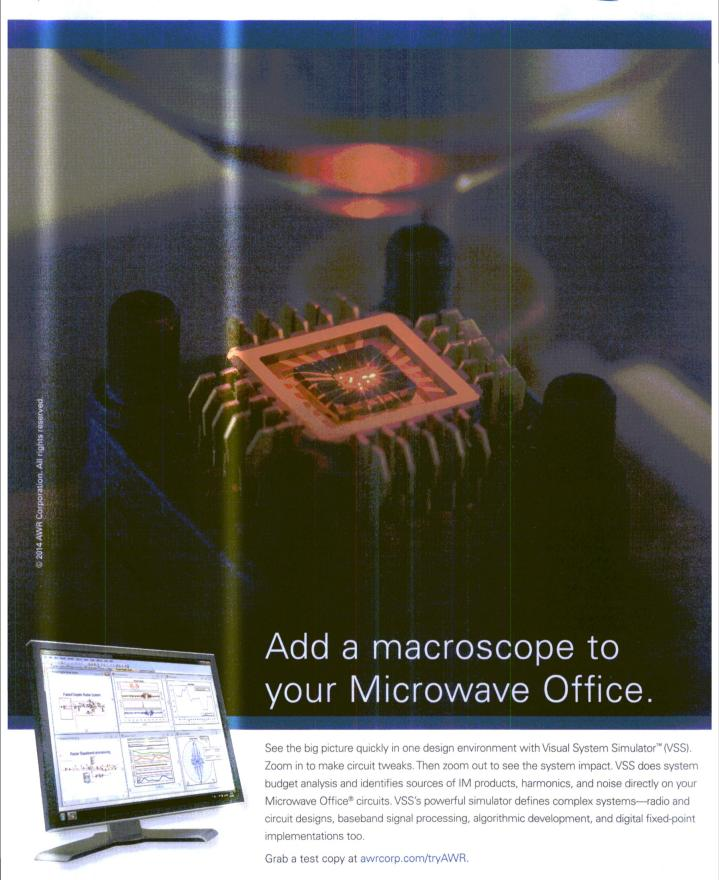


www.nardamicrowave.com • 631.231.1700

Six decades of technological

nnovation





VOLUME 53, ISSUE 6

This Issue

FEATURES

97 **COVER STORY:**

Amplifiers Gain Broadband Power

These solid-state amplifiers offer distortion-free performance in coaxial and drop-in packages for design flexibility in broadband applications.

54 Design A Ka-Band High-Gain LNA

Based on a commercial pHEMT semiconductor process, this amplifier aids applications from 30 to 36 GHz.

64 Compact Antenna Snares WiMAX/WLAN

This dual-band antenna covers the 3.1 to 3.8 GHz and 5.0 to 5.8 GHz bands in support of both WiMAX and WLAN wireless communications applications.

70 **DDS Model Tunes Doppler Simulation**

> An accurate model for a third-order direct-digital synthesizer can be used for computer simulations of satellite navigation receivers under different conditions.

Quadrupler Cuts Losses At W-Band 76

A unique design approach aids in the fabrication of a W-band quadrupler capable of as much as +2 dBm output power from 80 to 100 GHz.

Microstrip Antenna Boosts UWB Gain 84

> This compact slot antenna employs an FSS as a reflector to help boost gain over a wide impedance bandwidth for UWB applications.



40 **SPECIAL REPORT**

Jamming systems

INDUSTRY TRENDS & ANALYSIS

46 **RF ESSENTIALS**

Spectrum analyzers

50 **INDUSTRY INSIGHT**

SDR advances

PRODUCT TECHNOLOGY

PRODUCT TRENDS 100

Test chambers

102 **PRODUCT FEATURE**

Signal editing software

103 **PRODUCT BRIEFS**

NEWS & COLUMNS

- ON MWRF.COM 11
- **EDITORIAL**
- 18 **FEEDBACK**
- **NEWS** 20
- **COMPANY NEWS** 28
- **INSIDE TRACK** 33

with Nuvotronics Noel Heiks



- 36 **R&D ROUNDUP**
- MICROWAVES IN EUROPE 38
- 94 **APPLICATION NOTES**
- **ADVERTISER'S INDEX** 104
- **NEW PRODUCTS** 106

JOIN US ONLINE



follow us @MicrowavesRF

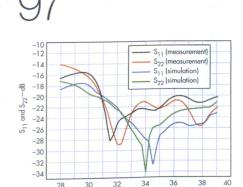


become a fan at facebook.com/microwavesRF

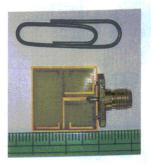








Frequency-GHz





PHASE STABLE THROUGH 70GHz

Rosenberger Rmor™ cables are designed for rugged environments for indoor and outdoor applications. Each shielded coaxial cable is protected with flexible, SPIRAL-wound 304 Stainless Steel armor coated with extruded Polyurethane. The connector ends are sealed and encapsulated with a pressure injection-molded polymer strain relief.

This combination of materials and technology provides superior ruggedization, environmental resistance, RF shielding effectiveness and stability under flexure and vibration.

Additional connector interfaces and armor/cable diameters are available on request.

DESCRIPTION

Rosenberger connectors, cable assembly, standard length 915mm or 36 inches

GENERAL ELECTRICAL SPECIFICATIONS

Impedance:
Operating frequency:
Return loss:

Cable insertion loss: Velocity of propagation (%): Capacitance:

Shielding effectiveness: Dielectric withstand voltage:

Amplitude & phase stable:

50 +/- 1 Ohms DC to 70 GHz

14 dB minimum up to 70 GHz .67 dB/ft @ 10.0 GHz

78 % nominal

24.7 pf/ft. nominal < -90 dB

< -90 dB 1000 Vrms

+/- .03dB & +/- 1° @10GHz

MECHANICAL SPECIFICATION

Cable jacket & armor outer diameter:

Minimum bend radius: Armor crush strength: Connector retention: Mating torque: 092 inches nominal &

.250 inches nominal

.5 inches

450 lbs/in (min) ≥25 lbs.

7-10 inch pounds

MATERIALS AND FINISHES

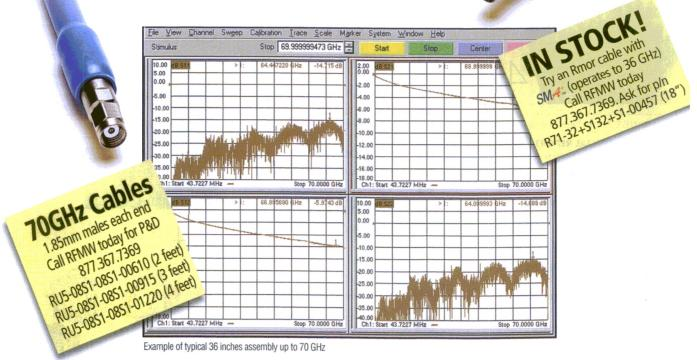
Armor type:

Connector environmental testing

Connector interface dimension

SPIRAL-wound 304 SS & Polyurethane blue jacket Per MIL-STD-202, Meth 101,106,107,204 & 213 JEC 60169-17 Per MIL-PRF-39012 DINEN122200

Note: Cable assemblies also available with interfaces such as 1.85mm, 2.4mm, 2.92mm, SMA+, SMA, N.





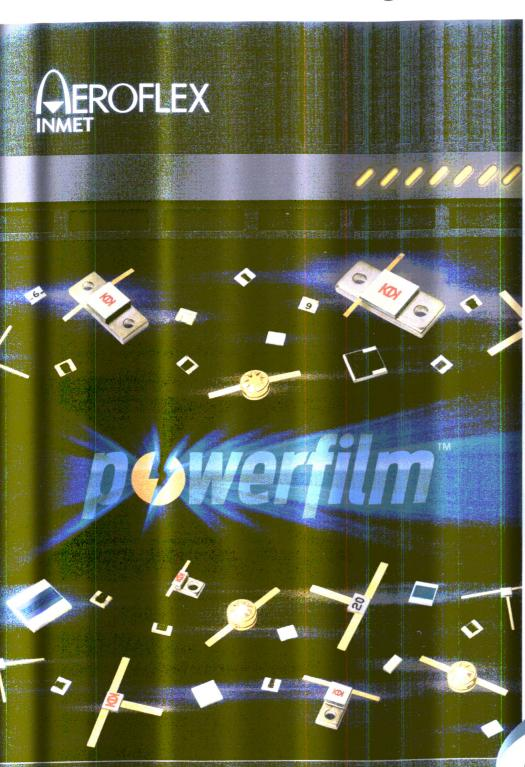
REALIZE A CLEAR COMPETITIVE ADVANTAGE

NXP has been at the forefront of smart RF and microwave solutions for more than 35 years, that's why we are a trusted leader in 4G base stations. Whatever your challenge, with a broad RF portfolio and collaborative approach, our application experts will help you advance your RF designs to power your competitive advantage.





Enhanced, Expanded, Perfected. Powerfilm™ attenuators go further.



Inspired by original designs produced by Aeroflex / KD decades ago, new Powerfili surface-mount attenuators from Aeroflex / Inmet are now produced in our new USA facility, and enhanced to include even more attenu ation range and power than ever before. Employing a proprietary, highly reliable thick/thin film processing approach, these devices are optimized for your highpower signal conditioning, leveling, gain optimization and matching network challenges.

Frequency Performance up to 18 GHz

Attenuation Ranges up to 20 dB

Power Ranges up to 100 Watts

They're easily designed-in, are readily available, and are priced competitively. Visit our website for detailed specifications.

888-244-6638 www.aeroflex.com/inmet

A passion for performance.

Modelithics®

Start designing today with Modelithics Global Models?

Scalable equivalent circuit models and S parameter data are available at Modelithics.com, in the simulator libraries of Agilent's ADS and

Genesys software, and in AWR's Microwave Office suite.



Low Frequency Power Combiners MECA introduces Low Frequency addition to the H-Series, 100-watt Wilkinson high power combiner/dividers. Available in 2 & 4-way configurations covering 5 to 500 MHz. VSWR of 1.30:1 accommodating load VSWR's of 2.0:1

or better! N and SMA connectors. Weatherproof IP 67 rated.

Low PIM Loads

MECA's Low PIM (-165 dBc Typ) Loads for DAS Applications feature industry leading PIM performance of -160 dBc Min all while handling full rated power to 85C. All of the terminations cover 0.698 - 2.700 GHz frequency bands in 7/16 DIN or Type N connectors as 30, 50, 100 & 150 wattrated, Ideal for IDAS / ODAS, In-Building, base station, wireless infrastructure, 4G and AWS. applications.





Low PIM Couplers

MECA's Low PIM (-160 dBc Typ) **Directional Couplers for DAS** Applications feature unique air-line construction that provides for the lowest possible insertion loss, high directivity and VSWR across the 0.800 - 2.500 GHz bands. Rated for 500 watts average power. Nominal coupling values of 15, 20, 30 & 40 dB

Low PIM Reactive Splitters MECA's Low PIM (-160dBc Typ) Reactive Splitters for DAS Applications, rugged construction and excellent performance across all wireless bands from 0.698 - 2.700 GHz make them ideal for in-building or tower top systems. Available 2-way and 3-way, 7/16 DIN and Type-N configurations. Rated for



BETTER BUILDINGS / BETTER PERFORMANCE

Dr. D.A.S. © Prescribes: MECA Low PIM Products & Equipments For next generation DAS there is only only one name in passives.

It's simple. Better signals equal better performance. Today's buildings personify the need for next-level Distributed Antenna Systems (DAS). And the engineers that are building them turn to MECA for passive components. American ingenuity and 53 years of experience have resulted in the deepest, most reliable product line of ready-to-ship and quick-turn solutions, such as:

Power Dividers: Up to 16 way and 18 GHz

Attenuators: Up to 60dB and 500W

Terminations: Up to 500W

Couplers: Up to 40dB and 1kW

Integrated Rack Units: Delivered in 3-6 weeks

They come with an industry leading 3 year guarantee and true MECA pride. Ready to build a better DAS? Start with a visit to www.e-MECA.com.

"delivered on time every time!!"

Low PIM Adapters

MECA's Low PIM (-165 dBc Typ) Adapters for DAS Applications feature industry leading PIM performance of -160 dBc Min. Available in 7/16 DIN, Type N to SMA and 4.1/9.5 Mini-DIN connectors. Ideal for IDAS / ODAS, In-Building, base station, wireless infrastructure. 4G and AWS applications.



Integrated D.A.S. Equipment

Let MECA create an integrated assembly with any of our RF/Microwave products on 19" panels, shelves or NEMA enclosures.



MECA's Low PIM (-160 dBc Typ) Adapters for DAS Applications feature industry leading PIM performance of -155 dBc Min.

Available in 7/16 DIN, Type N to SMA and 4.1/9.5 Mini-DIN connectors. Ideal for IDAS / ODAS, In-Building, base station, wireless infrastructure, 4G and AWS applications.



Dr. D.A.S. @ Prescribes ...



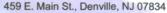


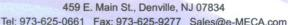
Look for the expanding lineup of MECA products in your iBwave library.



Microwave Electronic Components of America

The Professional's Choice for RF/Microwave Passive Components







More Q. Less Cu



These tiny new air core inductors have the highest Q and current handling in the smallest footprint.

Coilcraft's new SQ air core inductors have unmatched Q factors: most are above 200 in the 1-2 GHz range! That's 3 times higher than comparably sized 0805 chip coils.

And with their extremely low DCR, they can handle 4 to 8 times more current: up to 4.4 Arms.

SQ air core inductors are perfect for your LC filter and RF impedance matching applications. They come in 15 values ranging from 6 to 27.3 nH, all with 5% tolerance.

These coils

are significantly smaller than existing air core inductors. We reduced the footprint by using close-wound construction and keeping the leads close to the body. The square shape cuts the height to as low as 1.5 mm and creates flat top and bottom sur-







The square shape and narrow footprint reduce board space by 60-75% over conventional air core inductors.

Q factors are 3X higher than standard chip inductors

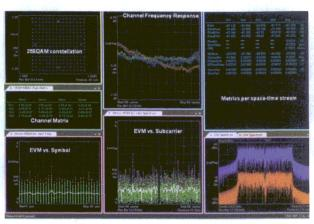
faces for easy automated handling and stable mounting.

See how the ultra-high Q and current handling of Coilcraft's new SQ air core inductors can maximize the performance of

your next design. For complete specifications and free evaluation samples, visit www.coilcraft.com/sq

Coilcraft

onmicrowaves&rf.com



WHAT'S THE DIFFERENCE

BETWEEN IEEE 802.11 AC AND 802.11AD?

The IEEE 802.11ac and 802.11ad specifications both promise to deliver increased capacity, speed, and performance in different ways, allowing users on-the-go to enjoy even their highest-data-rate applications. In this Web-exclusive report, Agilent Technologies' Liz Ruetsch breaks down the differences between the two.

To read the article in its entirety, go to www.mwrf.com/ test-amp-measurement/what-s-difference-between-ieee-80211ac-and-80211ad

NEWS UPDATES SENT TO YOUR DESKTOP

Don't believe everything you read, unless it's in the latest issue of Microwaves & RF **UPDATE.** The industry's longestrunning weekly e-mail newsletter, it combines insightful commentary with the latest product and industry business news. It is sent directly to your computer desktop each week, and often contains the little things that engineers love, such as links to free white papers

and even design software. If you're not already reading it, subscriptions are free, and available from the Microwaves & RF website at www.mwrf.com.

join us online 📴 📑



Fillenna EMI And RFI Noisa Fill MEMA Switches Are Printed For Mass

Putting Software Through Its Pace:

Corralling Materials







DAVID A. HALL

BOB NELSON

ALSO, BE SURE CHECK OUT THESE OTHER RECENT ARTICLES IN OUR CONTRIBUTED TECHNICAL EXPERT SERIES.

Visit www.mwrf.com/community/contributors.

THE EFFECT OF MOORE'S LAW ON RF INSTRUMENTS

DAVID A. HALL—Senior Product Marketing Manager for RF and Communications, National Instruments

UNDERSTANDING MEASUREMENT UNCERTAINTIES IN SPECTRUM ANALYSIS

BOB NELSON—Product Support Engineer, Agilent Technologies

The 2013 installment of the RF/ microwave industry's flagship event, the International Microwave Symposium, has come and gone. Luckily for you, it needn't live on just in memory. Visit www.mwrf. com/ims-2013-microwaves-rf-



reports-event to check out our show coverage, as well as www.engineering tv.com to view videos from the event.

MWRF.COM HAS ARCHIVES OF PRINT AND ONLINE ARTICLES DATING BACK TO OCTOBER 2002.

Visit mwrf.com today and click the "Back Issues" link. And while you're taking a look around the site, click on "Product Directory" to gain access to our complete directory of products and suppliers.



GO TO MWRF.COM



Ultra Small 2x2mm

TTENUATORS DC-20 GHz from 199 (ea.(qty. 1000)

absorptive attenuators, available in molded plastic or high-rel MIL requirements including vibration, PIND, thermal shock, hermetic nitrogen-filled ceramic packages. They are perfect gross and fine leak and more, at up to 125°C! building blocks, reducing effects of mismatches, harmonics, and intermodulation, improving isolation, and meeting other circuit level requirements. These units will deliver the precise attenuation you need, and are stocked in 1-dB steps from 0 to 10 dB, and 12, 15, 20 and 30 dB.

The ceramic hermetic RCAT family is built to deliver reliable, repeatable performance from DC-20GHz under the harshest conditions. With sample prices starting at

Save PC board space with our new tiny 2W fixed value only \$4.95 ea. (qty. 20), these units are qualified to meet

The molded plastic YAT family uses an industry proven, high thermal conductivity case and has excellent electrical performance over the frequency range of DC to 18 GHz, for prices as low as \$2.99 ea. (qty. 20).

For more details, just go to minicircuits.com - place your order today, and you can have these products in your hands as soon as tomorrow! (RoHS compliant

FREE Simulation Models! Modelithics

http://www.modelithics.com/mvp/Mini-Circuits/

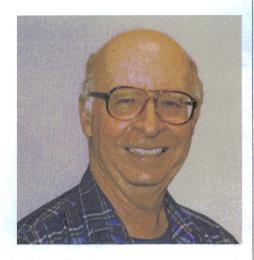


Plastic

Editorial

JACK BROWNE

Technical Contributor iack.browne@penton.com



Radar Is Driving Industry Differently

adar has long been a healthy application area for the RF/microwave industry, but it has also long been synonymous with military customers and subcontractors. For military radar use, requirements for devices, components, and systems were well established by the environmental and performance needs of those military radar systems. That being said, the commercial world is quickly adopting radar technology for collision avoidance systems, albeit at somewhat higher frequencies. Of course, without the support of military contracts, these higher-frequency systems must be designed economically and competitively.

One of the frequency bands that has caught a great deal of attention for commercial/consumer automotive radar systems is at 77 GHz, within a band that is not occupied by other applications and can effectively support collision-avoidance radar systems in commercial automobiles. The secrets are to fabricate electronic systems that can reliably and repeatably provide the performance needed for these systems, and to do so at a cost that can be competitively applied across a wide range of automobiles.

Because of the potential size of this market—with each automobile employing multiple antennas and 77-GHz radar receivers and transmitters to handle collisionavoidance protection for the front, rear, and sides of a vehicle—many major device, component, and subsystem manufacturers are exploring cost-effective solutions for 77-GHz automotive collision-avoidance radar systems.

Even suppliers of printed-circuit boards (PCBs) are testing different high-frequency materials for low dissipation at frequencies to 77 GHz and beyond. Interestingly, these frequencies that were once considered "exotic" because they were much higher than the traditional RF/microwave frequency range of DC to 18 GHz, are now drawing a growing number of device, circuit, system, and even PCB developers offering products capable of cost-effective performance at frequencies to 77 GHz and beyond.

The automotive radar market it is only just a start for what might be possible at these higher frequencies. With the increasing needs to move large amounts of data across relatively short distances in both commercial and military applications, lineof-sight communications links at 60 and 94 GHz are also growing in popularity. Not many years ago, electronic products at millimeter-wave frequencies were considered somewhat exotic. But driven by automotive applications, the use of 77 GHz and other millimeter-wave frequency bands may be as commonplace as getting in the car. **mw**

JOIN US ON SOCIAL MEDIA

@MicrowavesRF | facebook.com/microwavesrf



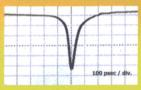
Impulse Generators 100 - 2000 MHz

Application:

- > Clock Reference
- > Sampling Circuit
- > Sharp Biasing or **Triggering Source**
- > Optical Modulator Driving







MODEL	INPUT (DRIVING) FREQ. (MHz)	TYPICAL IMPULSE OUTPUT VOLTAGE (V)	TYPICAL IMPULSE PULSE WIDTH (P SEC)	
GIM100A	100	-12	100	
GIM200A	200	-18	90	
GIM250A	250	-18	80	
GIM500A	500	-15	60	
GIM1000A	1000	-10	50	
GIM1500A	1500	-8	45	
GIM2000A	2000	-7	35	

Your Source for the Most Complete Line of Comb & **Impulse Generators**

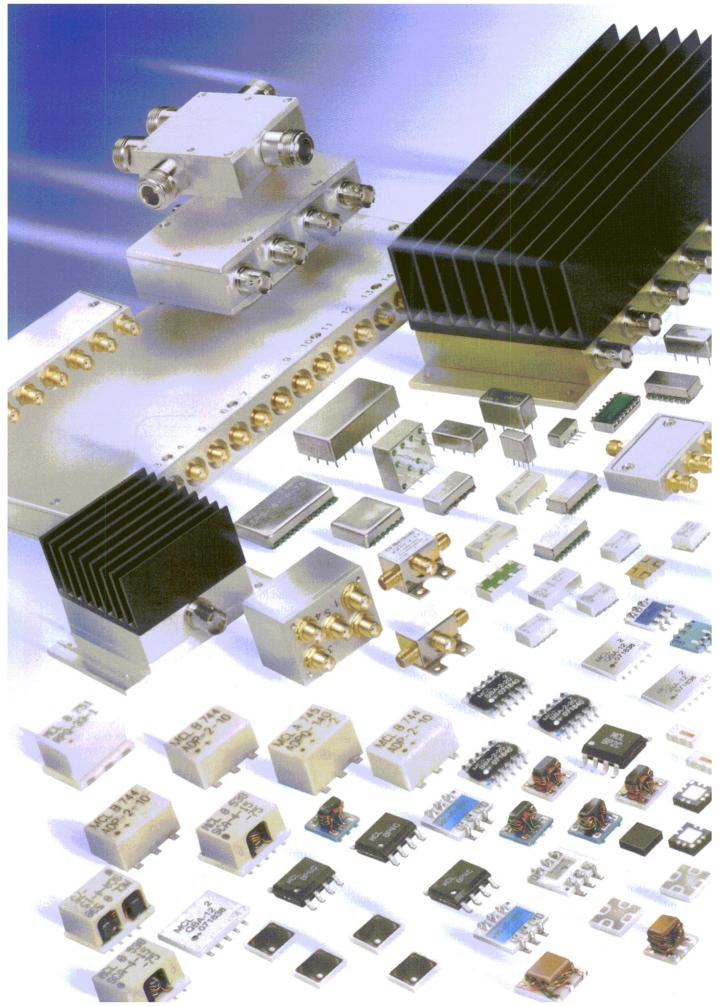
Other Herotek Products: Detectors . Limiters . Amplifiers Switches . Comb Generators Multipliers . Subassemblies



The Microwave **Products Source**

Herotek, Inc. 155 Baytech Drive San Jose, CA 95134 Tel: (408) 941-8399

Fax: (408) 941-8388 Email: Info @ herotek.com Website: www.herotek.com

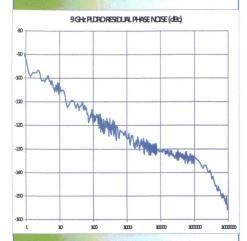






We have specialized in Low Phase Noise Fixed Frequency Sources since 1998.

A plot of our new quieter PLDRO line.



- Crystal reference phase noise to
 -130 dBc/Hz @ 100 Hz @ 100 MHz
- Dual loop output frequency resolution +/- 0.001 Hz
- Internal reference stability to +/- 10 ppb
- 5 1000 MHz External reference
- Frequency: 10 MHz to 35 GHz
- Power output: +10 to +24 dBm
- Wide operating temperature range: -55° to +85°
- Spurious: < -90 dBc

We welcome your custom requirements.



Nexyn offers the best performance and reliability on the market.

1287 Forgewood Ave. Sunnyvale, CA 94089 Tel: (408) 962-0895 Fax: (408) 743-5354 sales@nexyn.com

www.nexyn.com

JUNE | 2014

microwaves&rf

EDITORIAL

A Penton® Publication

CONTENT DIRECTOR: NANCY K. FRIEDRICH nancy.friedrich@penton.com
TECHNICAL CONTRIBUTOR: JACK BROWNE jack.browne@penton.com

 $\label{temperature} \begin{picture}{lll} TECHNICAL ENGINEERING EDITOR: {\it JEAN-JACQUES DELISLE} & jean-jacques.delisle@penton.com (a) & the control of the$

CONTENT PRODUCTION DIRECTOR: **MICHAEL BROWNE** michael.browne@penton.com

PRODUCTION EDITOR: RICHARD GAWEL richard.gawel@penton.com PRODUCTION EDITOR: JEREMY COHEN jeremy.cohen@penton.com PRODUCTION EDITOR: DENISE GRECO denise.greco@penton.com

ASSOCIATE CONTENT PRODUCER: ILIZA SOKOL iliza.sokol@penton.com
ASSOCIATE CONTENT PRODUCER: SARAH MANGIOLA sarah.mangiola@penton.com

EUROPEAN EDITOR: PAUL WHYTOCK p.whytock@btinternet.com

ASSOCIATE EDITOR: SALLY WARD-FOXTON sally.ward-foxton@penton.com

ART DEPARTMENT

GROUP DESIGN DIRECTOR: **ANTHONY VITOLO** tony.vitolo@penton.com CREATIVE DIRECTOR: **DIMITRIOS BASTAS** dimitrios.bastas@penton.com

SENIOR ARTIST: JAMES MILLER james.miller@penton.com

CONTRIBUTING ART DIRECTOR RANDALL RUBENKING randall.rubenking@penton.com

PRODUCTION

GROUP PRODUCTION MANAGER: JUSTIN MARCINIAK justin.marciniak@penton.com

PRODUCTION MANAGER: VICKI MCCARTY vicki.mccarty@penton.com

CLASSIFIED PRODUCTION COORDINATOR: LINDA SARGENT linda.sargent@penton.com

AUDIENCE MARKETING

AUDIENCE DEVELOPMENT DIRECTOR: **DEBBIE BRADY** debbie.brady@penton.com
ONLINE MARKETING SPECIALIST: **DAN KRAFT** dan.kraft@penton.com

FREE SUBSCRIPTION/STATUS OF SUBSCRIPTION/ADDRESS CHANGE/MISSING BACK ISSUES T | 866.505.7173 microwaves&RF@halldata.com

SALES & MARKETING

BRAND DIRECTOR, e DESIGN: **TRACY SMITH T** | 913.967.1324 **F** | 913.514.6881 tracy.smith@penton.com

REGIONAL SALES REPRESENTATIVES

BRAND CHAMPION: NORTHEAST/EASTERN CANADA: **DAVE MADONIA T** | 212.204.4331 **F** | 913.514.3966 dave.madonia@penton.com

MIDWEST/MID-ATLANTIC: **STEPHANIE CAMPANA T** | 312.840.8437 **F** | 913.514.3645 stephanie.compana@penton.com

PLEASE SEND INSERTION ORDERS TO: orders@penton.com

PENTON REPRINTS: WRIGHT'S MEDIA T | 877.652.5295 penton@wrightsmedia.com

CIRCULATION: CUSTOMER SERVICE T | 866.505.7173 F | 847.763.9673 electronicdesign@halldata.com

EUROPEAN SALES

EUROPE: MARK DURHAM T | +44 (0)7958 564137 mark.durham@penton.com

ASIA: **HELEN LAI T** | 886 2-2727 7799 | helen@twoway-com.com JAPAN: **HIROKAZU MORITA** T | -81 3 3261 4591 **F** | -81 3 3261 6126 TAIWAN: **CHARLES LIU T** | 886 2-2727 7799 **F** | 886 2 2728 -3686 KOREA: **JO YOUNG SANG** T | (011)82-2-739-7840 LIST RENTALS, CUSTOMER SERVICE—SUBSCRIPTIONS:

ONLINE MARKETING MANAGER: SARAH NOWOWIEJSKI T | (212) 204 4295

Sarah.nowowieiski@penton.com

PENTON REPRINTS: **WRIGHT'S MEDIA T** | (877) 652-5295 penton@wrightsmedia.com

ONLINE

ONLINE DEVELOPMENT DIRECTOR: VIRGINIA GOULDING virginia.goulding@penton.com

COMMUNITY LEADER: RYAN MALEC ryan.malec@penton.com
CONTENT OPTIMIZATION SPECIALIST: MATT LEE matt.lee@penton.com

DESIGN ENGINEERING & SOURCING GROUP

VICE PRESIDENT & MARKET LEADER: BILL BAUMANN

EXECUTIVE DIRECTOR OF CONTENT AND USER ENGAGEMENT: NANCY FRIEDRICH

GROUP DIRECTOR OF OPERATIONS: CHRISTINA CAVANO GROUP DIRECTOR OF MARKETING: JANE COOPER

RESEARCH MANAGER: JULIE RITCHIE

MARKETING & EVENTS SPECIALIST: ADRIAN PIAZZA

PENTON MEDIA INC.

CHIEF EXECUTIVE OFFICER: DAVID KIESELSTEIN david.kieselstein@penton.com
CHIEF FINANCIAL OFFICER: NICOLA ALLAIS nicola.allais@penton.com

 ${\tt SENIOR~VP,~DESIGN~ENGINEERING~GROUP:~\textbf{BOB~MACARTHUR}} \quad {\tt bob.macarthur@penton.com} \\$



Electronic Design | Machine Design | Microwaves & RF | Medical Design | Source ESB | Hydraulics & Pneumatics | Global Purchasing | Distribution Resource | Power Electronics | Mobile Dev & Besign | Defense Electronics | Auto Electronics | Electronic Design Europe | Engineering TV

RF Amplifiers and Sub-Assemblies for Every Application

Delivery from Stock to 2 Weeks ARO from the catalog or built to your specifications!

- Competitive Pricing & Fast Delivery
- Military Reliability & Qualification
- Various Options: Temperature Compensation, Input Limiter Protection, Detectors/TTL & More
- Unconditionally Stable (100% tested)

150 9001:2000 and AS91006: CERTIFIED

•	Uncondition	ally Stable	(100% te	sted)			
	OCTAVE BA Model No. CA01-2110 CA12-2110 CA24-2111 CA48-2111 CA812-3111	ND LOW N Freq (GHz) 0.5-1.0 1.0-2.0 2.0-4.0 4.0-8.0 8.0-12.0	Gain (dB) MII 28 30 29 29	Noise Figure (dB) 1.0 MAX, 0.7 TYP 1.0 MAX, 0.7 TYP 1.1 MAX, 0.95 TYP 1.3 MAX, 1.0 TYP	+10 MIN +10 MIN +10 MIN +10 MIN	3 3rd Order ICP +20 dBm +20 dBm +20 dBm +20 dBm +20 dBm	VSWR 2.0:1 2.0:1 2.0:1 2.0:1 2.0:1
	CA1218-4111 CA1826-2110 NARROW B CA01-2111 CA01-2113	12.0-18.0 18.0-26.5 BAND LOW 0.4 - 0.5 0.8 - 1.0 1.2 - 1.6	25 32 NOISE A 28 28 28	1.9 MAX, 1.7 IYP 3.0 MAX, 2.5 TYP ND MEDIUM PC 0.6 MAX, 0.4 TYP 0.6 MAX, 0.4 TYP 0.6 MAX 0.4 TYP	+10 MIN +10 MIN WER AMPI +10 MIN +10 MIN +10 MIN	+20 dBm +20 dBm LIFIERS +20 dBm +20 dBm +20 dBm	2.0:1 2.0:1 2.0:1 2.0:1 2.0:1
	CA23-3116 CA34-2110 CA56-3110 CA78-4110 CA910-3110 CA1315-3110 CA12-3114 CA34-6116 CA56-5114 CA812-6115 CA812-6116 CA1213-7110 CA1415-7110	2.7 - 2.9 3.7 - 4.2 5.4 - 5.9 7.25 - 7.75 9.0 - 10.6 13.75 - 15.4 1.35 - 1.85 3.1 - 3.5 5.9 - 6.4 8.0 - 12.0 8.0 - 12.0 12.2 - 13.25 14.0 - 15.0 17.0 - 22.0	29 28 40 32 25 25 30 40 30 30 28 30 28	0.7 MAX, 0.5 TYP 1.0 MAX, 0.5 TYP 1.0 MAX, 0.5 TYP 1.2 MAX, 1.0 TYP 1.4 MAX, 1.2 TYP 1.6 MAX, 3.0 TYP 4.5 MAX, 3.5 TYP 5.0 MAX, 4.0 TYP 4.5 MAX, 3.5 TYP 5.0 MAX, 4.0 TYP 6.0 MAX, 4.0 TYP 6.0 MAX, 4.0 TYP 5.0 MAX, 4.0 TYP	+10 MIN +10 MIN +10 MIN +10 MIN +10 MIN +33 MIN +33 MIN +30 MIN +33 MIN +33 MIN +30 MIN +31 MIN +31 MIN +31 MIN	+20 dBm +20 dBm +20 dBm +20 dBm +20 dBm +20 dBm +21 dBm +41 dBm +31 dBm	2.0:1 2.0:1 2.0:1 2.0:1 2.0:1 2.0:1 2.0:1 2.0:1 2.0:1 2.0:1 2.0:1 2.0:1
	Model No.	Freq (GHz)	Gain (dB) MI	N Noise Figure (dB)	Power-out @ P1-d	B 3rd Order ICP	VSWR
	CA0106-3111	6.0-18.0 6.0-18.0 2.0-18.0 2.0-18.0 2.0-18.0	26 32 36 26 22 25 35 30 30	1.9 Max, 1.5 TYP 2.2 Max, 1.8 TYP 3.0 MAX, 1.8 TYP 4.5 MAX, 2.5 TYP 2.0 MAX, 1.5 TYP 5.0 MAX, 3.5 TYP	+10 MIN +10 MIN +22 MIN +30 MIN	+20 dBm +32 dBm +40 dBm	2.0:1 2.0:1 2.0:1 2.0:1 2.0:1 2.0:1
	Model No. CLA24-4001 CLA26-8001 CLA712-5001 CLA618-1201	Freq (GHz) Ir 2.0 - 4.0 2.0 - 6.0 7.0 - 12.4 6.0 - 18.0	-28 to +10 c -28 to +10 c -50 to +20 c -21 to +10 c -50 to +20 c	Range Output Power IBm +7 to +1 IBm +14 to +1 IBm +14 to +1 IBm +14 to +1	Range Psat Po 11 dBm 18 dBm 19 dBm 19 dBm	+/- 1.5 MAX +/- 1.5 MAX +/- 1.5 MAX +/- 1.5 MAX +/- 1.5 MAX	VSWR 2.0:1 2.0:1 2.0:1 2.0:1
	Model No	Fron (GHz)	Gain (dR) MIN	Noise Figure (dB) Po	ower-out@P1-dB G	ain Attenuation Range	VSWR
973.899	CA1518-411UA	15.0-18.0	30	5.0 MAX, 3.5 TYP 2.5 MAX, 1.5 TYP 2.5 MAX, 1.5 TYP 2.5 MAX, 1.5 TYP 2.2 MAX, 1.6 TYP 3.0 MAX, 2.0 TYP	+12 MIN +18 MIN +16 MIN +12 MIN +16 MIN +18 MIN	20 dB MIN 20 dB MIN 22 dB MIN 15 dB MIN 20 dB MIN 20 dB MIN	2.0:1 2.0:1 1.8:1 1.9:1 1.8:1 1.85:1
	Model No.	Freq (GHz) G	ain (dB) MIN	Noise Figure dB F	Power -out @ P1-dB	3rd Order ICP	VSWR
Acade	CA001-2110 CA001-2211 CA001-2215 CA001-3113 CA002-3114 CA003-3116 CA004-3112	0.01-0.10 0.04-0.15 0.04-0.15 0.01-1.0 0.01-2.0 0.01-3.0 0.01-4.0	24 23 28 27 18 32	4.0 MAX, 2.2 TYP 3.5 MAX, 2.2 TYP 4.0 MAX, 2.2 TYP 4.0 MAX, 2.8 TYP	+10 MIN +13 MIN +23 MIN +17 MIN +20 MIN +25 MIN +15 MIN	+20 dBm +23 dBm +33 dBm +27 dBm +30 dBm +35 dBm +25 dBm	2.0:1 2.0:1 2.0:1 2.0:1 2.0:1 2.0:1 2.0:1
				rireless.com for			fering.

CIAO Wireless can easily modify any of its standard models to meet your "exact" requirements at the Catalog Pricing.

Visit our web site at www.ciaowireless.com for our complete product offering.

Ciao Wireless, Inc. 4000 Via Pescador, Camarillo, CA 93012

Tel (805) 389-3224 Fax (805) 389-3629 sales@ciaowireless.com

Feedback

MAKING THE MOST OF IMS

In reviewing recent issues of your magazine, I scoured your pages for details on the recent 2014 International Microwave Symposium (IMS) in Tampa. To be honest, I was a little disappointed by the lack of product preview information prior to the show. Admittedly, the best way to learn about new products at any IMS is to walk the floor and get in front of exhibitors to hear their pitch. But this is also a very time-consuming approach, since it can easily take 20 minutes per stop just to walk down one aisle at a big trade show.

With less than three days to cover such a large exhibition floor, with typically more than 500 exhibiting companies, it is nearly impossible to spend time with every company of interest. For this reason, it is especially important for publications such as yours to provide extended coverage of the IMS.

Joseph Starbuck

EDITOR'S NOTE

The International Microwave Symposium—with its excellent collection of technical presentations, workshops, and application reviews, along with its hundreds of manufacturers'

exhibition booths with existing and new products—is obviously one of the single most important events to occur in the RF/microwave industry each year. In recognizing the importance of the event to product specifiers and the companies providing new products, *Microwaves & RF* is expanding its online gallery of 2014 IMS new products into a subsite

of www.mwrf.com.

Starting with the 2014 IMS offerings, it will eventually extend to the full industry for 2014 and beyond. The subsite will provide a single source for searching out data on new products of all types, along with the capability to search for specific product types (such as low-noise amplifiers or spectrum analyzers).

Microwaves & RF welcomes mail from its readers.

The magazine reserves the right to edit letters appearing in "Feedback." Address letters to:

Jack Browne

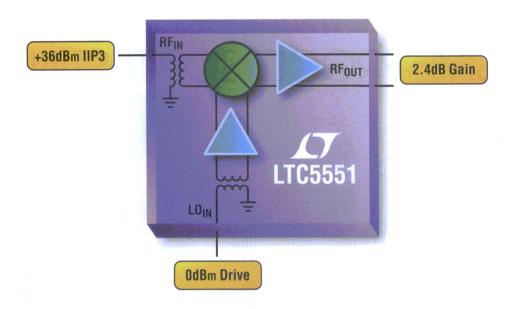
Technical Contributor jack.browne@penton.com Nancy Friedrich

Content Director nancy.friedrich@penton.com

DC-85 GHz **CUSTOMIZED DESIGN QUOTES IN 24 HOURS** www.pulsarmicrowave.com Power Dividers, DC-60 GHz **Directional Couplers** Single and Dual, to 60 GHz High Power, to 2500 watts Hybrids, to 40 GHz 90° & 180° Attenuators, to 18 GHz Digital, Analog, Linearized Bias Tees, to 85 GHz 30 KHz to 85 GHz Switches, to 18 GHz SP1T-SP8T **High Power Combiners** Also Available Modulators, and Image Reject Mixers

48 Industrial West, Clifton, NJ 07012 | Tel. 973-779-6262 | Fax: 973-779-2727 | sales@pulsarmicrowave.com

+36dBm IIP3 Mixer Boosts Dynamic Range with 2.4dB Gain



Wideband 300MHz to 3.5GHz Integrated Mixer Lowers Power and Reduces External Components

The LTC®5551's +36dBm IIP3, combined with 2.4dB conversion gain and 9.7dB noise figure, produces outstanding dynamic range performance. Its high gain saves an expensive IF amplifier stage while minimizing noise gain. And its 0dBm LO drive eliminates a high power RF amplifier, ensuring consistent performance without sensitivity to LO level or power supply variations.

Product Features

- 300MHz to 3.5GHz Frequency Range
- +36dBm IIP3
- 2.4dB Conversion Gain
- 9.7dB NF
- OdBm LO Drive
- Low Power: 670mW

LTC5551 Demo Board



(Actual Size)

🔻 Info & Free Samples

www.linear.com/product/LTC5551

LT, LT, LTC, LTM, Linear Technology and the Linear logo are registered trademarks of Linear Technology Corporation. All other trademarks are the property of their respective owners.



Cruise Missile Undergoes PASSIVE PROCESSOR TESTING

o perform precision strikes, the military typically turns to Tomahawk Block missiles to carry out the mission. The highly accurate, GPS-enabled precision weapon can change targets at a moment's notice, even in harsh environments. The latest iteration is the Tomahawk Block IV cruise missile. The new Block IV design, initiated in an effort to save cost and improve functionality, includes a two-way satellite data-link that makes it possible to retarget while in flight.

The Block IV recently underwent captive flight testing to demonstrate an advanced, next-generation, multifunction processor. The processor enables the missile to navigate and track moving targets through the use of radiofrequency signals.

The test equipped the Tomahawk's nosecone with passive antennas and the new modular processor. Fitted to a T-39 aircraft that simulated a normal flight regime, the passive seeker and processor successfully received numerous electronic signals from tactical targets in a complex, high-density electromagnetic environment.

Next year, Raytheon plans to test the



Over the past 30 years, Tomahawk cruise missiles have been used approximately 2300 times in combat and flight-tested more than 700 times. (Photo courtesy of Raytheon)

processor with an active seeker. The proposed event will demonstrate the processor's ability to broadcast active radar as well as passively receive electromagnetic information—a critical component in enabling the missile to strike moving targets on land and at sea.

Today's network-enabled Tomahawks allow controllers from across the globe to use almost any sensor to guide it to a target. The ability to multitask—sending back pictures while doing reconnaissance—is especially critical while carrying a 1000-lb warhead. ■

BITCOINS READY TO TAKE OFF...Into Outer Space?

BITCOINS, A CRYPTOCURRENCY based on a peer-to-peer (P2P) network, have now become the central components of a potential satellite launch. The project aims to bring the network to off-grid areas and in places plagued by expensive or faulty network connections, further expanding the cryptocurrency's reach. The bitcoin network

isn't governed by a central authority. Rather, a process called "mining" manages transactions and issues out money, all of which is balanced on a shared public ledger, or block chain.

A preliminary design contract between Dunvegan Space Systems and Deep Space Industries calls for the development of an

orbital system for the not-for-profit BitSat project. The constellation of small BitSats (small 10-cm boxes) will utilize an orbital node for the bitcoin P2P network to enhance resiliency against disruptions or outages. BitSats will also provide cross-check capabilities, verifying that blocks available on the terrestrial network haven't been spoofed while also providing the latest blocks to locations off the terrestrial grid.

This is not the first time bitcoins have met the space frontier. According to a Yahoo! News report, British billionaire Sir Richard Branson recently announced that his commercial space company, Virgin Galactic, would start accepting payments in the cryptocurrency for suborbital flights aboard SpaceShipTwo. So far, the Winklevoss twins—famous for their dispute with Facebook founder Mark Zuckerberg—are among Virgin Galactic's bitcoin-paying customers.

Back on Earth, bitcoins may be deemed a commodity rather than a currency by the IRS, but that hasn't stopped the digital transactions from changing the way we pay for things. RT.com examined the tumultuous bitcoin landscape, and noted that "the announcement comes at a curious time for the increasingly popular currency, with



some experts wondering if bitcoin's own success will ultimately lead to its demise. Governments and financial institutions have not been more encouraging, with the IRS announcing bitcoin would be regulated as a commodity rather than a currency, and the CEO of Chase bank questioning if users should trust bitcoin (price fluctuated from \$230 in April 2013 to below \$70 in July, then surpassing \$600 in November)."

The project is expected to cost around \$2 million—equal to about 4519 bitcoins—with funding provided by a crowdsourcing campaign. More details about the project will be made public later in 2014 via BitSats' Google Group. ■

FIRST-QUARTER MOBILE-PHONE SHIPMENTS Up 9% Over Last Year

GLOBAL MOBILE-PHONE SHIPMENTS

continue to escalate and an unexpected player joined the top 10 vendors, according to Strategy Analytics' recently released report. Shipments jumped 9%—the highest rate since 2011. Overall, Q1 2014 saw 408 million units shipped versus 372.7 million in Q1 2013. Of the total mobile-phone shipments, smartphones accounted for 7 in 10.

Demand for 3G and 4G models across Asia, Africa, and other countries represent the primary

driver of growth. However, growth in Asia was offset by rapid change in demand across Europe, the Middle East, Africa, and North America. Second-tier brands have gained momentum, too. Brands to watch include Coolpad, Lenovo, TCL-Alcatel, and Xiaomi, which had a strong quarter, evidenced by its first-ever ranking as a top 10 mobile vendor.

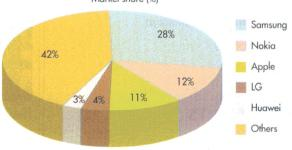
The top five mobile vendors are Samsung, Nokia, Apple, LG, and Huawei. Samsung grew 6% annually and shipped 113 million phones, landing 28% of the market in Q1 2014. However, Samsung's growth slowed due to competition from Chinese vendors. Still, the company ships more phones worldwide than Apple, LG, and Nokia combined. Nokia claims 12% market share, shipping 47 million

mobile phones worldwide, but still must fend off competition from Apple and other Android vendors. A key is new owner Microsoft, which will look to Nokia's upgraded X phone to stabilize potential future decline.

Apple, LG, and Huawei round out the top five mobile vendors. Apple shipped 43.7 million iPhones worldwide in Q1 2014 for a 10.7% market share—a slight increase from 37.4 million in Q1 2013. LG had a varied quarter, capturing 4% of the market. It

performed well in Europe, but weakly in China and India. Huawei captured a 3% share and is growing at twice the rate of the industry average. The company shipped 14.2 million phones, with its 3G and 4G Android gaining popularity in Asia and North America.





GO TO MWRE.COM 21

SECOND MUOS-SATELLITE RADIO Test Lab Begins Operations

GENERAL DYNAMICS C4 Systems opened the doors to a new radio testing labora-

tory for the Mobile User Objective System (MUOS) satellite-ground station communications that make up the soldier's network. MUOS ultra-high-frequency (UHF) satellites aim to provide more secure military communications by leveraging commercial

cellphone waveform technology. By adapting the wideband code-division multiple-access (WCDMA) architecture, the satellites can provide 16 times greater capacity than current UHF satellites.

Located in Scottsdale, Ariz., the U.S. Navy-approved laboratory is one of two that supports testing for radio terminals that will connect with the MUOS spaceground network. The lab is equipped with hardware and software that simulates radio connectivity with the network. Radios are provisioned with the WCDMA-based, MUOS-specific waveform to make secure voice calls and complete data transmissions at different data rates across the network. Communications flow to the satellites via UHF WCDMA links; the satellites relay the data via a Ka-band feeder link to one of four interconnected ground sites.

The lab will help the U.S. military and government find cost-effective and efficient ways to add MUOS-capable radios, such as Rockwell Collins' ARC-210 and General Dynamics' AN/PRC-155, to current communications networks. Recently, a team from Harris connected the AN/PRC-117G Falcon III radio to a MUOS system developed by Lockheed Martin.

The narrowband capability delivered through MUOS ensures reliable coverage even during situations such as national emergencies, disasters, and humanitarian relief. Once fully deployed, the MUOS constellation will consist of four geosynchronous satellites—plus an on-orbit spare—as well as the four ground stations. The constellation is expected to achieve full operational capability in 2015.



Testing the AN/PRC-155 Manpack Radio at the new laboratory in Scottsdale. (Photo courtesy of General Dynamics C4 Systems)

Redefining Frequency Synthesizers

With QuickSyn Technology



Design smaller and more efficient instruments with National Instruments QuickSyn synthesizers. The revolutionary phase-refining technology used in QuickSyn synthesizers enables blazing fast switching speeds, very low spurious and phase noise performance, wide frequency range, and small footprint.

QuickSyn Models

Full-Featured

Lite Version

FSL-0010 10 GHz

FSW-0010 10 GHz FSW-0020 20 GHz

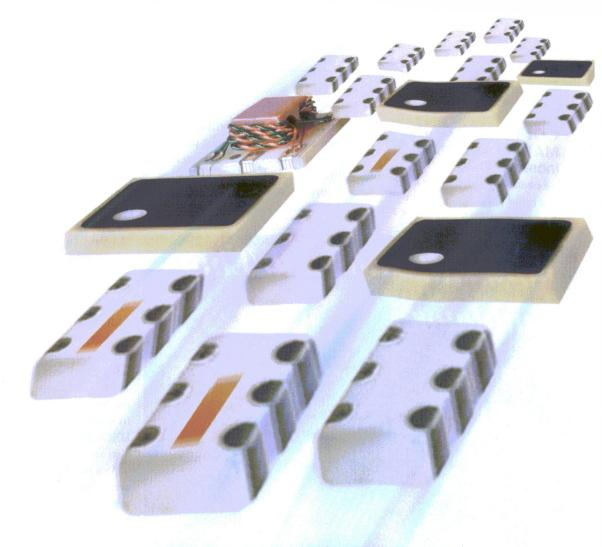
FSL-0020 20 GHz

ni-microwavecomponents.com/quicksyn 408 610 6810



©2014 National Instruments, Ail rights reserved, National Instruments, NI, and ni compare trademarks of National Instruments

Other good to be decompany cames listed and trademarks or trade games of their respective companies. 17281



90° SPLITTERS

5MHz to 8GHz

\$199 from 199

With over 70 different models, our two-way 90° splitters make the perfect building blocks for many designs including balanced amplifiers, IQ modulator/demodulators, single sideband modulators, image rejection mixers, voltage variable attenuators, phase shifters, and more! Use them for signal processing designs requiring 90° phase offset or to insulate your circuit from reflective elements. The industry's widest range of frequencies, extra low amplitude and phase unbalance, and packages as small as 0.08 x 0.05" make these hybrids essential tools for your RF design toolbox.

Tiny, robust, low-cost LTCC models are now available in small quantity reels, with standard counts of 20, 50, 100, 200, 500, 1000, or 2000 at no extra cost! For full performance details and product availability, visit *minicircuits.com*.

Order online today and have units in-hand as soon as tomorrow!



COROHS compliant

CONNECTED CAR MARKET Expects 15.4% Increase in 2014

THE CONNECTED CAR market is growing at a rapid pace. It also is undergoing major changes, thanks to the intro-

duction of new competition, global regulation, and increasing profit potential. Visiongain's commercial director, Sara Peerun, and head of reports, Daniel Harrison, recently shared some insights into this

industry based on the new report, "Top 20 Connected Car Companies 2014: mAutomotive, Telematics, Infotainment, Diagnostics, Connectivity, Safety & Security."

They emphasize the impact on the market as new players joined the foray this year. Specifically, telecommunications and Internet giants, competing with OEMs, are both starting to become prevalent in the connected car industry. Although OEMs currently lead the market, other types of companies will increasingly sell in-car technology and provide connectivity. Apple and Google, for example, are introducing operating systems to work with iPhone and Android. MNOs, like Verizon and Telematics. also are gaining interest.

As a result, different companies are shaping up to be industry leaders in the relatively new market. Car manufacturers and OEMs like



dBm

RF Test Equipment for Wireless Communications

dimCorp, Inc

32A Spruce Street ◆ Oakland, NJ 07436 Tel (201) 677-0008 ◆ Fax (201) 677-9444

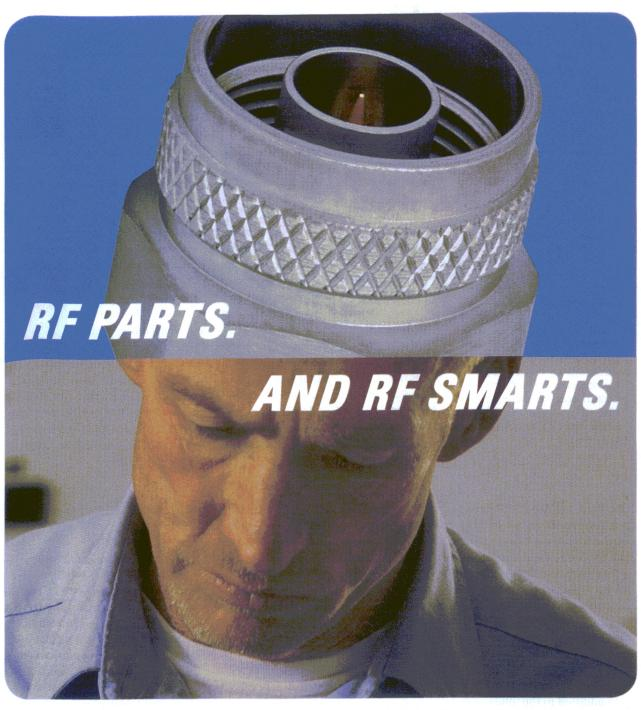
www.dbmcorp.com

KUDOS

API TECHNOLOGIES CORP—The UK
Trade & Investment (UKTI) GREAT
Business Innovation Award in
Technology was presented to API
Technologies Corp. during the annual BritWeek Miami event held in
South Florida. BritWeek Miami is
an alliance between UKTI and the
British Consulate General, which
was developed to highlight the
dynamic relationships between
Britain and Florida.

NORTHROP GRUMMAN CORP.—Charles Volk was awarded the Kershner Award at the Institute of Electrical and Electronics Engineers/Institute of Navigation's Position Location and Navigation Symposium. The prestigious Kershner Award was established in honor of Richard B. Kershner, the lead developer of the world's first navigation satellite system. Volk was honored for his work on navigation and inertial sensor systems.





Armed with the world's largest selection of in-stock, ready to ship RF components, and the brains to back them up, Pasternack Component Engineers stand ready to troubleshoot your technical issues and think creatively to deliver solutions for all your RF project needs. Whether you've hit a design snag, you're looking for a hard to find part or simply need it by tomorrow, our Component Engineers are at your service. Call or visit us at pasternack.com to learn more.







KUDOS

RAYTHEON—Chairman William H. Swanson was inducted into the U.S. News STEM Leadership Hall of Fame for his leadership in advancing STEM education and preparing the next generation of engineers and scientists. He was honored at a special ceremony during the 2014 U.S. News STEM Solutions National Leadership Conference at the Walter E. Washington Convention Center in Washington, D.C. In other Raytheon news, the company has once again been named to CR Magazine's 100 Best Corporate Citizens List, ranking 42. The annual list analyzes the performance of Russell 1000 companies, recognizing those that demonstrated outstanding corporate responsibility programs in 2013.

ANRITSU—The company's ME7834
Protocol Conformance Test system
has the highest number of approved IMS test cases for device
certification of any test platform,
Anritsu's accomplishment also
includes a number of unique and
industry-first GCF approvals for this
technology.

GM, Ford, and BMW will have a generous market share in 2014. Yet wireless-modem chipset providers like Qualcomm and Broadcom also will be prevalent. MNOs also will have a stake, such as AT&T and telematics software providers. Yet it is important to keep in mind that the connected car market is still relatively small. As a result, new players like Google and Apple could reshape it.

In addition to the influx of technology companies in this market, Peerun and Harrison note that regulatory efforts are driving connected cars forward. In the European Union, for example, eCall will be mandatory in every new vehicle by 2015. This automated call to emergency services is initiated after an accident with a minimum set of

PEOPLE

AGILENT TECHNOLOGIES—Named JAY AL-EXANDER has been named Keysight Technologies' chief technology officer. Agilent announced in September 2013

that it would separate into two publicly traded companies in 2014. Agilent's Electronic Measurement Group is expected to begin operating as Keysight



Technologies in August 2014. Alexander's appointment is effective immediately. In his new position, Alexander will lead Keysight's technology development, drive its product roadmap, and manage the company's resource allocation across divisions to transform Keysight's portfolio to proactively meet customers' needs.

ANRITSU CORP.—Appointed PETE ALEX-ANDER as vice president and general manager of Anritsu Co., the U.S. subsidiary of Anritsu Corp. Alexander will be responsible for all sales, marketing and field support operations for Anritsu's wireless, optical, microwave/ RF, and digital test solutions in North America and Latin America.

PRECISION DEVICES INC.—Announced the addition of SAM JOHNSON as vice president of engineering. Johnson brings extensive knowledge of filter design,



production, and testing to PDI. He has significant experience with cavity and coaxial/tubular filter designs covering DC to 20 GHz.

RAYTHEON—Named THOMAS A. VECCHI-OLLA as president, Raytheon International Inc., effective immediately. Vec-

chiolla has a proven track record and extensive experience in international business development and competitive pursuits. In his new role, he will be



responsible for leading Raytheon's international business team worldwide. Vecchiolla will report to John Harris, vice president, business development, Raytheon Co., and CEO, Raytheon International Inc. and will be based in Washington, DC.

emergency-related data (MSD). It is predicted to speed up emergency response time by 40% in urban areas and 50% in rural areas.

Additionally, Russia's Emergency Road Assistance (ERA)-Global Navigation Satellite System (GLONASS) is expected to

Regulatory efforts—
such as eCall in the
European Union—are driving
connected cars forward."

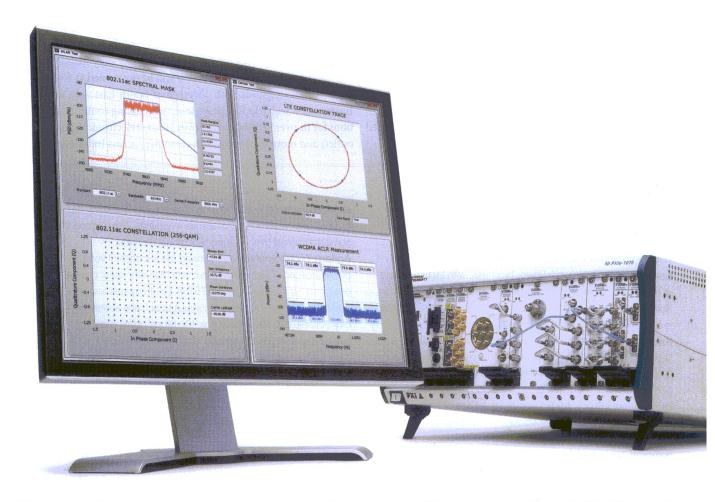
be required in all vehicles sometime this year. ERA-GLONASS is an emergency system like eCall. It will force foreign and domestic manufacturers to ensure that calls to emergency services can be made with basic connectivity technology. Also slated for 2014 is a vehicle tracking system

to combat Brazil's auto-theft problems. The stolen-vehicle-tracking (STV) device is called Contran 245.

In 2014, the connected car market is expected to be \$25.5 billion—an increase of 15.4% from 2013. Peerun and Harrison note that this growth is driven by both demand for wireless connectivity and global regulatory safety mandates. In countries where the demand for wireless connectivity is shown by high levels of smartphone and tablet adoption, the car is the next frontier for seamless connectivity. As safety regulations ease any privacy concerns on the part of drivers, the growth of telematics solutions should translate into prices dropping to levels that consumers will more readily pay. Given such an outlook, the connected car market indeed seems destined for growth.

Redefining RF and Microwave Instrumentation

with open software and modular hardware



Achieve speed, accuracy, and flexibility in your RF and microwave test applications by combining National Instruments open software and modular hardware. Unlike rigid traditional instruments that quickly become obsolete by advancing technology, the system design software of NI LabVIEW coupled with NI PXI hardware puts the latest advances in PC buses, processors, and FPGAs at your fingertips.

WIRELESS TECHNOLOGIES

National Instruments supports a broad range of wireless standards including:

LTE

802.11a/b/g/n/ac WCDMA/HSPA/HSPA+ GSM/EDGE CDMA2000/EV-D0

Bluetooth

>> Learn more at ni.com/redefine

800 813 5078

NATIONAL INSTRUMENTS

Company News

CONTRACTS

Redline Communications — Closed a significant contract with Hess Corp. to provide wireless networks for the oil giant's operations in the Bakken reserve area of North Dakota. Redline is providing complete turnkey installations of wireless digital oilfield networks, including engineering services for developing network designs optimized for the complex topography. This ubiquitous network coverage will allow people and machines to communicate to all Hess systems, regardless of where they are located.

RADWIN—Was selected by the Semirara Mining Corp.—the largest coal mine in the Philippines—for its high-capacity point-to-point solutions. Semirara is using RADWIN 2000 systems to create a private network to provide voice and data services to offices scattered across the mine site. EBDI, a Philippines-based system integrator, managed the entire installation.

REDLINEStrikes Hess
oilfield deal

SS/L Tapped to supply satellite **Space Systems/Loral (SS/L)**—Has been signed by EchoStar Corp. to provide the EchoStar XXIII, a high-power and very flexible Ku-band satellite capable of providing service from any of eight different orbital slots. Planned for launch in 2016, it is designed to provide service for 15 years or longer.

SSL also was chosen to provide a satellite to PT. Bank Rakyat Indonesia (Persero) Tbk (BRI), which would make BRI the first bank in the world to launch a communications satellite. Its goal is to provide a dedicated platform for banking connection services for the people of Indonesia. BRIsat is a C-band and Ku-band satellite that will be positioned at 150.5 degrees East longitude with coverage of South East Asia and Indonesia. It will help BRI provide secure banking communications for its over 9800 branches, over 100,000 electronic channel outlets and more than 50 million customers across Indonesia.

FRESH STARTS

Emerson—Will divest its Connectivity Solutions business unit to Bel Fuse Inc. The transaction, valued at \$98 million, is expected to close before the end of the fiscal year, with proceeds deployed for incremental share repurchase in 2014. Currently a part of Emerson's Network Power business, with 2013 revenue of more than \$80 million, Bannockburn, III.-based Connectivity Solutions offers fiber optic, RF, and microwave-coaxial technologies that safeguard network reliability.

Knowles Capacitors—Dielectric Laboratories, Novacap, Syfer Technology, and Voltronics have come together to form Knowles Capacitors, a new entity has a combined history exceeding 175 years and is a division of Knowles Corporation of USA, an independent publicly traded company. As one of the first moves under this new umbrella, the Voltronics brand has launched its V9000 series, specifically designed for the MRI industry.

National Technical Systems Inc.—Has successfully completed its American Association for Laboratory Accreditation (A2LA) audit for its Plano, Texas, facility and has added wireless/radio testing, product safety evaluations and Energy Star testing capabilities.

SemiGen Inc.—Announced that a series of fixed attenuator pads are now available from its RF Supply Center. SemiGen's advanced thin-film technology allows these attenuator pads to have full side wraps for SMT installation and a complete grounding backside for ease in attachment. SemiGen also offers a full range of RF/microwave and digital design/engineering services in collaboration with the microwave-engineering experts at Salt-whistle Technologies.

Würth Elektronik eiSos Group—The European supplier of electronic and electromechanical components has acquired Italian connector manufacturer Stelvio Kontek SpA. By buying up the company, Würth Elektronik eiSos will extend its global

activities in the connector business sector. The company has business operations in 50 countries worldwide with 13 production sites spread over all important global markets.

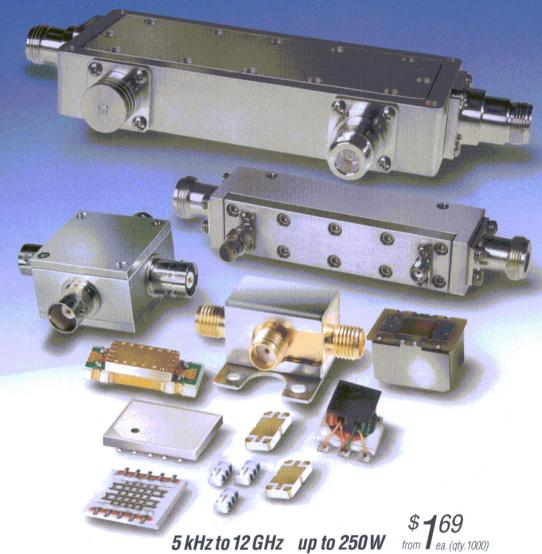
Agilent Technologies—Announced the successful verification of full Category 7 data throughput with Marvell's latest chipset design using the new Agilent E7515A UXM wireless test set. Agilent and Marvell worked in concert to achieve sustained bidirectional 300 Mbps downlink/100 Mbps uplink data throughput using 3GPP release 10 downlink and uplink carrier aggregation.

NYU WIRELESS—Aims to expand today's mobile and wireless capabilities to create a sustainable networked society using broadband wireless devices, networks, and applications. Through its Industrial Affiliates membership, Straight Path is making a commitment to support the center's research activities, including its pioneering work in understanding and characterizing the propagation environment at millimeter wave frequencies, including 28 and 39 gigahertz (GHz).

Huawei—Announced that its latest GSM-R solution has supported China's Da-Qin Railway Line with a successful 30,000-ton heavy-duty traction test, which increased China's railway hauling capacity by over 50%, enabling China to be one of the few countries in the world to conduct transportation of 30,000-ton heavy-haul trains in existing railway systems.

TriQuint Semiconductor Inc.—Appointed fast-growing Upstar Technology as its new distributor in China for TriQuint's high-performance mobile products. TriQuint has already created buzz and captured numerous design wins in China—the world's largest wireless communications market—at a time of explosive growth driven by rapid consumer adoption of mobile devices and accelerating buildouts of LTE networks for leading smartphones.

Directional/Bi-Directional COUPLERS



5 kHz to 12 GHz

Now! Looking for couplers or power taps? Mini-Circuits has 279 236 models in stock, and we're adding even more! Our versatile, low-cost solutions include surface-mount models down to 1 MHz, and highly evolved LTCC designs as small as 0.12 x 0.06", with minimal insertion loss and high directivity. Other SMT models are designed for up to 100W RF power, and selected core-and-wire models feature our exclusive Top Hat™, for faster pick-and-place throughput.

At the other end of the scale, our new connectorized air-line couplers can handle up to 250W and frequencies as high as 12 GHz, with low insertion loss (0.2 dB @ 9 GHz, 1 dB @ 12 GHz) and exceptional coupling flatness! All of our couplers are RoHS compliant. So if you need a 50 or 75 Ω , directional or bi-directional, DC pass or DC block coupler, for military, industrial, or commercial applications, you can probably find it at minicircuits.com, and have it shipped today!



USB & ETHERNET RESULTATION RESULTATION RESULTATION REPORTS AND ADMINISTRATION RESULTATION RESULTATION

Efficiency for your test setup. Economy for your budget.



New Feature! Switch Cycle Counting

DC to 18 GHz from \$385 ea.

We're adding more models and more functionality to our line of RF switch matrices. All models now feature switch cycle counting with automatic calibration interval alerts based on actual usage, an industry first! This function improves test reliability and saves you money. Our new RC-series models feature both USB and Ethernet control, so you can run your test setup from anywhere in the world! Rugged aluminum cases on all models house our patented mechanical switches with extra-long life of 10 years/100 million cycles of guaranteed performance!*

USB Control Switch Matrices

Model	# Switches (SPDT)	IL (dB)	VSWR (:1)	Isolation (dB)	$RF P_{MAX}$ (W)	Price \$ (Qty. 1-9)	
NEW USB-1SP4T-A18 USB-1SPDT-A18 USB-2SPDT-A18	1 (SP4T) 1 2	0.25 0.25 0.25	1.2 1.2 1.2	85 85 85	2 10 10	795.00 385.00 685.00	
USB-3SPDT-A18 USB-4SPDT-A18 USB-8SPDT-A18	3 4 8	0.25 0.25 0.25	1.2 1.2 1.2	85 85 85	10 10 10	980.00 1180.00 2495.00	

Our easy-to-install, easy-to-use GUI will have you up and running in minutes for step-by-step control, full automation, or remote operation. They're fully compatible with most third-party lab software, † adding capabilities and efficiency to existing setups with ease! Visit minicircuits.com today for technical specifications, performance data, quantity pricing, and real time availability – or call us to discuss your custom programming needs – and think how much time and money you can save!

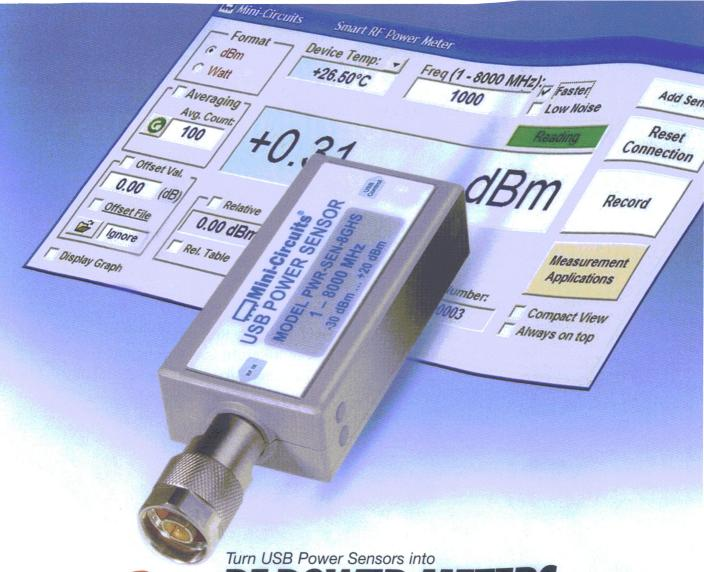
NEW USB and Ethernet Control Switch Matrices

Model	# Switches (SPDT)	(dB)	VSWR (:1)	Isolation (dB)	RF P _{MAX} (W)	Price \$ (Qty. 1-9)	
RC-1SP4T-A18	1 (SP4T)	0.25	1.2	85	2	895.00	
RC-1SPDT-A18	1	0.25	1.2	85	10	485.00	
RC-2SPDT-A18	2	0.25	1.2	85	10	785.00	
RC-3SPDT-A18	3	0.25	1.2	85	10	1080.00	
RC-4SPDT-A18	4	0.25	1.2	85	10	1280.00	
RC-8SPDT-A18	8	0.25	1.2	85	10	2595.00	

^{*}The mechanical switches within each model are offered with an optional 10 year extended warranty. Agreement required. See data sheets on our website for terms and conditions. Switches protected by US patents 5,272,458; 6,650,210; 6,414,577; 7,633,361; 7,843,289; and additional patents pending.

TSee data sheet for a full list of compatible software.





Smart RF POWER METERS

from -35 up to +20 dBm 9 kHz to 8 GHz

- •True RMS model now available! Lightning-fast measurement, as quick as 10 ms*
- Compatible with most test software[†] Up to 55 dB dynamic range Measurement averaging

Don't break your bank with expensive conventional power meters. Mini-Circuits USB Power Sensors turn almost any Linux® or Windows® based computer into a low-cost testing platform for all kinds of RF components. Reference calibration is built in, and your USB port supplies required power. Our GUI offers a full range of watt or dB measurements, including averaging, frequency sweeps, and multi-sensor support.

Our power sensors can be carried in your pocket, or mounted remotely for manual or automated system monitoring (internet connectivity required). Data can be viewed on-screen or exported to Excel® spreadsheets for reporting and analytic tools. Mini-Circuits Power Sensors cost half as much as you might expect, so why do without? Place an order today, and we can have it in your hands as early as tomorrow.

All Power Sensor models include:

- Power Sensor Unit
- Power Data Analysis Software
- •SMA Adaptor (50Ω only)
- USB Cable

* Measurement speed as fast as 10 ms with PWR 8 FS. All other models as fast as 30 ms.

† See datasheets for an extensive list of compatible software. Windows and Excel are registered trademarks of Microsoft Corporation in the US and other countries. Linux is a registered trademark of Linus Torvalds. Neither Mini-Circuits nor Mini-Circuits Power Sensors are affiliated with or endorsed by the owners of the above-referenced trademarks.



Model	Frequency	Price \$ ea (Qty 1-4)
PWR-4GHS	9 kHz-4 GHz	795.00
PWR-2.5GHS-75	100 kHz-2.5 GHz	795.00
PWR-6GHS	1MHz-6 GHz	695.00
PWR-8GHS	1MHz-8 GHz	869.00
PWR-8FS	1MHz-8 GHz	969.00
NEW! PWR-4RMS	50 MHz-4 GHz	1169.00

(RoHS compliant



MEW ATC 506WLS Series Ultra-Broadband Inductors

For Coverage Through 40+ GHz

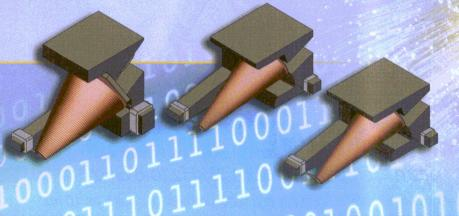
Ideal for Ultra-Broadband Decoupling Networks and Bias Tee
Applications for Optical Communication Systems using High Speed
Digital Logic

Attributes:

- Ultra-Broadband Performance
- Operating Temperature Range: -55°C to +125°C
- Ultra-Low Insertion Loss
- Lead-free, RoHS Compliant Terminations

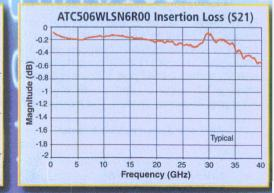
Advantages:

- Flat Frequency Response
- Excellent Return Loss Through 40 GHz
- Unit-to-Unit Performance Repeatability
- Rugged Powdered Iron Core



Series - Case Size	Inductance Range	Operating Frequency Range*	Insertion Loss typ.**	Current Handling (DC max.)***
506WLS - Case M	0.47 μH to 3.8 μH	1.1 MHz through 40+ GHz	0.5 dB	182 mA to 815 mA
506WLS - Case N	1.47 μH to 10.7 μH	1.3 MHz through 40+ GHz	0.4 dB	150 mA to 694 mA

^{*}Lower -3 dB roll-off frequency **Shunt Mounted ***Current for 100 °C temperature rise





AMERICAN

ATC North America sales@atceramics.com

TECHNICAL

ATC Europe saleseur@atceramics.com

CERAMICS

ATC Asia sales@atceramics-asia.com

ENGINEERS'
CHOICE®
ISO 9001 REGISTERED

Inside

with Noel Heiks,

Interview by JEAN-JACQUES DELISLE

JD: Nuvotronics' goals and identity have been dynamic due to the shifting landscape of grant-based work. What capabilities and technologies do you want Nuvotronics to be known for as the firm comes into its own?

NH: Nuvotronics continues to produce highly advanced 3D architectures for microwave modules and systems. We hope to be known as the ones who can fit a diplexer into that $100\times$ smaller footprint, deliver 500+ RF feed connections in one shot, or hit that performance metric again and again without tuning. We aim to be the supplier who can deliver what no one else can from DC to beyond 300 GHz.

JD: What factors have influenced Nuvotronics' move to a larger-format process?

NH: In 2013, we opened a new facility in North Carolina with an 8-in. wafer line. (We started with a 6-in. line.) This step moved us along our roadmap toward larger wafer and panel sizes. We produce phased-array front ends and other large-format modules with many RF and DC lines currently in scales from 1 to 10 cm. As long as yield remains high, a larger product is more economical because assembly complexity is reduced. In addition, we produce many devices like filters and power modules, where—although they are small form factor—they are made more cost-effective as substrate size grows.

JD: What market trends are driving the miniaturization of RF networks?

NH: Millimeter-wave technology is booming with a predicted 63% compound annual growth rate (CAGR) for the industry through 2016. As frequencies go up, miniaturization becomes a huge issue for traditional microwave-system manufacturers. Waveguide launches, transitions, combiners, and antennas all become painfully small—difficult to machine and integrate—unless you have a manufacturing technology capable of tolerances like a micron (rather than a mil).

Unmanned, man-portable, and aerospace platforms also are driving miniaturization and size, weight, and power (SWaP) across all frequencies. Say a customer needs to pack 20 W of Ka-band power into a few ounces. How are they going to achieve their requirements? An answer would be to use innovations in high-density, miniaturized RF networks and, of course, the latest gallium-nitride (GaN) and gallium-arsenide (GaAs) monolithic microwave integrated circuits (MMICs). JD: What markets are the highest consumers of miniaturized RF networks?

NH: We've seen miniaturization already in the phones we carry every day. Communications is a huge consumer of small, sophisticated RF devices. For the military alone, communications is projected to be a \$30 billion market by 2019.² This demand has driven huge volumes and vast miniatur-

News

ization in RF networks and will continue to do so in the coming years. In particular, we are looking forward to future volumes in millimeter-wave communications, where hundreds of thousands of millimeter-wave radios will be needed per year by 2018.³ JD: What benchmarks is the industry striving for in terms of size, speed, cost, yield, etc.?

NH: Cost and yield benchmarks for commercial applications are more stringent than in defense. But budget constraints in the defense sector also are pushing those targets. For some RF components, yield above 99% is expected. In contrast, more cutting-edge devices have looser constraints. (Think millimeter-wave MMIC dies and anything that uses them.) Regarding size benchmarks, we have customers that need a nearly 10× reduction in footprint, weight, or power, particularly for space applications.

JD: What is enabling miniaturized RF network technology?

NH: Competition between MMIC foundries and design firms has resulted in high-performance, multi-function ICs in dramatically reduced chip form factors. These devices are burdened by numerous RF, DC, and control interconnects in a tight pitch, where signal isolation is difficult to achieve. Novel flat antenna designs have introduced the industry to miniaturized planar beam-steering products. Yet the industry has lacked the feed and interconnect architecture to weave MMICs and planar antennas together, ideally incorporating the feeds, passives, MMIC interconnects, waveguide launches, and hundreds of isolated DC and RF lines all in a compact, low-loss footprint. Nuvotronics has developed a unique additive manufacturing technology for mixed metal-air-dielectric microfabrication to enable this 3D RF miniaturization.

JD: What new applications are being enabled by miniaturized RF networks?

NH: I mentioned millimeter-wave communications as a target application. Not only land-based, but airborne millimeter-wave SATCOM is driving miniaturization. Commercial aircraft and even unmanned drones are being targeted to carry small, lightweight terminals that will need miniaturization throughout. Look at DARPA's Mobile HotSpots program, retrofitting drones with millimeter-wave terminals to make them mobile WiFi hubs. That program is a great example of the need to miniaturize the RF antenna, front end, and power amplifier.

JD: How are miniaturized RF networks helping to advance GaN MMIC technologies in terms of thermal management? NH: Although the industry is making dramatic advances in

NH: Although the industry is making dramatic advances in GaN, the packaging of such solutions is often an afterthought, while it could mean everything in terms of performance and reliability. Taking a typical PolyStrata power module as an example, we incorporate the combining interconnects, and even filters, in a microfabricated all-metal 3D backplane. A low-loss architecture is provided via air-dielectric transmission lines. We are advancing our solutions toolbox further under a DARPA-funded program called ICECOOL. The goal of that program is to address thermal management for high-power MMIC die.



JD: How do these technologies address yield and reliability?

NH: Let's compare a traditional machined diplexer to a microfabricated component. With the machined part, you get something bulky (a traditional E-band diplexer is 100 times larger than Nuvotronics' version) that is handcrafted, assembled, and tuned. With a wafer-level fabrication technology, what you design is what you get. For higher-level integrated products, microfabrication techniques can still hit commercial-level yields on initial prototype builds without tuning or tweaking. The key parts of the product are simply made at the wafer level. As a result, thousands of parts can be cranked out at one time with micron-level precision and repeatability.

Reliability concerns in new technologies are dealt with the same way they have been in the past—with rigorous qualification testing. We work closely with our customers to develop qualification plans for their particular applications, with space applications being the most stringent. Unlike traditional microelectromechanical systems (MEMS), our structures are primarily made of metal that is often millimeters thick. So, they are quite robust, substrate-free structures. The structures we create are under our control not only electromagnetically, but also mechanically, starting early in the design phase. ^{5,6}

With any new technologies, there is going to be an initial chasm to cross. That hurdle is no different for miniaturized RF networks. However, the demand piling up in millimeter-wave, mobile, and unmanned systems drives even the most reticent of industries to embrace innovation and work with small companies like Nuvotronics. We are excited to be a part of the solution for this increasingly wireless world.

REFERENCES

- 1. "Millimeter wave gear forecast to grow at 63% CAGR; Ethernet microwave growing 5-fold by 2016," Infonetics.
- "Military Communications Market (SATCOM Terminals, Commercial off The Shelf (COTS), Military Communication Security, Tetra Radio, JTRS, Software Defined Radio, Radio Communication, Tactical Communication) – Worldwide Forecasts & Analysis (2014 - 2019)," Markets and Markets.
- 3. "Millimeter Wave Technology Market by Components (Sensors, Radio, Networking), Products (MM Scanners, MM RADARs, MM Small Cells), Applications (Communications, Aerospace, Healthcare, Automotive, Industrial) Analysis & Forecast to 2020," Markets and Markets.
- 4. "Darpa Turns Aging Surveillance Drones Into Wi-Fi Hotspots," Allen McDuffee, Wired.
- 5. "Transmission lines withstand vibration," S. Huettner, *Microwaves & RF*, March 2011.
- "Test and verification of micro coaxial line power performance," P. Ralston, K. Vanhille, A. Caba, M. Oliver, S. Raman, 2012 IEEE MTT-S International Microwave Symposium, Montreal, Canada, June 2012.

OMNIYIG DINC. CELEBRATING 41 YEARS IN BUSINESS

Omniyig's advanced products are designed into some of the world's most sophisticated systems, including commercial, EW, and ECM programs such as the ALQ-99, ALQ-117, ALR-172, ALR-56C, ALR-62, ALR-64, ALR-67, ALR-69, APR-39, WLR-8, Rapport III and we are on board the F-15, F-16, F-18, EA6B, EF111, B-1, B2 Stealth, L-130, F-35 and more.

FUNDAMENTAL YIG-TUNED OSCILLATOR

Frequency Range

2.0 to 18.5 GHz

Min. RF Power Output

RF Power Output Variation

Max. 2nd Harmonic (typ)

FM Noise @ 100 KHz Away

-120 dBc

0-10 Volt Analog or 12 Bit Digital Driver Available!



ModelFreq Rg.HarmonicRF PowerYOM3977DD2-8 GHz> 45dBc> 13dBmYOM3979DD8-18GHz> 45dBc> 13dBmOperating Temperature -54C to +85C

0-10 Volt Analog or 12 Bit Digital Driver Available!

DUAL BAND REJECT YIG FILTERS

Model Freq Rg. 40dbBW Ins Loss
MR3278DD 2-8 GHz > 45dBc < 2.0dB
MR3280DD 8-18GHz > 45dBc < 2.0dB
Operating Temperature -54C to +85C

0-10 Volt Analog or 12 Bit Digital Driver Available!

• YIG FILTERS

YIG OSCILLATORS

- YIG MULTIPLIERS
- LIMITERS
- DETECTORS
- COMB GENERATORS
- FRONT END TUNERS
- SUB SYSTEMS

Since 1973, **Omniyig** has continued technology improvement with expansions in Yig technology and new microwave products in thousands of designs developed and built for Customers Worldwide. MIL-E-5400 Class II, MIL-STD-883, in frequencies 0.5 GHz to 40.0 GHz, both Octave & Multi-Octave.

Ask Around - Omniyig Delivers.



3350 Scott Blvd., Bldg. #66 • Santa Clara, CA 95054 [t] 408.988.0843 • [f] 408.727.1373 Omniyig@ix.netcom.com • http://www.Omniyig.com Since 1973 | *Celebrating 41 Years!*



L- AND KA-BAND ANTENNAS SHARE THE SAME PATCH

Y PLAYING TO the strengths of both the L- and Ka-bands, a shared-aperture communications antenna could operate at a high data rate in good weather without completely losing its connection in inclement weather. In collaboration with Cobham Satcom, researchers from the Technical University of Denmark—Thomas Smith, Ulrich Gothelf, Oleksiy Kim, and Olav Breinbjerg—have developed a shared aperture antenna array. It leverages a cost-effective printed-circuit-board (PCB) substrate for multiband antenna operation. Using a frequency-selective surface as the groundplane of the Ka-band reflectarray structure enables a compact structure. The L-band patch antenna array sits directly behind the reflectarray.

A concentric, dual split-loop element is designed for the Ka-band reflectarray with a concentric, dual-loop ground-plane of equal trace width (0.2 mm). Adjustment of the split-loop elements

changes the reflection phase. It also can be used to adjust the center frequencies over a nearly 10-GHz range.

The Ka-band reflectarray was validated in the DTU-ESA Spherical Near-Field Antenna Test facility. It performed with receive and transmit aperture illumination efficiencies of 56% and 41%, respectively. A commercial L-band patch-array antenna was used to demonstrate the Ka-band translucence of the Ka-band reflectarray. It displayed only minor degradation of the L-band patch array's performance. The measurements for that patch array were conducted from 1500 to 1700 MHz with a varying directivity of ±0.15 dB and maximum cross polarization below ±2.5 dB.

See "An FSS-Backed 20/30 GHz Circularly Polarized Reflectarray for a Shared Aperture L- and Ka-Band Satellite Communication Antenna," *IEEE Transactions on Antennas and Propagation*, Feb. 2014, p.661.

GAN MMICS FOR SMALL CELLS GET A DOHERTY POWER BOOST

SING A 0.25-µM gallium-nitride-on-silicon-carbide (GaN-on-SiC) process, a monolithic-microwave-integrated-circuit (MMIC) power amplifier (PA) promises to meet the power, size, and cost considerations of small-cell applications. With support from the IT R&D Program of MSIP/KEIT, Republic of Korea, Cheol Ho Kim, Seunghoon Jee, Gweon-Do Jo, Kwangchun Lee, and Bumman Kim designed and tested the 2.14-GHz hybrid-Doherty PA. To achieve low part count and reasonable efficiencies in a compact package, the team used an unconventional power-splitting technique.

For the nonsymmetrical configuration, different-sized PAs were used. The peak amplifier was sized larger than the carrier amplifier for greater backoff characteristics, resulting in a higher peak-to-average power ratio (PAPR). This helped the PA achieve a higher data rate capable of supporting 4G and LTE requirements. To further reduce size, low-loss chip inductors were placed around the MMIC die. They reduced the inductor circuit footprint by a factor of 10.

Exhibiting a high drain efficiency of 52.7%, the PA provided output power to +22.2 dBm. It achieves an adjacent power leakage rate of -49.6 dBc for an LTE signal. The peak-to-average power ratio (PAPR) reached 7.1 dB after the digital-predistortion linearization. See "A 2.14-GHz GaN MMIC Doherty Power Amplifier for Small-Cell Base Stations," *IEEE Microwave and Wireless Components Letters*, April 2014, p. 263.

RF SENSORS BIODEGRADE UNDER PRESSURE

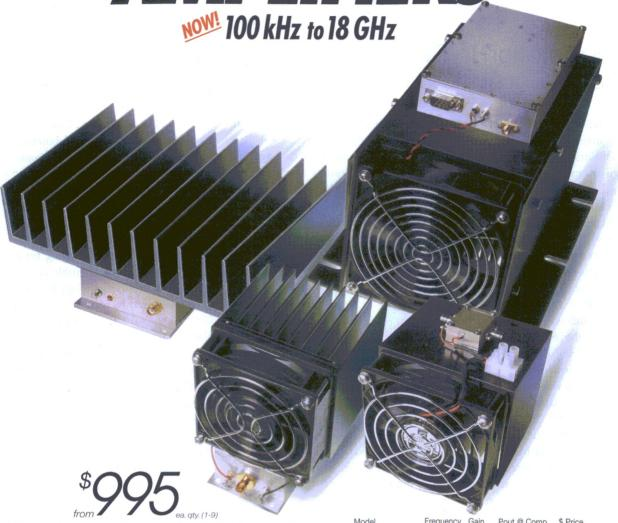
WHEN TEMPORARY WIRELESS sensors are used for medical applications, multiple surgeries are needed to install and remove the sensor. If a wholly biodegradable sensor were used, the removal surgery would become unnecessary. To save patients a costly and potentially painful second surgery, Mengdi Luo, Adam Martinez, Chao Song, Florian Herrault, and Mark Allen from the Georgia Institute of Technology explored materials to create an RF biodegradable pressure sensor.

SPolyactic acid (PLLA) and polymer liquid crystal (PLC) biodegradable plastics were used to construct the films that operate as the sensor substrate. The conductor materials for the inductor coils and capacitor plates for the sensor were formed from zinc and iron. The coils and plates were electrodeposited on the film using a standard plating bath. The metallic structures and insulating layers were deposited on a flat film that is folded to produce the multi-layer pressure sensor.

Several tests were performed to characterize the biodegradability of the components and the structure. A 0.9% saline solution was used to immerse the metallic pressure-sensor components in a heated mechanical vibration chamber. After a 300-hr. test, the iron oxides were the only remaining material that was not dissolved in the solution. In resonant-frequency testing in saline and air, a similar decline in resonant frequency to increased applied pressure is observed. There is a marked shift in resonant frequency between the air and saline environments. See "A Microfabricated Wireless RF Pressure Sensor Made Completely of Biodegradable Materials," Journal of Microelectromechanical Systems, Feb. 2014, p. 4.

UP TO 100 Watt

AMPLIFIERS



High-powered performance, across wide frequency ranges. These class A/AB linear amplifiers have set a standard throughout the RF & microwave industry. Rugged and reliable, they feature over-voltage and over-temperature protection, including the ability to withstand opens and shorts! And they're all in stock, whether with a heat sink/fan (for design labs and test benches), or without (for quick integration into customer assemblies). Go to minicircuits.com, where it's easy to select the models that meet your needs, including new features like TTL-controlled RF output. Place an order today, and you can have them in your hands as soon as tomorrow—or if you need a custom model, just give us a call for an engineer-to-engineer discussion of your requirements!

		0677			
Model	Frequency (MHz)	Gain (dB)	Pout (1dB (W)	@ Comp. 3 dB (W)	\$ Price (Qty. 1-9)
ZVE-3W-83+ ZVE-3W-183+ ZHL-5W-2G+ ZHL-5W-1 ZHL-10W-2G	2000-8000 5900-18000 800-2000 5-500 800-2000	36 35 45 44 43	2 2 5 8 10	3 3 6 11 13	1295 1295 995 995 1295
ZHL-16W-43+ZHL-20W-13+ZHL-20W-13SW+ LZY-22+ ZHL-30W-262+	1800-4000 20-1000 20-1000 0.1-200 2300-2550	45 50 50 43 50	13 13 13 16 20	16 20 20 32 32	1595 1395 1445 1495 1995
ZHL-30W-252+ LZY-2+ LZY-1+ • ZHL-50W-52	700-2500 500-1000 20-512 50-500	50 46 43 50	25 32 37 40	40 38 50 63	2995 2195 1995 1395
ZHL-100W-52ZHL-100W-GAN+ZHL-100W-13+	50-500 20-500 800-1000	50 42 50	63 79 79	79 100 100	1995 2395 2195

Listed performance data typical, see minicircuits.com for more details.

• Protected under U.S. Patent 7,348,854



Microwaves in

PAUL WHYTOCK | European Editor

Collaboration To Develop Low-Power

IP For WiGig And 4G Backhaul Apps

HENRY NURSER, CEO OF BLU WIRELESS



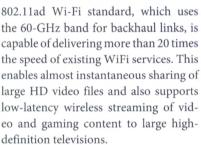
PAUL WHYTOCK

NEW PARTNERSHIP agreement between UK-based Blu Wireless Technology and Cadence

Design Systems, San Jose, Calif., aims to

advance and promote a set of design IP software for designers to develop low-power solutions for emerging 60-GHz WiGig and Fourth-Generation (4G) cellular backhaul market sectors.

Blu Wireless maintains that the 60-GHz market is being driven by consumer demand for high-definition video via smartphones, laptops, and tablets. The IEEE



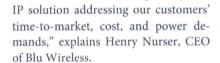
Analysts think that globally this market could have an annual value of \$5 billion (USD) by 2018. In addition to this application, 4G base station operators are also using the 60-GHz band for high-speed unlicensed wireless links between small cells that can be mounted on street furniture. The demand for these small cells is also being driven by the fast download requirements of mobile video and is forecast to be worth over \$3 billion (USD) annually by 2018.

As part of the working agreement between the two companies, CDNS will

contribute its analog/mixed-signal IP expertise while Blu Wireless will share its experience with 60-GHz band design.

"As our customers turn to 28 nm

and beyond for designs for the 60-GHz communications market, it is important for them to be confident that they can rely on robust mixed-signal and interface IP from Cadence that has been matched to our HYDRA baseband architecture (see "Behind Hydra Technology"). By working with Cadence, we will be able to provide a complete system



MILLIMETER-WAVE SOLUTIONS

Blu Wireless also has a collaboration agreement with wireless research company InterDigitalTechnology. It has successfully concluded the first phase of its work, which involved the investigation of millimeter-wave solutions for smallcell base stations and access points. A demonstration platform resulting from this work is expected to enable operators to evaluate this technology in order to cost-effectively increase 4G and Fifth-Generation (5G) cellular backhaul. The platform will also be suited to research and development exploration for 5G millimeter-wave mobile-access services. It will combine InterDigital's multi-hop backhaul technology with Blu Wireless's HYDRA baseband evaluation platform, which was developed for IEEE 802.11ad WiFi systems and has been further optimized to speed throughput in backhaul applications. mw

BEHIND HYDRA TECHNOLOGY

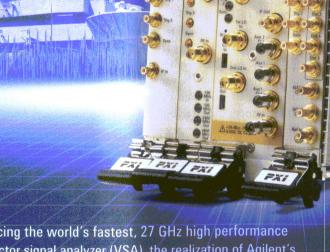
HYDRA BASEBAND TECHNOLOGY uses a heterogeneous multiprocessing architecture, mixing fixed-function digital-signal-processing (DSP) blocks with highly optimized parallel vector DSPs. This mixture provides a pool of DSP processors and fixed-function blocks that are arranged in clusters that optimize data flow. Each cluster has a heterogeneous controller that automatically and optimally utilizes these units, switching units off between executing tasks to preserve power.

The high-level software that maps onto the heterogeneous controller uses a threaded data-flow model. Software threads that define the wireless DSP pipeline are dispatched in order as a "virtual pipeline" in a series of interlocking threaded subtasks. The controller automates the threaded data flow through the heterogeneous DSP resources. These subtasks are executed on each DSP unit driven by data-flow completions that move data concurrently between them. Any arbitrary combination of dispatched virtual pipelines can be dispatched, and the real-time data flow defines the execution, timing, and order.

Agilent's Electronic Measurement Group is becoming Keysight Technologies.



Agilent M9393A PXIe performance vector signal analyzer



Introducing the world's fastest, 27 GHz high performance PXIe vector signal analyzer (VSA), the realization of Agilent's microwave measurement expertise in PXI. The M9393A integrates core signal analysis capabilities and proven measurement software with modular hardware speed and accuracy. So you can tailor your system to fit specific needs today and tomorrow. Deploy the M9393A and acquire the performance edge in PXI.

Λ	19393	A PX	le performance \	/SA

Frequency Range 9 kHz to 27 GHz

Analysis Bandwidth Up to 160 MHz

Frequency Tuning 150 µs

Amplitude Accuracy ± 0.15 dB



Scan QR code to hear directly from M9393A design engineers.

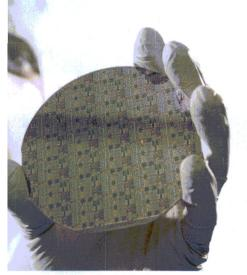
© Agilent Technologies, Inc. 2014

Download new app note on innovative techniques for noise, image and spur suppression.www.agilent.com/find/M9393APXI

u.s. 1-800-829-4444 canada 1-877-894-4414



Agilent Technologies



 GaN-based RF/microwave integrated electronics are revolutionizing the maximum frequency and power expectations of devices for military and commercial applications. (Courtesy of Raytheon)

Special Report

JEAN-JACQUES DELISLE | Technical Engineering Editor

Gan AESAs Enable New Jammer

The U.S. Navy is stepping up its electronic-warfare capability by contracting Raytheon to build the latest in stand-off jamming systems for its aircraft.

o match and even exceed the electronic-warfare (EW) capability of modern systems, the U.S. Navy has commissioned a \$279.4-million contract to enhance the jamming features of the EA-18G Growler airframe. This decision came after a realization that the stealth capability of warfighters is dramatically reduced when confronted with the latest in radar technologies. Active jamming and other advanced EW techniques are necessary to maintain air superiority in the modern battlespace.

The contract called for jamming technology that brings next-generation jamming assets to the U.S. Navy—hence the name, the next-generation jammer or NGJ. Raytheon, which was awarded the contract, will implement a highly efficient AESA-based (actively electronically steered array) jamming system with powerful and wideband gallium-nitride (GaN) technology.

The EA-18G is a variant of the F/A-18F Super Hornet Block II made by Boeing. The U.S. Navy commissioned it to replace the EA-6B Prowler aircraft. The goal of the upgrade is to present a platform for airborne electronic attacks (AEAs) that could adapt to the latest in EW requirements, which include suppression of enemy air defenses, stand-off/escort jamming, nontraditional electronic attack, self-protect/time-critical strike support, and continuous capability enhancement.

Such features rely on the ability to locate, record, replay, and jam hostile communications while tracking across an extremely broad frequency range. Maintaining the ability to communicate with allied forces while operating jamming electronics is another critical requirement.

"Stand-off jamming" implies another layer of defense separate from a self-protect system, which is only capable of individual defense or stand-in systems that only defend aircraft within a limited escort range. The stand-off system would be able to mask an entire fleet of airships from an extremely long range.

The NGJ is being designed to break the acquisition cycle of radar installations in the search or early-warning phase of detection. S-band radar installations are the threat most often considered, as they are used in most surface-to-air (SAM) missile systems and other anti-access/area denial (A2/AD) systems. "As that would be your queen on the board, you would want to protect those high-value assets. If you remove the Growlers, you remove the cover and everyone is exposed," says Andy Lowery, the NGJ chief engineer for Raytheon

WHY THE UPGRADE?

To provide these features, the current AN/ALQ-99 Tactical Jamming System (TJS) required replacement. The ALQ-99 is a ram-air, turbine-powered mid-band jamming array that uses mechanically steered technology. It comprises mostly analog technology and delivers turbine power to roughly 27 kW. The power conversion and RF-transmission electronics in the ALQ-99 were designed with older technology. As a result, it cannot use the turbine-generated power in a highly efficient manner. This limits both range and target suppression abilities.

To cover the ultra-high-frequency (UHF) to X-band range, the appropriate mechanically steered arrays require time-consuming installation. This missionization structure only allows a Growler to offer EW capability for a single narrow-frequency range. The NGJ program is designed to reinvent the methods used for jamming technology to eliminate these drawbacks.

"This particular program is completely on the other end of the spectrum. It taps into state-of-the-art technologies from tip to tail. It has a very advanced set of technologies and leverages brand new designs and developments," notes Lowry.

Several global factors are contributing to the drive to improve the jamming systems of modern warfighters. For instance, the power and sensitivity of potentially hostile radar systems

JUNE 2014 MICROWAVES & RF



CERAMIC FILTERS

LOW PASS BANDPASS HIGH PASS

NOW! Passbands Covering DC to 18 GHz

Over 200 models as small as 0.06 x 0.03"! These tiny, hermetically sealed filters utilize our advanced Low Temperature Co-fired Ceramic (LTCC) technology to offer superior thermal stability, high reliability, and very low cost. Supporting a wide range of applications with high stop band rejection and low pass band insertion loss in tiny packages, they're a perfect fit for your system requirements. Visit minicircuits.com for comprehensive data sheets, PCB layouts, free high-accuracy simulation models, and everything you need to choose the model for your needs. Order direct from our web store, and have them in your hands as soon as tomorrow!

Now available in small-quantity reels at no extra charge: Standard counts of 20, 50, 100, 200, 500, 1000 or 3000. Save time, money, and inventory space!

Wild Card Filter Kits, KWC-LHP, only \$98



- Choose any 8 LFCN or HFCN models
- Receive 5 of each model
- · A total of 40 filters for a great value
- Order your KWC-LHP Filter Kit TODAY!

OROHS compliant U.S. Patents 7,760,485 and 6,943,646

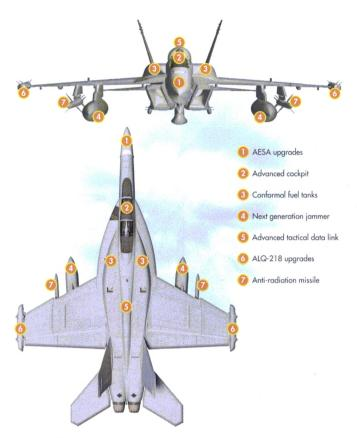
Modelithics

9 9

Free, High-Accuracy Simulation Models for ADS

www.modelithics.com/mvp/Mini-Circuits.asp





2. Many design configurations are possible with the modular mounting systems on the EA-18G platform. Additional space also is available, thanks to the move toward conformal fuel tanks on the dorsal side of the platform. (Courtesy of Raytheon)

is allowing for much longer range as a byproduct of their increased signal-to-noise ratio (SNR). Today, more countries are producing large numbers of radar installations in dense configurations. The technological sophistication of these radar systems mitigates traditional stealth technology, due to improved signal-processing techniques and jamming avoidance.

To counter these enhancements, the NGJ upgrades the jamming capability of the EA-18G with GaN power/thermal-management systems. It uses the electronic scan nature of the AESAs to contend with numerous radar systems. At the same time, it increases back-end system capability with highly sophisticated computer control along with rapid reprogrammability.

THE COMPONENTS

Physically, the NGJ is composed of two pods attached to the port and starboard modular attachments of the Growler. Each pod houses four AESAs with a full-bandwidth pair of arrays in both the front and back of each pod. One array in each pair covers the higher range. The other array covers the lower end of the threat-band frequency range. This structure eliminates the need for missionization and costly reconfiguration.

The internal computer contains processors, technique generators, and a scope of receiver capabilities. A major advancement of the

3. The goal of the NGJ program is to equip the EA-18G airframe with full 360-deg. EW wideband capability that can be adapted to best handle situations that arise. (Courtesy of Raytheon)

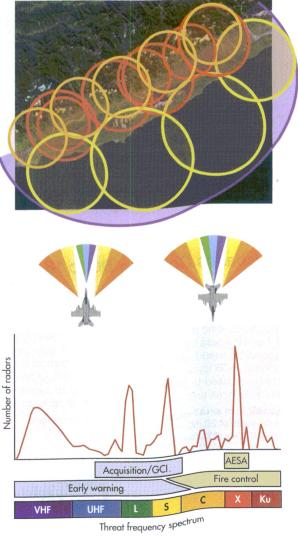
Jamming Systems

NGI is that each of the AESAs can receive and transmit through the whole range of its frequency operation. Additionally, the arbitrary NGJ signal generation offers a wide range of signals that can be transmitted through the apertures and arrays.

Polarization is another control method that the signal generators can perform. It enables the NGJ to perform smart jamming functions. In those scenarios, the NGJ can receive signals from a specified threat and respond to information gathered from those signals with counter-jamming action. Such actions do not rely on control from the EA-18G techniques generator or electronic support measures (ESMs).

The array modules include electronics that use GaN highpower amplifiers (HPAs). Those amplifiers drive the power signals through the circulators and apertures to the array elements. The AESAs can therefore form high-energy RF beams with advanced signal capability that can be steered by a highly advanced and rapidly reprogrammable computer.

"Due to the nature of it being an AESA, you can form many beams or a super beam with a lot of energy. It is agile, so you can dart from one system to another system on the ground almost instantaneously," says Lowry.



The computers driving the NGJ system also communicate with the Growler's common electronics unit (CEU), which has the enhanced ability to link with military-communications networks. In essence, this makes the NGJ system an extremely mobile, high-power, wideband, networked, and steerable long-range software-defined radio (SDR). There are many potential applications for the NGJ system, although currently the NGJ is geared specifically for jamming.

In addition, each pod is a fully selfsustaining system capable of generating its own highly efficient power, cooling, and transmission. The pods require no ship-generated power or resources other than instructions. An edge in efficiency is acquired by using a submerged ramair turbine technique that enables air power to be extracted. The articulating cores can be completely enclosed during flight, which creates an extremely streamlined pod design for lower drag.

"When they are ready for a jamming mission, it can deploy taking in air and produce an excess of three times more power from the airstream than the ALQ-99," Lowry says.

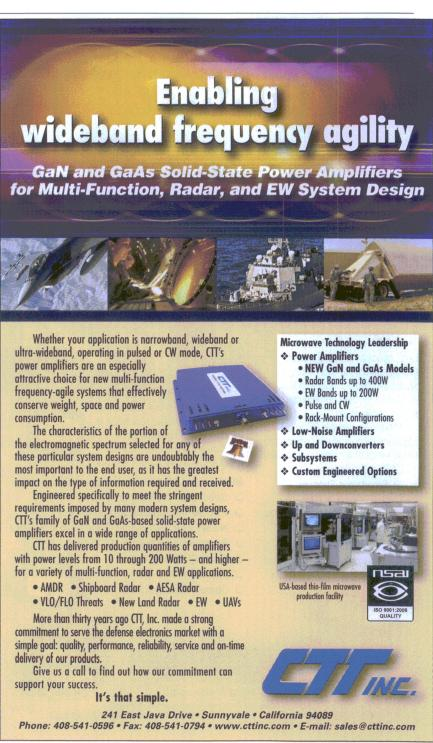
Once this air-based mechanical energy is converted to AC electrical energy, it is converted into high-voltage DC. Another conversion produces low-voltage DC power primarily for the GaN-based electronics driving the four arrays and the intelligent subsystems.

WORKING WITH GAN

Raytheon has been developing GaN technology for 15 years. In addition to delivering higher frequency, bandwidth, and power from RF devices that are defense-ready, GaN technology offers a much smaller footprint, larger wafer sizes, increased yields, and higher efficiencies. Currently, Raytheon is manufacturing its GaN circuits in its foundry in Andover, Mass. The Pentagon awarded this foundry with a manufacturing readiness level (MRL) of eight, which is the highest rating for any organization in the defense industry for that technology sector.

All of GaN technology's strengths make it a very attractive solution for

defense applications, which may have been a key factor in Raytheon winning the NGJ contract. Of course, the benefits of GaN technology don't come without critical design considerations. Working with extremely high-frequency and high-power components in a very dense space requires the dissipating of heat that is produced by its operation, preventing poor efficiencies and device failure.



GO TO MWRF.COM 43

"If you can't spread the heat, the device will burn itself out. Or you will at least have to back off the power and not use the device to its full potential," says Lowry.

The cooling system used in the NGJ is based on a singlephase system similar to a car-radiator fluid system. But it boasts far greater sophistication and more modern design. This type of thermal-management system was chosen for its robust nature. It can operate reliably across a wide range of environmental conditions.

Additionally, the design lends itself to very high heat dissipation for its size. Stock cold plates with advanced adhesives are used to sink the thermal energy from the AESA. The thermal energy is further spread throughout a larger heat-dissipation system using an ethylene-glycol and water-mixture-based liquid.

The amount of heat flux generated by the latest GaN devices in such a small area could exceed the heat flux of a nuclear explosion, making the heat-dissipating technology critically important. This is a more exaggerated problem with GaN devices compared to gallium-arsenide (GaAs) devices, due to GaN technology having power density and bandwidth capacity that is many times greater than GaAs. Research and development is still being invested in discovering the best performing adhesives and thermal spreaders.

The goal of the thermal-management system is to provide a secure fixture under extreme G-forces and excellent grounding while spreading the heat from the pinpoint generation zones of the GaN devices. Diamond thermal spreaders are of particular interest, as they have extremely high thermal conductivity. Using diamond as a semiconductor substrate for a GaN-on-diamond insulator process could solve many of the thermal stress issues that arise with GaN technology.

TESTING THE SYSTEM

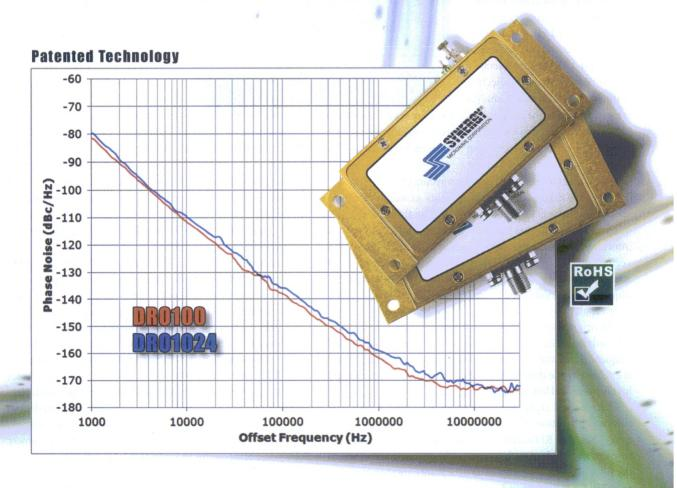
Such a sophisticated and configurable system, which will be deployed in an extreme environment, also faces a challenge in testing prior to production. Many of the subsystems can be tested in an isolated environment. When the subsystems are compiled into a larger structure, however, the nature of the system makes it a daunting testing scenario.

"When you start to multiply all of the states that a single beam can have across all of those dimensions, you end up getting a huge amount of data points. Each state would have to be calibrated and configured when making the AESA," says Lowry.

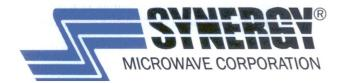


Exceptional Phase Noise Performance Dielectric Resonator Oscillator

DR0100 & DR01024
10GHz 10.24 GHz



Call Factory For Your Specific Requirement



Phone: (973) 881-8800 | Fax: (973) 881-8361

E-mail: sales@synergymwave.com Web: WWW.SYNERGYMWAVE.COM

Mail: 201 McLean Boulevard, Paterson, NJ 07504

Spectrum Analyzers: Real Time to Real Accuracy

When frequency spectrum and modulation information on unknown signals is needed, spectrum and signal analyzers are there to hunt down even spurious elements.

sis provide the test and measurement foundations for RF/microwave applications ranging from simple component test to advanced pulsed-radar techniques (Fig. 1). Spectrum analysis began in the mid-1900s with moderately performing frequency-selective voltmeters. Now, modern analyzers can measure the amplitude, phase, modulation, and even timedomain information in everything from racks inside specialized test

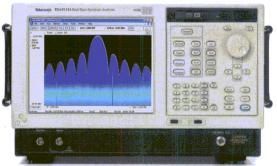
labs to handhelds in external harsh environments.

There are many deployment formats as well as types of spectrum-analysis techniques (Fig. 2). The three basic types of spectrum analyzers that can measure radiated spectral information include the swept-tuned spectrum analyzer (SA), vector signal analyzer (VSA)—or fast Fourier transform (FFT) analyzer—and real-time spectrum analyzer (RTSA). The techniques and methods used by each type of analyzer vary, as do their capabilities.

The original spectrum analyzers used a swept-tuned superheterodyne architecture that measured signal power versus frequency, and that same method is used today. This capability is enabled by the downconversion of a received signal using a highly linear and low-noise mixer.

The received signal is picked up by sweeping a very narrowband resolution filter along the analyzer's frequency-sweep range. Next, an RF/microwave power detector is used to capture the amplitude at each sequential frequency stage in which the filter is swept. The amplitude data points are then stored in memory for collection and analysis. Each amplitude data point is mapped to the displayed frequency range on the analyzer's visual interface.

Today's swept-tuned SAs are very capable of providing highdynamic-range measurements with good phase noise and lowdistortion products. "The lower-speed ADCs (analog-to-digital



1. Modern spectrum analyzers are built with high-resolution colored displays. Some can display time-based signal information in a spectral plot using color differentiation. (Courtesy of Tektronix)

converters) of a swept-tuned analyzer perform a cleaner acquisition," says Eric Brown, signal analyzer strategic planner for Agilent Technologies (www.agilent.com).

The problem is that signals that vary faster than the sweep could be inaccurately represented or completely missed in the acquisition. With swept-tuned SAs, there also is no reliable way to discover if the signals are being misrepresented or lost. Commercial and tactical applica-

tions often use impulse and rapid changing signals with digital modulation for communications and radar. More detailed information on the quality of those transmissions may be desired, which has led to the development of vector spectral measurements or signal analysis.

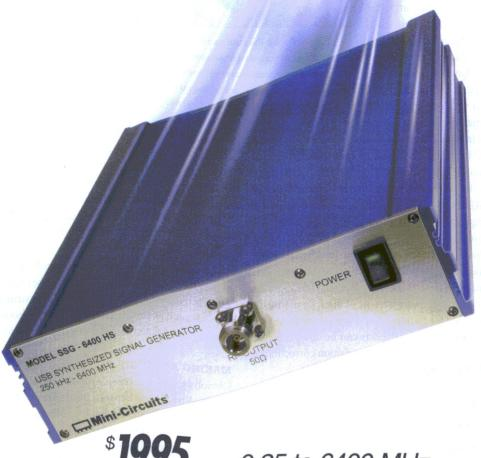
Vector signal analyzers solve some of the limitations of the swept-tuned SA by simultaneously capturing a much wider frequency window for analysis. A VSA will digitize the total RF power present within the intermediate-frequency (IF) bandwidth of the instrument's passband. This digitized information is then stored in memory, where it can be downconverted, filtered, and processed after being mapped to the frequency domain using FFT algorithms. Whereas swept-tuned SAs only detect amplitude, a VSA also captures the phase information of the frequency. This allows for more advanced processing using digital-signal-processing cores and advanced demodulation techniques.

Frequency-modulation (FM) deviation, code-domain power (CDP), and error-vector magnitude (EVM) can all be described with a VSA. Additionally, channel power, power over time, and spectrograms can be derived from the basic magnitude and phase data captured by a VSA. Some VSAs come equipped with the infrastructure for two-channel measurements.

A potential drawback of the VSA capture process is the processing and conversion time of the ADC during an acquisition. This technique leaves a "blind spot" between acquisitions,

USB & SCAL Ethernet SCATORS

To fit your budget.



Control your test setup via Ethernet or USB with a synthesized signal generator to meet your needs and fit your budget! The SSG-6400HS and the new SSG-6000RC feature both USB and Ethernet connections supporting HTTP and Telnet protocols, giving you more choices and more freedom.

Small enough to fit in your laptop case, all models provide sweep and hopping capabilities over frequencies and power levels and are designed for easy integration with other test equipment using trigger and reference ports. They even feature built-in automatic calibration scheduling based on actual usage!

Our user-friendly GUI software, DLLs, and programming instructions are all included so you can control your SSG through our software or yours! Visit minicircuits.com today to find the right model for your application!

0.25 to 6400 MHz

Models Available from Stock at Low Prices!

SSG-6400HS \$4,995

- 0.25 to 6400 MHz
- -75 to +10 dBm output Pout
- AM, PM, FM, and pulse modulation
- USB and Ethernet control

SSG-6000RC \$2,795

- 25 to 6000 MHz
- -60 to +10 dBm Pout
- Pulse modulation
- USB and Ethernet control

Pout et control

SSG-4000LH \$2,395

- 250 to 4000 MHz
- -60 to +10 dBm Pout
- Pulse modulation
- Low harmonics (-66 dBc tvp.)
- USB control

SSG-4000HP \$1,995

- 250 to 4000 MHz
- High power, -50 to +20 dBm Pout
- Pulse modulation
- USB control

Mini-Circuits®

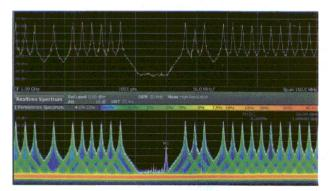
where highly transient effects may not be acquired or identifiable after digitization. To trigger on transient events effectively with a VSA, prior knowledge of the events is needed. Note that low-power signals in the same acquisition window as higher-power signals may not significantly impact a VSA trigger, even if the event is predicted, due to scaling effects. If a signal changes slightly in frequency, but not amplitude, a trigger also may neglect the signal.

One solution to these challenges is to use a series of ADCs with overlapping IF bandwidths in a staggered capture approach. The

digitized signal information could then be processed live while advanced triggering techniques could be used to achieve a positive effect. This is the basic concept behind an RTSA. In fact, this approach grants the analyzer an additional key function: discovery. "All of the ADCs are processed so fast that they overlap with the previous acquisition. This ensures that no information will be lost," says Brown.

As the amplitude, phase, and modulation domain data is captured in real time, the multi-domain data also can be represented in the time domain for time-aided analysis. Using this approach, a densely used band with many streams of digitally modulated data can be monitored for transient responses. At the same time, the quality of the digital modulations can be analyzed. This method enables amplitude and phase acquisition corrections to be applied in real time, improving detection.

Real-time spectrum analyzers can ensure proper operation of frequency-hopping devices or the tuning structure of a voltage-controlled oscillator (VCO). Both examples have potentially random or glitch behavior that would be invisible to a swept-tuned SA or VSA. Also, RTSAs can produce a time-as-temperature plot that measures the occurrence rate of dynamic signals and depicts them using a color code. In doing



3. A fast-hopping radio signal can be displayed on a real-time signal analyzer in conventional spectrum-analyzer mode (upper) with a maximum hold trace after several seconds as well as in real-time mode (lower). (Courtesy of Rohde & Schwarz)



2. To enhance the field capabilities of RF test and measurement equipment, spectrum and signal-analyzer functions are built into the latest portable and rugged models. (Courtesy of Agilent Technologies)

so, it can differentiate frequent and infrequent transients (*Fig. 3*).

Real-time signal analysis can capture a breadth of information about several signals. Yet the acquisition speed necessary to perform real-time capture and processing necessitates lower-resolution and higher-speed ADCs. The maximum frequency capture of an RTSA also is limited by the bandwidth of its ADCs, which limits the area of investigation. Although each technique has its drawbacks, certain applications could benefit from each.

Swept-tuned SAs boast the highest dynamic range and optimal linearity. As a result, they excel at integrated phase-noise measurements. These measurement advantages enable a swept-tuned SA to measure with the least distortion. Properly equipped VSAs, which can perform coherent two-channel measurements, are similar to a network-analyzer two-port structure. These cross-spectrum measurements between two channels enable precise phase measurement and time correlation of pulses.

Along with catching transients, an RTSA can capture and export real-time in-phase and quadrature (IQ) data. RTSAs also excel at measuring the dynamic and transient performance of devices, such as those that use frequency-hopping techniques or highly modulated data in a potentially spurious environment.

MAKING A CHOICE

Obviously, cost and complexity may be a concern for some SA users as they choose between the different SA options. "To start, you need to understand what type of signals you are looking for. Other factors include the skill set of the user, how many turnkey features the user will need to be efficient, and what environment the instrument will play in," Brown recommends.

Increased integration and advances in digital conversion have enabled more digital capability as well as more compact analyzers. "Modern analyzers have moved the digitization further into the block diagram, which has allowed for more software features," Brown notes. Some of these new software features include user-interface improvements, which allow for triggering on transients using two-dimensional (2D) sector triggers, multidomain correlated displays, and remote viewing and control.

The latest test and measurement equipment is highly software upgradable. And if the need arises, optional software packages for more advanced features are often available. Additionally, devices like multi-domain oscilloscopes, portable analyzers, and network analyzers frequently have spectrum/signal-analysis capability built into the machines. If not, it can be included as an optional add-on. The latest SA instruments can even use each of the various SA techniques, depending upon the measurement being performed.

Another Industry First:

20 MHz - 18 GHz Frequency Coverage in 2 small modules!





Aethercomm has developed another industry first!

We offer 20 MHz to 18 GHz of frequency coverage, with typical power levels of 40 watts CW in two small RF power amplifiers. This is 2+ decades of coverage in these modular and robust RF power amplifiers. This gives system designers flexibility in their designs and also reduces costs. The band breaks on these SSPA's are 20 MHz to 6 GHz and 6 GHz to 18 GHz. Power rolls to 20-25 watts at 20 MHz and 18 GHz. These state of the art, GaN SSPA's are in production now.

Please contact the factory with any further information or visit our website at www.aethercomm.com for more product and company capabilities.



Tel 760.208.6002
sales@aethercomm.com

SDRS Leap Ahead

Advancements in GPPs and FPGAs have merged with software-based development platforms to enable the latest in communications technology.

IN TODAY'S RAPIDLY evolving and dynamic wireless world, hardware that can adapt to a myriad of different environments is becoming more critical. From tactical communications to the common smartphone, highly configurable hardware can remove the design/development and end-user costs associated with having to upgrade system hardware for a simple feature change. Instead, a software upgrade can be instantly transmitted through the existing wireless infrastructure as soon as an upgrade becomes available.

By developing their own software, users also can implement a host of desired features without significant knowledge of the underlying hardware. Such scenarios—which would have been a dream only a few years ago—are now very much a reality, thanks to software-defined radios (SDRs) and Universal Software Radio Peripherals (USRPs; *Fig. 1*).

To create a layer of digital abstraction, SDRs leverage the power of modern general-purpose processors (GPPs) and clever reprogrammable-logic systems, such as field-programmable gate arrays (FPGAs). De-embedding the hardware from the digital plane eliminates the need to physically adjust RF/microwave components to enable behavioral feature changes, such as implementing the latest LTE standards. When an SDR operates as a USRP with virtual hardware instrumentation, it can extract and analyze information within complex RF signals.

Accurate analog-to-digital converters (ADCs), which are placed on either generic or application-specific peripherals, map RF signals to a lower frequency. The ADCs can digitize

those signals using downconversion. These signals are then converted into digital recreations of the waveforms. Processing is done using digital-signal-processing (DSP) techniques that are often implemented with the DSP cores of a FPGA.

Clearly, such flexible radio architectures could enable the same hardware to be used to implement a wide



1. Many modern SDRs have the ability to link with other SDRs for test & measurement and research & development purposes. (Courtesy of National Instruments) range of telecommunications applications. This task could be done on the fly, without the designer needing significant RF/microwave knowledge, and potentially using community-generated code. As a result, this approach easily translates into dramatically lower development and upgrade costs.

Beyond telecommunications, SDR features also offer a host of advantages. Among other benefits, for example, tactical radios could adjust their communication algorithms based upon field conditions. Test and measurement instruments can receive cost-effective,

software-licensed upgrades, which allows them to advance with the latest techniques. For their part, consumer products gain the ability to adapt to various wireless network situations for an optimum user experience. The applications that can benefit from SDR approaches are essentially infinite, given the ability to more easily generate the software backbone.

According to James Kimery, director of marketing for National Instruments, "Today, what's driving a lot of momentum with SDR technology is that the software elements are available. Software is more plentiful and there is a community where code is shared, which helps with rapid adoption." Yet the hardware to implement advanced SDR technology is still relatively expensive for certain applications. As a result, SDRs are more often used in applications in which the cost of the initial unit is offset by inexpensive upgradability and versatility. Two examples are tactical/public-safety radios and cellular base stations.

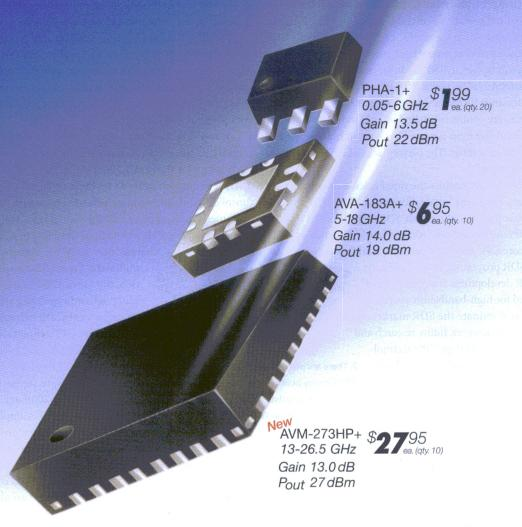
As the range of SDR applications is vast, so is the rest of the

SDR landscape—especially considering form factors, capabilities, software tools, and companies offering SDR solutions. Companies like Rohde & Schwarz offer highly rugged and flexible SDRs for mission-critical systems (*Fig. 2*). For low-cost rapid-prototyping structures, firms like Analog Devices and Peregrine make whole RF-transceiver systems-



 Many tactical radios systems are designed with SDR backbones, which are capable of rapid software upgrades and modularity. (Courtesy of Rohde & Schwarz)

50 MHz to 26.5 GHz THREE AMPLIFIERS COVER IT ALL!



Mini-Circuits' New AVM-273HP+ wideband, 13 dB gain, unconditionally stable microwave amplifier supports applications from 13 to 26.5 GHz with 0.5W power handling! Gain flatness of ± 1.0 dB and 58 dB isolation make this tiny unit an outstanding buffer amplifier in P2P radios, military EW and radar, DBS, VSAT, and more! Its integrated application circuit provides reverse voltage protection, voltage sequencing, and current stabilization, all in one tiny package!

The AVA-183A+ delivers excellent gain flatness (±1.0 dB) from 5 to 18 GHz with 38 dB isolation, and 19 dBm power handling. It is unconditionally stable and an ideal LO driver amplifier. Internal DC blocks, bias tee, and

microwave coupling capacitor simplify external circuits, minimizing your design time.

The PHA-1+ + uses E-PHEMT technology to offer ultra-high dynamic range, low noise, and excellent IP3 performance, making it ideal for LTE and TD-SCDMA. Good input and output return loss across almost 7 octaves extend its use to CATV, wireless LANs, and base station infrastructure.

We've got you covered! Visit minicircuits.com for full specs, performance curves, and free data! These models are in stock and ready to ship today!

FREE X-Parameters-Based
Non-Linear Simulation Models for ADS

Model ithics*

http://www.modelithics.com/mvp/Mini-Circuits.asp



on-a-chip (SoCs) that lend themselves to SDR implementation.

Even small hobbyist companies, such as Great Scott Gadgets and Ettus Research, are rolling out affordable SDR prototyping units that previously would have been too expensive for the hobbyist consumer. Meanwhile, companies like National Instruments and Nutaq are producing high-performance SDR modules and test/measurement equipment.

Driving this boom of SDR hardware and software development is the increased accessibility to integrated, low-power, and high-performance RF transceivers, Kimery says. "RF integrated circuits (ICs) are continually being offered in wider frequency ranges with smaller form factors. They consume less power and have a rich set of abilities. The performance of FPGAs also can't be underestimated."

Such DSP density enables the rapid calculation of complex mathematics. Given the innate property of FPGA DSP systems for parallelization, they also enable SDR configurations that use multiple FPGAs in tandem. Other technologies, such as GPU

and multicore CPU combinations, may lend themselves to SDR processing in the future. As FPGA SDR development is currently more streamlined for high-bandwidth operation, FPGAs may dominate the SDR markets for the time being. However, future research and developments could adapt GPU technology to take advantage of its parallel-processing capabilities.

3. Therefore, SDRs.

Of course, implementing DSP technologies using FPGAs invites a challenge: Software must be developed that can use

these devices' extensive capabilities. Ultimately, software performance depends upon the environment in which the software is designed. But its success also depends on the length of time that it takes for the software to be developed. To increase the ease and speed of software development for SDR applications, organizations like GNU Radio, Mathworks, and NI have developed graphically based programming languages.

This style of programming could lead to a more intuitive programming design, which enables a software system to more closely resemble the hardware that it controls. Some examples of these environments include GNURadio, Matlab/Simulink, and Labview. With a well-developed hardware and software partnership, SDR technology could be adapted to almost any telecommunications application.

Given the increased interest in smart automobile systems, for instance, the Institute for Electrical and Electronics Engineers (IEEE) has developed standards for wireless access in vehicular environments (WAVE or IEEE 802.11p). One aim of automobile manufacturers has been to eliminate the wired connectivity between the many sensors and subsystems within a vehicle. Doing so has the ability to reduce costs and service time while enabling new features and allowing user customization. SDR

technology could benefit this market, as highly integrated SDR devices could be used and flexibly configured throughout the automobile environment.

An area that is drawing attention from the industry as well as research and development groups is millimeter-wave technology. Building traditional radio architectures that are suited for millimeter-wave applications is generally costly, highly specialized, and prone to error. A millimeter-wave structure's behavior is highly influenced by its direct environment. As a result, it must change its behavior according to environmental stimulus to provide adequate performance.

Meanwhile, millimeter-wave technology is advancing very rapidly, as there is a lot of interest in using millimeter-wave technology for the next 3GPP installment of Fifth-Generation (5G) telecommunications. Yet these rapid developments and unsolidified standards make investing in current hardware for millimeter-wave applications a potential risk. A highly adapt-

changes may allow for higher-performing millimeter-wave technologies. In addition, the use of USRP components may reduce the hardware configuration risks.

able SDR with built-in flexibility to environmental

Recent advances in SDR technology include hardware offerings like GPPs integrated with an FPGA in a single device, a "cell-phone"-grade complete RF front-end module, and advances in software support for SDRs. The Xilinx Zynq-7000 series of programmable SoCs, for example, includes the ARM Core Cortex processors, a

wealth of I/O, on-chip memory, and a programmable logic center. In theory, strapping a Zynq device to an integrated RF front-end module would create a standalone and capable SDR with minimal hardware development and an already rich software environment.

Meanwhile, Peregrine's Global 1 RF front end is reported to achieve gallium-arsenide (GaAs) -level performance using silicon-on-insulator (SoI) CMOS technology. In doing so, it could potentially replace the RF front end of a cell-phone with LTE capability.

In summary, more capable DSP cores are being included with advanced programmable-logic devices. This trend elevates the importance of the software that can harness these powerful devices. At the same time, the latest RF system-integration approaches are preparing to enable radio platforms with virtually infinitely configurable hardware and a rapidly reprogrammable structure. These advances could even allow for previously untapped markets for SDRs—namely, wireless Internet and cellular—to see a revolution in flexibility. Considering the push for 5G technologies and the proliferation of the Internet of Things, SDR technology may pave the way to massive-element wireless systems.

3. There are many project—or hobbyist level—SDRs being built with sophisticated performance characteristics that can reach 6 GHz.

(Courtesy of Hacker RF)

Launch Your Ideas

talk with our engineering team today

TRM Microwave is a recognized leader in the design and manufacture of standard and custom high-reliability, passive RF and microwave components. TRM offers you:

- Proven Technology Our extensive Space and DoD heritage means less risk for your team and projects. Our full line of Directional Couplers, Power Dividers and Hybrids cover the full power spectum from milliwatts to kilowatts, in frequency ranges from DC to 40 GHz.
- Engineering Expertise We have more than 250 years of combined engineering experience and offer rapid turnaround times on your prototypes. We are experts at utilizing the best combination of ferrite, coaxial, microstrip and airstrip technology to meet your challenging size, weight and power requirements.
- Ready-To-Build Catalog Parts More than 4,000 designed parts means less NRE fees for your project. We respond to quotes in 24 hours, there is no minimum order and parts come with a five-year warranty. Delivery, stock to 6 weeks.
- Continuity of Service We are celebrating 44 years of service as an independently owned business. From sourcing of quality materials to optimized manufacturing processes and equipment, TRM is committed to delivering the best solution to our customers.

Speak with our applications engineering team today! Call us Toll-Free at 888.677.6877 or visit our web site at trmmicrowave.com.



Space Qualified Clock Divider - HF Band

High Power Coupler - 1 - 6 GHz



High Power Reactive Divider - 2 - 6 GHz



Beamformer Power Divider - X-Band







IS09001:2008 Certified

603.627.6000 280 South River Road Bedford, NH 03110 info@trmmicrowave.com trmmicrowave.com



Design Feature

ZIQIANG YANG | Associate Professor SHAOTENG CHI | Master's Degree Candidate TAO YANG | Professor
YU LIU | Associate Professor

HAO PENG, Ph.D.

School of Electronic Engineering, University of Electronic Science and Technology of China, Chengdu 611731 People's Republic of China; yangziqiang 1981@gmail.com

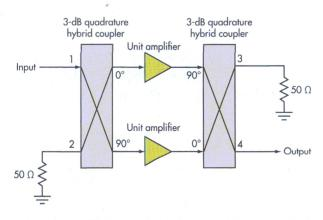
Design A Rased on a commercial pseudomorphic high-electron-mobility-transistor (pHEMT) semiconductor process, this amplifier aids applications from 30 to 36 GHz. High-Gain LNA

illimeter-wave frequencies offer great capacity for a wide variety of short-distance communications links—for systems ranging from wireless local area networks (WLANs) and collision-avoidance radars to satellite-communications (satcom) systems and radiometry systems. But to use these bands, low-noise amplifiers (LNAs) are needed for receiver front ends, and these amplifiers must provide suitable gain along with minimal noise.

Fortunately, a high-gain LNA was developed using a commercial 0.15- μ m pseudomorphic high electron-mobility transistor (pHEMT) process and a balanced topology for increased instability with the high gain. The LNA achieves more than 34-dB gain from 30 to 36 GHz, with gain flatness of better than 0.8 dB and noise figure of less than 2.6 dB. And it all comes in a chip measuring just $4.3 \times 1.9 \text{ mm}^2$.

Many high-frequency LNAs have been designed and based on gallium-arsenide (GaAs) semiconductor technology for its noteworthy high gain and low noise at millimeter-wave frequencies. A balanced configuration offers numerous benefits in performance at these frequencies, with a typical balanced amplifier configuration consisting of two identical unit amplifiers and two quadrature hybrid couplers (Fig. 1). Input signals are split into quadrature signals by a coupler and fed to the two unit amplifiers. A coupler at the output combines the outputs of the two unit amplifiers. The simple but robust architecture is designed for ease of installation in 50 Ω . high-frequency systems.

At the input of the balanced amplifier, reflected signals from the two unit amplifiers are 180° out of phase and cancel each other out. For the same reason, at the output of the balanced

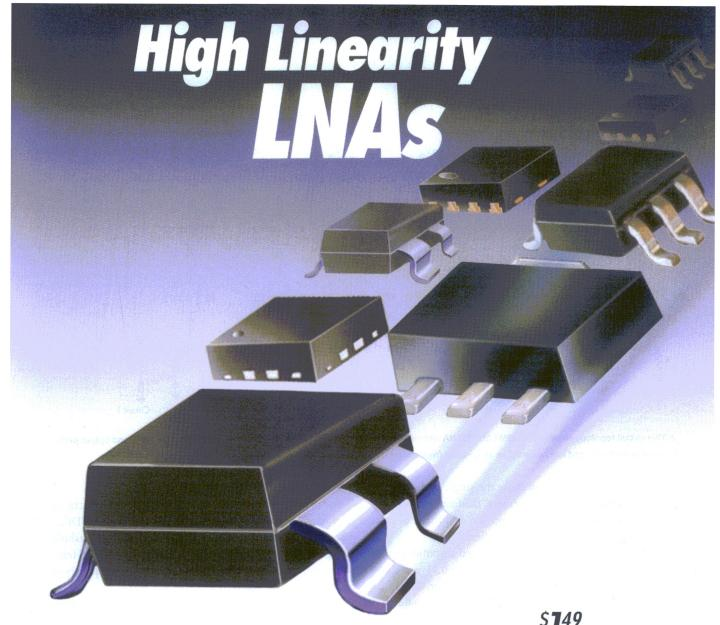


 This circuit schematic diagram represents the balanced millimeterwave amplifier, which features two identical unit amplifiers and two quadrature hybrid couplers.

amplifier, reflected signals will also be canceled, resulting in good input and output return-loss behavior for the balanced amplifier. The balanced amplifier also provides better stability compared to a single-ended amplifier.⁹⁻¹¹

In a balanced amplifier, each unit amplifier is terminated with a fixed load, which is close to 50 Ω . So the actual loads at the input and output of the balanced amplifier only minimally affect the loads of the two unit amplifiers. Instead, the single-ended amplifier is affected by actual loads.

The amplifier may be unstable in some frequency ranges, especially if the actual load is a filter. A filter behaves as a $50-\Omega$ load only in the passband. In the stopband, the filter will behave as a purely reactive load to the amplifier.



NF as low as 0.5 dB · IP3 up to 43 dBm · DC current 20 mA and up from ea.(qty. 20)

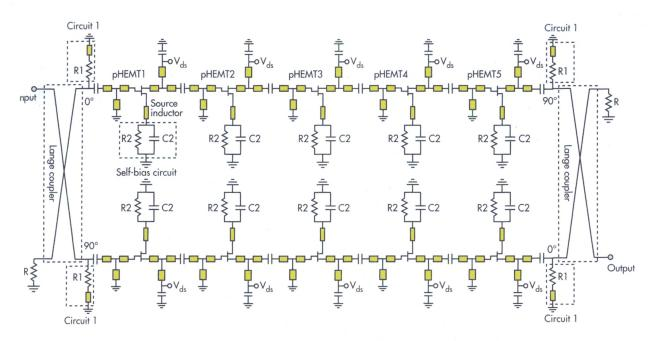
Pick your parameters, and meet your needs at Mini-Circuits! With over 20 low noise/high linearity amplifier models to choose from, you'll likely find the output power, gain, DC current, and broad bandwidths required to upgrade almost any 3-to-5V circuit—from cellular, ISM, and PMR to wireless LANs, military communications, instrumentation, satellite links, and P2P—and all at prices that preserve your bottom line!

Model	Freq. (MHz)	Gain (dB)	NF (dB)	IP3 (dBm)	P _{out} (dBm)	Current (mA)	Price \$ (qty. 20)
PMA2-162LN+ PMA-5452+	700-1600 50-6000	22.7 14.0	0.5	30 34	20 18	55 40	2.87 1.49
PSA4-5043+	50-4000	18.4	0.75	34	19	33 (3V) 58 (5V)	2.50
PMA-5455+	50-6000	14.0	0.8	33	19	40	1.49
PMA-5451+	50-6000	13.7	0.8	31	17	30	1.49
PMA2-252LN+	1500-2500	15-19	0.8	30	18	25-55 (3V) 37-80 (4V)	2.87
PMA-545G3+	700-1000	31.3	0.9	33	22	158	4.95
PMA-5454+	50-6000	13.5	0.9	28	15	20	1.49
-		All lines					

Our catalog models are in stock and ready to ship, so why wait? Go to minicircuits.com for all the details, from data sheets, performance curves, and S-parameters to material declarations, technical notes, and small-quantity reels—as few as 20 pieces, with full leaders and trailers. Place an order today, and see what these tiny, high-performance amplifiers can do for your application, as soon as tomorrow!

Model	Freq. (MHz)	Gain (dB)	NF (dB)	IP3 (dBm)	P _{out} (dBm)	Current (mA)	Price \$ (qty. 20)
PGA-103+	50-4000	11.0	0.9	43	22	60 (3V) 97 (5V)	1.99
PMA-5453+	50-6000	14.3	0.7	37	20	60	1.49
PSA-5453+	50-4000	14.7	1.0	37	19	60	1.49
PMA-5456+	50-6000	14.4	0.8	36	22	60	1.49
PMA-545+	50-6000	14.2	0.8	36	20	80	1.49
PSA-545+	50-4000	14.9	1.0	36	20	80	1.49
PMA-545G1+	400-2200	31.3	1.0	34	22	158	4.95
PMA-545G2+	1100-1600	30.4	1.0	34	22	158	4.95
PSA-5455+	50-4000	14.4	1.0	32	19	40	1.49





2. This circuit topology shows the pHEMT MMIC LNA and its use of multiple pHEMT devices and Lange couplers at the input and output ports to achieve high gain and low noise figure at Ka-band frequencies.

The purely reactive load can cause the single-ended amplifier to become unstable. Furthermore, the failure of one unit amplifier will only cause a gain drop of 6 dB instead of catastrophic failure for the balanced amplifier.

To demonstrate the use of this balanced amplifier design approach, an LNA was designed based on a 0.15-µm GaAs pHEMT process. By employing more amplifier stages, the LNA exhibits a higher gain than the previous balanced LNAs.^{1,5} The input and output return losses of the LNA are improved by using two optimized Lange couplers at the RF input and output ports, respectively, which also help maintain impedance matching across the frequency band of interest (Ka band).

With application of a self-bias technique, the LNA can be

biased from a single power supply. The LNA exhibits high gain of more than 34 dB with gain flatness within 0.8 dB, and a noise figure of less than 2.6 dB from 30 to 36 GHz. The LNA is stable at any frequency within its operating range.

Active devices for the LNA are grown on 6-in. GaAs substrates using a commercial 0.15-µm pHEMT process. The process provides GaInAs/AlGaAs pHEMT devices, using electron-beam lithography to define 0.15-µm T-gates. The lownoise pHEMTs consist of single-sided doped structures with a single recess. Connections are made by means of air

bridge or slot viahole connections.

The process achieves devices with peak transconductance $(g_{\rm m})$ of 550 ms/mm at a gate-drain voltage of -0.1 VDC, a gate-drain breakdown voltage of +9 VDC, and a threshold voltage of -0.45 VDC. The process delivers devices with transition frequency, $f_{\rm t}$, of 95 GHz, and maximum frequency of oscillation, $f_{\rm max}$, of 160 GHz.

Low input and output return loss can be achieved by means of Lange couplers at the LNA's input and output ports. Each of the LNA's unit amplifiers incorporates five common-source field-effect transistors (FETs), combining to form the balanced monolithic Ka-band amplifier shown in *Fig. 2*. The active devices are all 2 \times 40 μm . The input matching networks of the first two amplifier stages were designed for opti-

Source	Reference 5	Reference 1	This work
Topology	two-stage balanced	three-stage balanced	five-stage balanced
Technology	0.1-µm GaAs MHEMT	0.15-µm GaAs MHEMT	0.15-µm GaAs pHEM1
Frequency (GHz)	20 to 40	27.3 to 50.7	30 to 36
Gain (dB)	20	23	34
Noise figure (dB)	<2.5	3.7 (average)*	≤2.6
S ₁₁ /S ₂₂ (dB)	72-1 <u>71</u> -33	≤–13	≤-19.7
Self-bias	no	no	yes
Area (mm²)	4.3×2.0	2×2	4.3×1.9

^{*}The average equivalent noise temperature is 390.42 K.

Build a leaner DAS with our conduction-cooled flatpacks

Offering you up to 550 W average and 10 kW of peak power, Aeroflex / Weinschel's conduction-cooled, fixed attenuators and terminations are designed to fit your next Distributed Antenna System (DAS) challenge.

These ruggedized, compact,

These ruggedized, compact, low-profile components fit in the tightest spaces. Their connectors are equipped with proprietary, high-temperature, support beads and they are designed specifically for common DAS bands through 6 GHz.

- -55° C to 100° C
- Temperature Indicators
- Optional Low PIM Models
- Customization Available

These standardized,
Weinschel-quality components are available quickly
and at a great value. Visit our
website today for complete
details.

800-638-9222 / 301-846-9222 www.aeroflex.com/weinschel

AEROFLEX WEINSCHEL	422
Mana Control of the C	
	Tait II A III III III III III III III III I
Fixed Coaxial Attenuators Model Frequency Avg. Peak Avg. Power Po	Hable Swa Connector Type

Coaxial Terminations

DC to 2.5

DC to 4.0

DC to 6.0

DC to 6.0

DC to 6.0

DC to 6.0

DC to 10.0

100

50

550

250

400

100

50

10

5

10

10

10

10

59

72

253

257

258

268

284

Model	Frequency (GHz)	Avg. Power (W)	Peak Power (kW)	SWR	Connector Type Available
1441	DC to 4.0	50	5	1.20	Type N
1470	DC to 6.0	100	10	1.20	SMK (2.92mm) or N
1471	DC to 6.0	250	10	1.20	SMK (2.92mm) or N
1472	DC to 6.0	400	10	1.20	SMK (2.92mm) or N
1473	DC to 6.0	400	10	1.20	SMK (2.92mm) or N
1476	DC to 10.0	50	5	1.25 to 1.40*	SMK (2,92mm) or N

10, 20, 30, 40

3, 6, 10, 20, 30

10, 20, 30, 40

10, 20, 30, 40

10, 20, 30, 40 6, 10, 20, 30, 40

3, 6, 10, 20, 30, 40

1.15

1.20

1.10 to 1.20*

1.10

1.10 to 1.25*

1.10 to 1.15*

1.10 to 1.30*

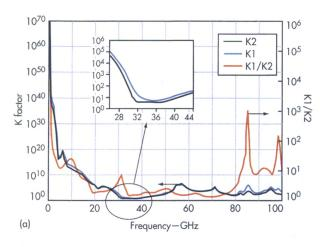
Type N

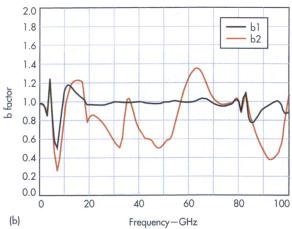
Type N

SMK (2.92mm) or N

* Varies with frequency.







3. These plots show the simulated stability factor (K) for the whole LNA and the unit amplifier: (a) for the K factor and K_1/K_2 and (b) the b factor.

mum noise match for low noise figure, while the remaining amplifier stages were conjugate-matched for increased gain. The output matching networks were conjugate-matched for high gain.

Since the input and output return losses depend on the Lange couplers, the two unit amplifiers were optimized for gain, gain flatness, and noise figure. To bias the LNA from a single power supply rail, a self-bias circuit, consisting of a bypass capacitor (C_2) and a resistor (R_2) , was used. For the best noise figure, bias voltages were selected to ensure that the amplifier operates in its low-noise region.

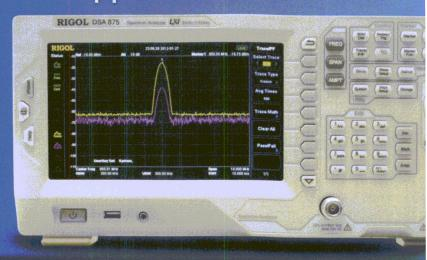
The drain-source voltage (V_{ds}) and the gate-source voltage (V_{gs}) were selected at +2 VDC and -0.19 VDC, respectively, with the aid of computer software simulations. The source

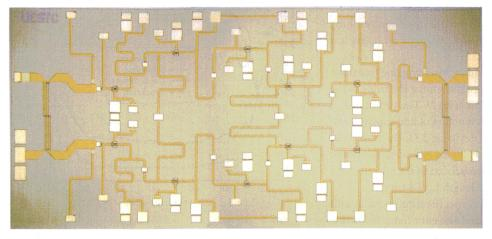
NEW DSA875

Spectrum Analyzer

Ideal for WiFi & 2.4 GHz Apps

- 100 kHz to 7.5 GHz Frequency Range
- Low Noise Floor of Typ. -136dBm DANL
- Available Tracking Generator
- EMI and VSWR Packages
- View 3rd Harmonic of 2.4 GHz Wireless Signals





 This microphotograph reveals the amplifier fabricated with the commercial pHEMT process.

The coupler was computer-simulated with the aid of a commercial, three-dimensional (3D) electromagnetic (EM) simulation program. The simulated results of the Lange coupler indicate insertion loss of better than 3.52 dB, with amplitude balance of less than 0.48 dB and

phase balance of less than 0.53 deg. from the reference 90-deg. phase difference.

For a pHEMT device, the load reflection coefficient, Γ_{opt} , is generally much different than S_{11}^* , the conjugate reflection coefficient of S_{11} . This implies that an amplifier that is designed for minimum noise figure would also be mismatched for a maximum power-transfer condition.

However, by choosing an appropriate transistor size—and using series inductive feedback circuits at the source electrode

current was selected at 12.7 mA, so that resistors (R_2) were chosen with value of 15 Ω to set a gate-source voltage (V_{gs}) of –0.19 VDC.

Lange couplers, which readily provide broadband, 90-deg. phase splits of input signals, are detailed in design and operation in refs. 12 and 13. The Lange coupler for the current amplifier was designed with four fingers for use from 29 to 37 GHz, exceeding the frequency range (30 to 36 GHz) actually required by the LNA.



of the pHEMT devices—it may be possible to achieve values of Γ_{opt} and S_{11}^{*} that are somewhat closer together, resulting in better output-power performance while still achieving low noise figure.

The source inductor is formed by inserting one transmission line, with length L_s , between the source electrode of the pHEMT and the self-bias circuit (Fig. 2). The values of Γ_{opt} and ${S_{11}}^{\star}$ are then calculated as a function of line length L_s and the gate width of the pHEMT device at 33 GHz to find the optimum values of L_s and gate width for best noise figure and output power. This analysis approach led to the selection of a gate width of 2 \times 40 μm and line length L_s of 80 μm .

Gain flatness is an important specification in radar and communication systems, ^{14,15} and the gain flatness for this LNA was targeted for performance within 0.8 dB. Gain flatness is limited by different active device characteristics, such as maximum available gain (MAG). Normally, MAG decreases linearly as frequency increases.

As a result, highpass reactive matching circuits are adopted for the input and output matching networks to compensate. The matching networks provide an upward frequency slope to compensate for the gain rolloff of the pHEMT devices, resulting in flat gain performance from 30 to 36 GHz.

LNA stability is another critical design consideration. By using a balanced topology, the stability of the LNA is better than the stability of the single-ended LNA. Due to the large gain characteristics of pHEMT devices in the lower frequency range, the LNA is more likely to have stability problems in this frequency band. Therefore, a low-loss resonator-type circuit is adopted to stabilize the LNA.

The stabilization circuit, consisting of a transmission line and a resistor (R_1) , as shown in Fig. 2 (circuit 1), has a weak resonance in the vicinity of 20 GHz. Resistor R_1 acts as a dumping resistor at around 20 GHz to reduce the gain of the LNA in this frequency band. At the same time, this circuit does not degrade the LNA's noise and gain performance levels within its target operating frequency range.

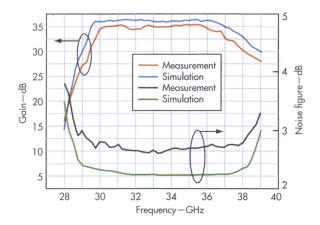
The Rollet's condition, as defined in Eqs. 1-3:16

$$K = [1 - |S_{11}|^2 - |S_{22}|^2 + |\Delta|]/2|S_{12}S_{21}| > 1 \quad (1)$$

$$b = 1 + |S_{11}|^2 |S_{22}|^2 |\Delta|^2 > 0 \quad (2)$$

$$\Delta = S_{11}S_{22} - S_{12}S_{21} \quad (3)$$

is used to check the stability of the LNA. When these two conditions are simultaneously satisfied, the LNA will be unconditionally stable. The simulated stability factor is shown in *Fig. 3*. Parameters K_1 and b_1 are stability factors for the whole LNA, while parameters K_2 and b_2 are stability factors for the unit amplifier. Parameters K_1 and K_2 are maintained above 1, while parameters b_1 and b_2 are maintained over 0 for the frequency



5. These plots show the simulated and measured noise figures and associated gains for the LNA with drain-source voltage ($V_{\rm gs}$) and gate-source voltage ($V_{\rm gs}$) of +2 VDC and -0.19 VDC, respectively.

range of 0 to 100 GHz, implying that the LNA will effectively be stable at any frequency. Meanwhile, parameter K_1 is greater than K_2 in all frequency ranges, indicating the better stability of the balanced amplifier compared to a single-ended amplifier.

The designed five-stage balanced LNA was fabricated by a commercial 0.15- μ m pHEMT semiconductor process, with a microphotograph of the chip shown in *Fig. 4*. The LNA chip measures 4.3 \times 1.9 mm. Its noise figure and S-parameters were measured at room temperature while the device was still on wafer (using commercial wafer probes and associated test equipment).

Figure 5 shows the simulated and measured noise figures and associated gains for the LNA. The gain is greater than 34 dB with 0.8-dB gain flatness from 30 to 36 GHz. The noise figure is less than 2.6 dB for the same bandwidth. The simulated and measured results are in close agreement.

Figure 6 shows the simulated and measured input and output reflection coefficients, S_{11} and S_{22} . The input and output return losses were found to be greater than 19.7 dB from 30 to 36 GHz, showing the effectiveness of the amplifier's input and output matching networks. As the *table* shows, the LNA compares well with recently reported GaAs-based balanced LNAs. 1,5

Its gain is greatly improved by the five-stage cascade structure, while its chip area was not significantly increased by its layout. It has a beneficial dual-Lange-coupler design and makes effective use of self-biasing and a single power supply, for ease of installation in a number of different applications.

ACKNOWLEDGMENT

This work was supported by the National Natural Science Foundation of China (Grant No. 61006026).

HOW POWER

5-500 WATTS PRODUCTS

POWER DIVIDERS COME

Model #	Frequency (MHz)	Insertion Loss (dB) [Typ./Max.] ◊	Amplitude Unbalance (dB) [Typ./Max.]	Phase Unbalance (Deg.) [Typ./Max.]	Isolation (dB) [Typ./Min.]	VSWR (Typ.)	Input Power (Watts) [Max.] a	Package
2-WAY								
CSBK260S	20 - 600	0.28 / 0.4	0.05 / 0.4	. 0.8 / 3.0	25 / 20	1.15:1	50	377
DSK-729S	800 - 2200	0.5 / 0.8	0.05 / 0.4	1/2	25 / 20	1.3:1	10	215
DSK-H3N	800 - 2400	0.5 / 0.8	0.25 / 0.5	1/4	23 / 18	1.5:1	30	220
P2D100800	1000 - 8000	0.6 / 1.1	0.05 / 0.2	1/2	28 / 22	1.2:1	2	329
DSK100800	1000 - 8000	0.6 / 1.1	0.05 / 0.2	1/2	28 / 22	1.2:1	20	330
DHK-H1N	1700 - 2200	0.3/0.4	0.1/0.3	1/3	20 / 18	1.3:1	100	220
P2D180900L	1800 - 9000	0.4/0.8	0.05 / 0.2	1/2	27 / 23	1.2:1	2	331
DSK180900	1800 - 9000	0.4 / 0.8	0.05 / 0.2	1/2	27 / 23	1.2:1	20	330
3-WAY								
S3D1723	1700 - 2300	0.2/0.35	0.3 / 0.6	2/3	22 / 16	1.3:1	5	316
4-WAY								
CSDK3100S	30 - 1000	0.7 / 1.1	0.05/0.2	0.3 / 2.0	28 / 20	1.15:1	5	169S
With matched oper	ating conditions					Mark Park Control of the Control	State of the State of the Late of the State	

HYBRIDS Z



Model #	Frequency (MHz)	Insertion Loss (dB) [Typ./Max.] ◊	Amplitude Unbalance (dB) [Typ./Max.]	Phase Unbalance (Deg.) [Typ./Max.]	Isolation (dB) [Typ./Min.]	VSWR (Typ.)	Input Power (Watts) [Max.]	Package
90°								
DQS-30-90	30 - 90	0.3/0.6	0.8 / 1.2	1/3	23 / 18	1.35:1	25	102SLF
DQS-3-11-10	30 - 110	0.5 / 0.8	0.6/0.9	1/3	30 / 20	1.30:1	10	102SLF
DQS-30-450	30 - 450	1.2 / 1.7	1 / 1.5	4/6	23 / 18	1.40:1	5	102SLF
DQS-118-174	118 - 174	0.3 / 0.6	0.4 / 1	1/3	23 / 18	1.35:1	25	102SLF
DQK80300	800 - 3000	0.2/0.4	0.5 / 0.8	2/5	20 / 18	1.30:1	40	113LF
MSQ80300	800 - 3000	0.2/0.4	0.5 / 0.8	2/5	20 / 18	1.30:1	40	325
DQK100800	1000 - 8000	0.8 / 1.6	1/1.6	1/4	22 / 20	1.20:1	40	326
MSQ100800	1000 - 8000	0.8 / 1.6	1/1.6	1/4	22 / 20	1.20:1	40	346
MSQ-8012	800 - 1200	0.2 / 0.3	0.2/0.4	2/3	22 / 18	1.20:1	50	226
180° (4-PORTS)	and the second second		L		1.3.		
DJS-345	30 - 450	0.75 / 1.2	0.3/0.8	2.5/4	23 / 18	1.25:1	5	301LF-1
In evenes of theore	tical coupling loss of 3	0.4P						

COUPLERS ROHS

Model #	Frequency (MHz)	Coupling (dB) [Nom]	Coupling Flatness (dB)	Mainline Loss (dB) [Typ./Max.]	Directivity (dB) [Typ./Min.]	Input Power (Watts) [Max.] •	Package
KFK-10-1200	10 - 1200	40 ±1.0	±1.5	0.4/0.5	22 / 14	150	376
KDS-30-30	30 - 512	27.5 ±0.8	±0.75	0.2 / 0.28	23 / 15	50	255 *
KBS-10-225	225 - 400	10.5 ±1.0	±0.5	0.6 / 0.7	25 / 18	50	255 *
KDS-20-225	225 - 400	20 ±1.0	±0.5	0.2/0.4	25 / 18	50	255 *
KBK-10-225N	225 - 400	10.5 ±1.0	±0.5	0.6 / 0,7	25 / 18	50	110N *
KDK-20-225N	225 - 400	20 ±1.0	±0.5	0.2 / 0.4	25 / 18	50	110N *
KEK-704H	850 - 960	30 ±0.75	±0.25	0.08 / 0.2	38/30	500	207
SCS100800-10	1000 - 8000	10.5 ±1.5	±2.0	1.2 / 1.8	8/5	25	361
KBK100800-10	1000 - 8000	10.5 ±1.5	±2.0	1.2 / 1.8	8/5	25	322
SCS100800-16	1000 - 7800	16.8 ±1.5	±2.8	0.7 / 1.0	14/5	25	321
KDK100800-16	1000 - 7800	16.8 ±1.5	±2.8	0.7 / 1.0	14/5	25	322
SCS100800-20	1000 - 7800	20.5 ±2.0	±2.0	0.45 / 0.75	12/5	25	321
KDK100800-20	1000 - 7800	20.5 ±2.0	±2.0	0.45 / 0.75	14/5	25	322
KEK-1317	13000 - 17000	30 ±1.0	±0.5	0.4 / 0.6	30 / 15	30	387
A A A A			A THE CONTRACT OF THE PARTY OF	Unless noted products of	na DaUC sameliant		

Add suffix - LF to the part number for RoHS compliant version.

Unless noted, products are RoHS compliant



Phone: (973) 881-8800 | Fax: (973) 881-8361

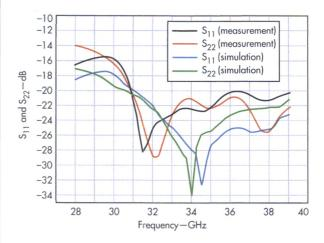
E-mail: sales@synergymwave.com Web: WWW.SYNERGYMWAVE.COM

Mail: 201 McLean Boulevard, Paterson, NJ 07504

With matched operating conditions

High Performance Modular EW Subsystems **Up and Down Converters** Low Noise RF Synthesizer IF Synthesizer Low Spurious Signal Content Modular VPX Backplane Interface Visit us at IEEE IMS • Booth 332 • Tampa, FL CRANE AEROSPACE & Microwave Solutions MERRIMAC® • SIGNAL TECHNOLOGY www.craneae.com/mw6

pHEMT Amplifier



6. These plots show the S_{11} and S_{22} performance of the LNA with V_{ds} and V_{qs} of +2 VDC and -0.19 VDC, respectively.

REFERENCES

1. S.H. Weng, W.C. Wang, H.Y. Chang, C.C. Chiong, and M.T. Chen, "A Cryogenic 30-50 GHz balanced low noise amplifier using 0.15-µm MHEMT process for radio astronomy applications," in IEEE 2012 International Symposium on RFIT, 2012, pp. 177-179.

2. D.M. Kang and H.S. Yoon, "80-110 GHz MMIC amplifiers using a 0.1-µm GaAsbased mHEMT technology," Microwave and Optical Technology Letters, Vol. 54, No. 8, 2012, pp. 1978-1982.

3. C.M. Hu, C.Y. Huang, C.H. Chu, D.C. Chang, Y.Z. Juang, J. Gong, C.F. Huang, and C.M. Chin, "A 60-GHz three-stage low noise amplifier using 0.15-µm gallium-arsenide pseudomorphic high-electron mobility transistor technology," Microwave and Optical Technology Letters, Vol. 54, No. 2, 2012, pp. 329-332.

 Y.S. Lin and S.S. Wong, "A 60-GHz low-noise amplifier for 60-GHz dual-conversion receiver," Microwave and Optical Technology Letters, Vol. 51, No. 4, 2009, pp. 885-891.

5. W.R. Deal, M. Biedenbender, P. Liu, J. Uyeda, M. Siddiqui, and R. Lai, "Design and Analysis of Broadband Dual-Gate Balanced Low-Noise Amplifiers," IEEE Journal of Solid-State Circuits, Vol. 42, No. 10, 2007, pp. 2107-2115.

 P.J. Riemer, B.R. Buhrow, J.B. Hacker, J. Bergman, B. Brar, B.K. Gilbert, and E.S. Daniel, "Low-power W-band CPWG InAs/AISb HEMT low-noise amplifier," IEEE Microwave and Wireless Components Letters, Vol. 16, No. 1, 2006, pp. 40, 42

7. J.B. Hacker, J. Bergman, G. Nagy, G. Sullivan, C. Kadow, L. Heng-Kuang, A.C. Gossard, M. Rodwell, and B. Brar, "An ultra-low power InAs/AISb HEMT Ka-band low-noise amplifier," IEEE Microwave and Wireless Components Letters, Vol. 14, No. 4, 2004, pp. 156-158.

8. B. Aja, M.L. de la Fuente, J.P. Pascual, M. Detratti, and E. Artal, "GaAs pHEMT broadband low-noise amplifier for millimeter-wave radiometer," Microwave and Optical Technology Letters, Vol. 39, No. 6, 2003, pp. 475-479.

 A.F. Osman and N.M. Noh, "Wideband LNA design for SDR radio using balanced amplifier topology," in 4th Asia Symposium on Quality Electronic Design, 2012, pp. 86-90.

10. I. Malo-Gomez, J. D. Gallego-Puyol, C. Diez-Gonzalez, I. Lopez-Fernandez, and C. Briso-Rodriguez, "Cryogenic Hybrid Coupler for Ultra-Low-Noise Radio Astronomy Balanced Amplifiers," Microwave Journal of Theory and Techniques, Vol. 57, No. 12, 2009, pp. 3239-3245.

11. Wantcominc.com, "Merits of balanced amplifier," Application Note AN-101, www.wantcominc.com/Application_Notes/AN-101.pdf.

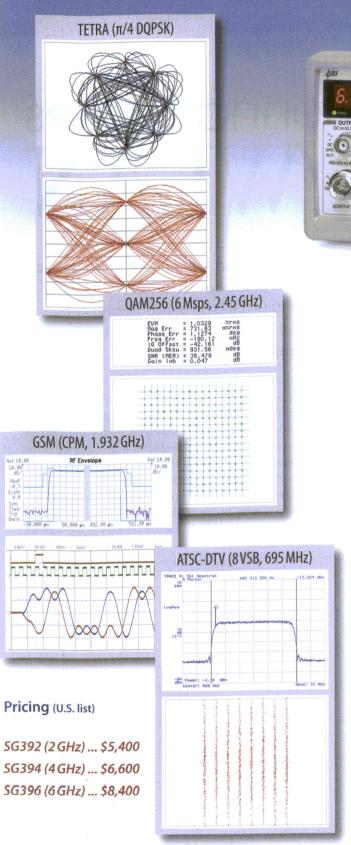
12. R.M. Osmani, "Synthesis of Lange Couplers," IEEE Transactions on Microwave Theory & Techniques, Vol. 29, No. 2, 1981, pp. 168-170.

13. W.P. Ou, "Design equations for an interdigitated directional coupler," IEEE Transactions on Microwave Theory & Techniques, Vol. 23, No. 2, 1975, pp. 253-255.

14. Y.H. Yu, Y.S. Yang, and Y.J. Chen, "A Compact Wideband CMOS Low Noise Amplifier With Gain Flatness Enhancement," IEEE Journal on Solid-State Circuits, Vol. 45. No. 3, 2010, pp. 502-509.

15. D.H. Zhang, W.R. Zhang, D.Y. Jin, H.Y. Xie, X. Zhao, B.Y. Liu, and Y.Q. Zhou, "The feedback technology for gain flatness and stability of UWB LNA," 2011 International Conference on Electric Information and Control Engineering, pp. 6260-6216. G. Gonzalez, Microwave Transistor Amplifiers: Analysis and Design, Prentice-Hall, Inc., Englewood Cliffs, NJ, 1984.

Vector Signals at the touch of a button





- 2 GHz, 4 GHz & 6 GHz models
- · Dual baseband arb generators
- Vector & analog modulation
- I/Q modulation inputs (300 MHz RF BW)
- ASK, FSK, MSK, PSK, QAM, VSB & custom I/Q
- Presets for GSM, EDGE, W-CDMA, APCO-25, DECT, NADC, PDC, ATSC-DTV & TETRA
- GPIB, RS-232 & Ethernet interfaces

The SG390 Series **Vector Signal Generators** — taking communications testing to a new level.

The SG390 series has outstanding features and performance: complete vector and analog modulation, dual baseband arb generators, I/Q inputs with 300 MHz RF bandwidth, low phase noise, and an OCXO timebase are all included.

We've also made communications testing quick and easy — everything is available from the front panel of your instrument. Pulse shaping filters, TDMA gating signals, additive white noise, and event markers are all there. Use the built-in pattern or PRBS generators to create data, or upload your own symbol data. Map your symbols to any constellation and transmit at rates up to 6 Msps — it's that simple.

Design Feature

CHANGIZ GHOBADI | Professor

MARYAM MAJIDZADEH | Engineer

Electrical Engineering Department, Urmia Branch, Islamic Azad University, Urmia, Iran; e-mail: Ch.Ghobadi@urmia.ac.ir (Changiz Ghobadi) and Maryam_Majidzadeh37@yahoo.com (Maryam Majidzadeh).

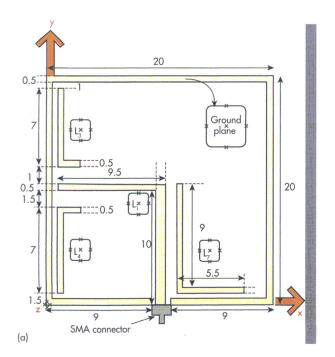
Compact Antenna Snares Will AX/WILAN

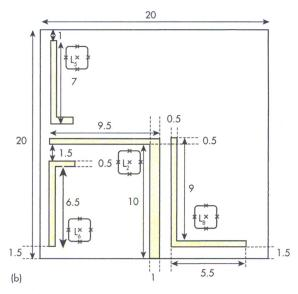
ntennas will usually form the most visible parts of a communications system. For wireless systems that are apparently everpresent—such as Worldwide Interoperability for Microwave Access (WiMAX) and wireless local area network (WLAN) systems—antennas that can cover the required bandwidths in the smallest packages possible offer great appeal for many system designers. An effective way to work with WiMAX and WLAN systems while shrinking the antennas is to use the same antenna for both systems, a dual-band antenna capable of handling both bands in one compact antenna body.

The growing demand for WiMAX and WLAN capabilities in mobile devices brings with it the need for antennas capable of handling multiple communications standards. To this end, multiband antennas have evolved into structures capable of This dual-band antenna with its compact ground plane covers the 3.1 to 3.8 GHz and 5.0 to 5.8 GHz bands in support of both WiMAX and WLAN wireless communications applications.

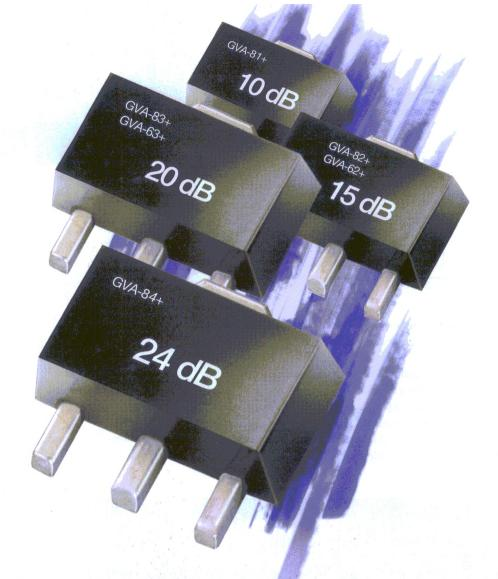
handling multiple frequency bands by means of a single antenna body, with significant reductions in both size and cost. A number of interesting multiband antennas have already been reported. Another antenna designed for WLAN and WiMAX uses a rectangular ring and an S-shaped strip on the top of the substrate, along with a crooked U-shaped strip and three straight strips located on the back layer of the design. 2

Reference 3 addresses a printed broadband asymmetric dual-loop antenna which consists of two asymmetric radiated loops and asymmetric feeding structure suitable for WiMAX





1. The configuration in (a) shows top view of the antenna structure and (b) shows bottom view of the antenna structure.



+20 dBm Power Amplifiers with a choice of gain

4MPLIFIERS

DC to 7 GHz

from **94**¢ ea. (qty. 1000)

The GVA-62+ and -63+ add gain flatness as low as ± 0.7 dB across the entire 100 MHz to 6 GHz range to our GVA lineup! The GVA series covers DC* to 7 GHz with various gain options from 10 to 24 dB and wide dynamic range to fit your application. Based on high-performance InGaP HBT technology, these patented amplifiers all provide +19 dBm or better output power

and IP3 performance as high as +41 dBm. GVA amplifiers are unconditionally stable and designed for a single 5V supply. All models are in stock for immediate delivery! Visit minicircuits.com for detailed specs, performance data, export info, free X-Parameters, low prices, and everything you need to choose your GVA today! US patent 6,943,629

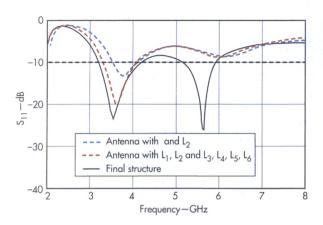
*Low frequency cut-off determined by coupling cap, except for GVA-60+, GVA-62+ and GVA-63+ low cut-off at 10 MHz.

FREE X-Parameters-Based Non-Linear Simulation Models for ADS Model ithics

http://www.modelithics.com/mvp/Mini-Circuits.asp

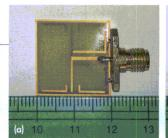


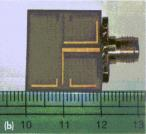
WiMAX/WLAN Antenna



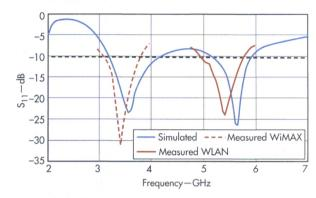
These curves show the simulated VSWR performance for the three antennas in the antenna design process.

and WLAN applications. A compact triband antenna was introduced in ref. 4, with a metallic strip etched on the back side of the substrate. In ref. 5, a partial ground and a Y-shaped radiating patch consisting of two unequal monopole arms and a modified circular monopole were combined to create a triband antenna. In ref. 6, a multiband single-feed antenna with two arms was designed for Global Positioning System (GPS), digital commu-





3. These are (a) top and (b) bottom views of the fabricated antenna.



4. The curves plot the simulated and measured S_{11} behavior of the proposed antenna.

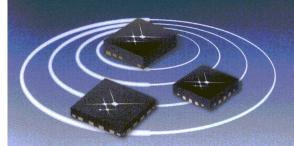
nication system (DCS), and 2.4/5.8-GHz WLAN applications. Ref. 7 reported of a dual-band antenna implemented with L- and E-shaped radiating elements to generate two resonant modes.

The current report presents a novel dual-band structure for WiMAX and WLAN use (*Fig. 1*). The same configuration was adopted for both the top and bottom substrate layers. The antenna was printed on FR-4 circuit laminate in a compact $20 \times 20 \times 1$ mm³ size. It operates over the dual frequency bands of 3.1 to 3.8 GHz for WiMAX and 5.0 to 5.8 GHz for WLAN systems.

To better understand this antenna, its design can be explained in three basic steps. In the first step, an inverted L-shaped element, denoted L_1 , is used as the feeding and radiating patch system. A parasitic element with the same configuration, marked as L_2 in $Fig.\ 1$, is located on the back side of the substrate. In the second step, four L-shaped elements designated as L_3 , L_4 , L_5 , and L_6 , are embedded in the antenna body both on the top and back layers of the substrate. In the third step, parasitic elements L_7 and L_8 are also included in the antenna structure beside the radiating patch.

Antenna performance simulations were carried out with the aid of the High Frequency Structure Simulator (HFSS) software from ANSYS (www.ansys.com),





SKYWORKS

Broadband RF and Analog Solutions

Integrated Single-Stage PIN Diode Limiter Module 0.5 to 6.0 GHz



SKY16601-555LF



- For broadband receiver protection in microwave communication applications
- Low insertion loss: 0.1 dB
- Low distortion: IIP3 = 32 dBm
- Package: MLP 2L 2.5 x 2.5 x 0.75 mm

2.4 GHz 802.15.4 / ZigBee® / Smart Energy Front-end Module



SKY66109-11



- For connected home, security, smart appliance, and smart thermostat applications
- Integrated PA with output power: up to 24 dBm
- Typical low noise figure: 2 dB
- Supply range: 2–3.6 V
- Package: MCM 20-pin 4 x 3 x 0.9 mm

650-950 MHz Broadband, High Gain and **Linearity Diversity Downconversion Mixer**





- For high dynamic range 2G/3G/4G base station receiver system
- Conversion gain: 8.1 dB
- Noise figure: 9.3 dB
- Package: QFN 36L 6 x 6 x 0.85 mm

Broadband Automotive SPDT Switch



- For in-vehicle infotainment, remote keyless entry (RKE), and telematics applications
- AEC-Q100 qualification in progress
- Typical input P_{1 dB}: 30 dBm @ 3 V
- Low insertion loss: 0.3 dB @ 0.9 GHz
- Low DC power consumption
- Package: QFN 6L 2 x 1.25 x 0.9 mm

5 GHz, 802.11n/ac Front-end Module



SKY85706-11

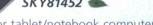


- For mobile/portable 802.11n/ac and system applications
- Integrated high performance 5 GHz PA with harmonic filter, LNA with bypass, and SPDT
- Transmit / receive gain: 30 / 11 dB
- · Output power: 18 dBm @ 3% EVM, 64 OAM 54 Mbps
- Package: QFN 16L 2.5 x 2.5 x 0.45 mm

Six-Channel, High Efficiency White LED **Driver with Touch Screen Driver Supply**



SKY81452



- For tablet/notebook computer, monitor, and other portable device applications
- Input voltage range: 2.5 to 5.5 V
- Frequency range: 600 kHz to 2 MHz
- Up to 93% efficiency
- Package: WLCSP 25-bump 2.44 x 2.44 x 0.65 mm

Skyworks' GreenTM products are compliant to all applicable materials legislation and are halogen-free. For additional information, please refer to Skyworks Definition of GreenTM, document number SQ04-0074. New products are continually being introduced at Skyworks.









WiMAX/WLAN Antenna

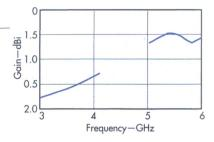
for which the S₁₁ curves were extracted and depicted in Fig. 2. The antenna with elements L₁ and L₂ operates at frequencies from 3.5 to 4.0 GHz, which does not fulfill the requirements of WiMAX applications. By including elements L₃ and L₄ on the top side and L₅ and L₆ on the back side of the substrate, a resonance is excited at 3.5 GHz, which results in frequency coverage of 3.2 to 4.0 GHz for WiMAX. By embedding elements L₇ and L₈ in the final structure, another resonance is excited at 5.5 GHz, while the second operating band at 5.2 to 5.9 GHz is created.

A prototype of the experimental antenna was fabricated and characterized to analyze its performance under real operating conditions. Figure 3 shows the fabricated antenna. The same configuration was adopted on both sides of the antenna structure. Figure 4 compares simulated and measured S₁₁ curves for the design, and the measurements confirm that the structure operates over the frequency band of 3.1 to 3.8 GHz for WiMAX and 5 to 5.8 GHz for WLAN applications.

Figure 5 displays antenna peak gain for the WiMAX and WLAN bands. Relatively stable and acceptable peak gain suitable for these communication systems was obtained for the antenna in its two operating bands. To better understand the performance of the dual-band antenna, the E- and H-plane radiation patterns were studied at 3.5 and 5.5 GHz. The omnidirectional radiation patterns obtained at those two test frequencies indicate good performance for the WiMAX and WLAN frequency bands.

To assess the performance of this dualband antenna, it was compared with three previous multiband antenna designs in terms of total size, ground-plane size, and operating frequency bands. The current design is capable of WiMAX and WLAN operation with somewhat smaller size and ground plane than the other three dualband antennas. By suitable placement of the L-shaped parasitic elements and accurate tuning of their dimensions, good performance was obtained.

The three earlier antenna designs in



5. These curves show the antenna's peak gain over the WiMAX and WLAN frequency bands.

refs. 2, 4, and 5 have ground planes of 390.6, 514.8, and 495 mm², respectively, compared to a ground plane of only 38 mm² for the new dual-band antenna design. This small ground-plane area makes this new dual-band antenna an attractive alternative for applications in which WiMAX and WLAN frequency coverage is required and antenna size must be minimized.

The new antenna delivers good performance in its bands of 3.1 to 3.8 GHz and 5.0 to 5.8 GHz for WiMAX and WLAN systems, respectively, while requiring a much smaller ground plane than competitive antenna designs. It offers numerous advantages that make it a quite reasonable choice for communications systems in need of dual-band coverage from a compact antenna structure. mw

ACKNOWLEDGMENT

This work was supported by a research grant provided from Urmia Branch, Islamic Azad University, which is gratefully acknowledged.

1. Y.S. Shin and S.O. Park, "A Compact Loop Type Antenna for Bluetooth, S-DMB, Wibro, WiMax, and WLAN Applications," IEEE Antennas & Wireless Propagation Letters, Vol. 6, 2007, pp. 320-323.

2. Y. Xu, Y.C. Jiao, and Y.C. Luan, "Compact CPW-fed Printed Monopole Antenna with Triple-Band Characteristics for WLAN/WiMAX Applications," Electronics Letters, Vol. 48, 2012, pp. 1519-1520.

3. C.M. Peng, I.F. Chen, and J.W. Yeh, "Printed Broadband Asymmetric Dual-Loop Antenna for WLAN/ WiMAX Applications," IEEE Antennas & Wireless Propagation Letters, Vol. 12, 2013, pp. 898-901.

4. M.J. Hua, P. Wang, Y. Zheng, and S.L. Yuan, "Compact Tri-Band CPW-Fed Antenna for WLAN/WiMAX Applications," Electronics Letters, Vol. 49, 2013, pp. 1118-1119.

5. T. Wu, X.W. Shi, P. Li, and H. Bai, "Tri-Band Microstrip-Fed Monopole Antenna with Dual-Polarization Characteristics for WLAN and WiMAX Applications," Electronics Letters, Vol. 49, 2013, pp.1597-1598.

6. R.K. Raj, M. Joseph, B. Paul, and P. Mohanan, "Compact Planar Multiband Antenna for GPS, DCS, 2.4/5.8 GHz WLAN Applications," Electronics Letters, Vol. 41, 2005, pp. 290-291.

7. X.L. Sun, L. Liu, S.W. Cheung, and T.I. Yuk, "Dual-Band Antenna with Compact Radiator for 2.4/5.2/5.8 GHz WLAN Applications," IEEE Transactions on Antennas and Propagation, Vol. 60, 2012, pp. 5924-5931.

DUAL DIRECT CONVERSION RECEIVER

Highly Integrated, High Performance, Modular Design Supporting Scalable MIMO Architectures



Analog, Digital & Mixed-Signal ICs, Modules, Subsystems & Instrumentation



HMC8363-DCR Complete, Intergrated, Multi-Carrier GSM Compliant Receiver Solution for 600 MHz to 4000 MHz



Typical Applications

- Multi-Carrier Multi-Standard Cellular Base Stations
- Microwave Point-to-Point
- Adaptive IF Strips
- Test Equipment
- Software Defined Radios

Features

- Arbitrarily Programmable BW: 7 MHz to 100 MHz
 - Unprecedented BW Accuracy: +/- 2.5%
- Integrated DSP
 - Real-time image rejection: > 90 dBc
 - Real-time DC-Offset Compensation
- Fractional LO with Spurious Free Performance
 - < -90 dBc/Hz Spurious
- High Performance ADCs
 - 80 dBc SFDR, 75 dBFS SNR at 500 MSPS
- 153 dB of Distributed Programmable Gain











Design Feature

OU GANG | Professor ZHANG GUO-ZHU | Associate Professor

College of Electronic Science and Engineering, National University of Defense Technology, Changsha 410073, People's Republic of China

DDS Model Tunes Doppler Simulation

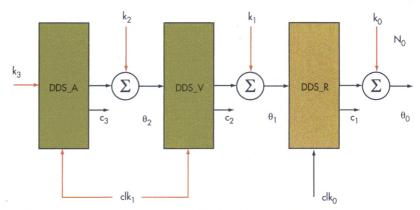
An accurate model for a third-order direct-digital synthesizer can be used for computer simulations of satellite navigation receivers under different conditions.

depends on signal simulation to evaluate a satellite navigation receiver under high-dynamic-range conditions. 1,2 A third-order

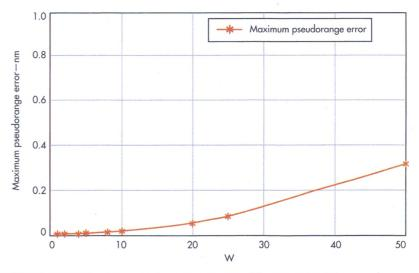
direct-digital synthesizer (DDS) is invaluable for such simulation and testing, and the accumulation clock rate for each of the three DDS stages can either be the same or different. Numerous reports have been based on the use of same-clock conditions for these multiple-stage DDS sources,^{3,4} with few studies of higher-order, hybridclock DDS sources, structured with multiple cascade accumulators with different accumulation clock rates.⁵ To better understand these hybrid-clock, third-order DDS sources, a simulation model was developed and a model was derived for its output phase behavior. Hopefully, the straightforward model can be applied to better understand the application of DDS sources in phasesensitive applications, including for use in satellite navigation receivers.

The performance and versatility of high-frequency DDS sources has been well documented in recent years for a wide range of applications in commercial, industrial, and military markeets. These are signal sources that are capable of reasonably low phase noise and overall excellent spectral purity, with oiutstanding switching speed over fairly wide frequency tuning ranges. The function of a DDS

accumulator can be expressed as a simple relationship (Eq. 1), where the output of the DDS accumulator is represented as acc(n), with n as the clock number index, n_0 as the clock number when the accumulator resets, x as the initial value,



1. This diagram represents the hybrid-clock third-order DDS model.



2. This plot shows maximum pseudoranging errors for different values of W.

and k as the accumulation step.⁴ When the DDS accumulator is implemented in a field-programmable gate array (FPGA), the output always lags behind the input by one clock cycle.

$$acc(n) = \begin{cases} x & n = n_0 \\ x + \sum_{m=n_0+1}^{n} k(m) & n > n_0 \end{cases}$$
 (1)

Figure 1 shows a third-order, hybridclock DDS model with three cascaded DDS accumulators (defined as DDS_A, DDS_V, and DDS_R, respectively). The first stage accumulator runs with a different accumulation clock rate from the other two accumulators.

Parameters k_0 through k_3 are the initial accumulation parameters of each accumulator stage; parameters θ_0 through θ_2 are the outputs of each different accumulator stage; N_0 is the word length of parameter k_0 ; and c_1 through c_3 are the bits that must be truncated when adding the accumulator output to the initial accumulator parameter. Parameters clk_0 and clk_1 are clock signals driving the first and additional accumulator stages, respectively, as represented in Eq. 2:

$$clk_0 = W \times clk_1 \tag{2}$$

In Eq. 2, the clock frequency division coefficient, $W \ge 1$, is an integer. In the case of W = 1, the DDS model degenerates into the same-clock model presented in ref. 4.

Based on the model of Fig.~1, the output of each accumulator stage can be derived when W is an unknown parameter. The output of the last stage DDS, DDS_R—supposing the number of the accumulation clock is n, Y = [n/W], where the square brackets denote rounding the contained value to an integer—results in Eq. 3:

See Eq. 3 on p. 74.

For a satellite navigation signal simulator, a simulated signal Doppler is

ANALYZING A SINGLE THIRD-ORDER DDS					
Clock frequency division coefficient W	Occupied slice	Static power consumption(mW)	Dynamic power consumption (mW)		
1	221	97	39		
10	204	95	4		



71

generated due to radial variable motion between the receiver and satellite. The relationship of parameters in the model must satisfy the conditions presented in Eq. 4.⁴:

$$p(n) = \frac{f_T}{c} \left(R + \frac{v}{f_c} n + \frac{a}{2f_c^2} n^2 + \frac{\hat{a}}{6f_c^3} n^3 \right)$$
 (4)

where:

R = the initial pseudorange amount;

v = the initial velocity;

a = the accelerated velocity;

 \hat{a} = the amount of jerk;

 f_T = the transmit signal frequency; and

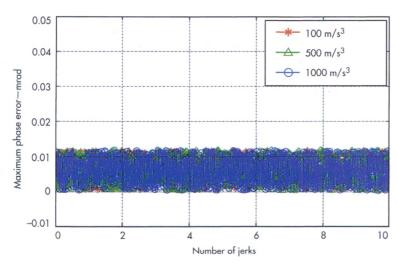
In order to obtain initial accumulation parameters k_0 through k_3), it can be presumed that the output phase of the third-order DDS satisfies Eq. 5 at n=0,W,2W...iW for $i\in Z+:$

$$p(iW) = \frac{\theta_0(iW)}{2^{N_0}}$$
 (5)

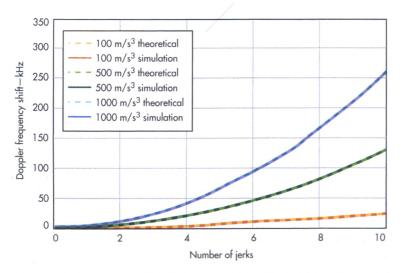
If Eq. 5 is the constraint condition, and N_0 and c_0 through c_3 are treated as known parameters, the values of k_0 through k_3 in Eq. 3 can be obtained by means of Eq. 6:

See Eq. 6 on p. 74.

 f_c = the clock rate of DDS_R.



3. These are simulation results for maximum phase errors with different amounts of jerk applied.



4. These are simulation results of Doppler frequency shifts with different jerk rates applied.

To prove that Eq. 6 satisfies Eq. 5 at any $i \in \mathbb{Z}_+$, mathematical induction can be applied. The proven steps are easily derived.

Compared with the results of ref. 4, the calculation results of the same-clock condition is the case of W = 1 in Eq. 6, and when W > 1, the hybrid-clock third-order DDS will generate a larger pseudorange error than a same-clock DDS. In case of $f_c = 100$ MHz and W \leq 50, and ignoring word-length quantization errors, the third-order DDS output pseudorange errors under the high-dynamic-range conditions represented by v = 1000 m/s; a = 1000 m/s^2 ; and $\hat{a} = 1000 \text{ m/s}^3$ will be simulated.

For a third-order DDS simulation run time of 10 ms, *Fig. 2* shows the maximum pseudorange errors that will occur for different values of the accumulator variable W. According to this simulation, as the value of parameter W increases, the maximum pseudorange error caused by the hybrid clock increases correspondingly. In the case of values of W \leq 10, the maximum pseudorange error is smaller than 10^{-10} m.

As part of an analysis, Doppler simulation errors for the hybrid-clock third-order DDS can be mainly attributed to the quantization error of the word length at each stage. Therefore, the word length of each accumulator stage must be designed accordingly, to minimize quantization errors. In Eq. 7, parameters ΔR , Δv , Δa , and $\Delta \hat{a}$ represent the resolution of the pseudorange, the velocity, the acceleration, and the jerk amount, respectively. For the case of $k_i = 1$, the corresponding parameter should be

smaller than the resolution. The word length obtained from Eq. 6 can be expressed in terms of Eq. 7:

$$\begin{cases} N_0 = \left[lb \frac{c}{f_T \Delta R} \right], \\ c_1 = \left[lb \frac{cf_c}{f_T \Delta v} \right] - N_0, \\ c_2 = \left[lb \frac{cf_c^2}{f_T \Delta aW} \right] - N_0 - c_1, \\ c_3 = \left[lb \frac{cf_c^3}{f_T \Delta \hat{a}W^2} \right] - N_0 - c_1 - c_2, \end{cases}$$

$$(7)$$

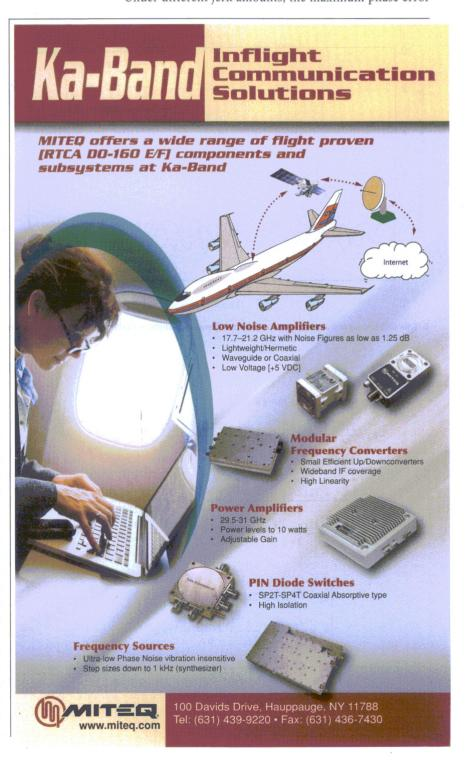
The square brackets in Eq. 7 represent rounding to an integer value. It should be evident from Eq. 7 that the lower bounds of word length parameters for all three accumulators are $N_0 + c_1$, $N_0 + c_1 + C_2$, and $N_0 + c_1 + c_2 + c_3$, respectively.

When W = 1, Eq. 7 reverts to the results for a same-clock third-order DDS. Considering the initial accumulation parameter calculation expressions, it is clear that the same-clock third-order DDS simulation model can be unified with the hybrid-clock simulation model, and the word length obtained when W > 1 is shorter than the one when W = 1.

Using a 1561.098-MHz BeiDou2 B1 carrier signal simulation as an example, 6 the reductions in word length can be analyzed while W > 1. For this example, the sampling frequency is assumed to be 100 MHz, the clock frequency division coefficient W can be 1 or 10, $\Delta R = 5$ cm, $\Delta v = 1$ mm/s, $\Delta a = 10$ mm/s², and $\Delta \hat{a} = 10$ mm/s³. The values of $N_0 = 2$ and $c_1 = 33$ do not matter whether W = 1 or 10. For $c_2 = 23$ and $c_3 = 26$ when W = 1 and $c_2 = 20$ and $c_3 = 23$ when W = 10, three bits of resolution are reduced at each DDS stage.

The model was used to simulate the performance of a hybrid-clock third-order DDS. Simulation parameters were similar to those used previously, with W = 10, and with word-length parameters of $N_0 = 6$, $c_1 = 33$, $c_2 = 20$, and $c_3 = 23$.

With an initial velocity of 0, the acceleration is 0 m/s², and the jerk rates are 100 m/s³, 500 m/s³, and 1000 m/s³, respectively. To avoid errors from a long accumulation period, caused by DDS word-length quantization, the hybrid-clock, third-order DDS is initialized every other 10 ms during simulation. Under different jerk amounts, the maximum phase error



73

GO TO MWRF.COM

at every 10-ms simulation interval is always less than 0.02 mrad (*Fig. 3*).

During this simulation, the phase sequence of the DDS_R within each simulation interval is obtained; a direct phase modeling method was adopted to estimate the Doppler frequency shift produced.⁷ The simulation results are shown in *Fig. 4* and the corresponding Doppler frequency-shift

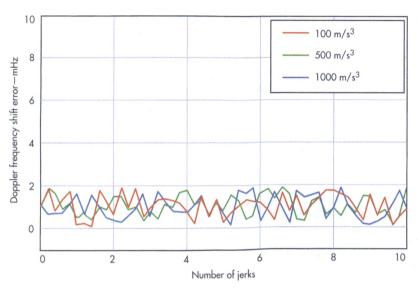
errors in *Fig. 5*. The simulation results are compared to the theoretical values (the dashed lines) and how they line up for different jerk rates, and with data sampling intervals in both figures increased to 200 ms. The jerk rates in both cases are presented as the number of jerks per second, from 0 to 10, with the higher jerk rates resulting in more significant Doppler frequency shifts. This span of jerk rates allows designers to

gauge expected performance for an FPGA in a DDS application when subjected to different conditions.

As Fig. 5 shows, even under different jerk rates, the hybrid-clock third-order DDS can maintain high Doppler simulation accuracy, and the Doppler frequency shift error is always less than 2 mHz. The table compares resource and power consumption results of the latter two accumulators for cases of W = 1 and W = 10, detailing the differences in static power consumption and dynamic power consumption for these two values of W.

To compare the simulation results to an actual unit, the FPGA used for analysis in the table was a model XC6SLX150 from Xilinx (www.xilinx.com), and the power consumption analysis was produced with the aid of an XPower Analyzer from Xilinx. For W = 10, the accumulation clock rate of the last two DDS accumulator stages is reduced to 1/W of the same-clock condition, which results in a dynamic power consumption reduction of approximately 1/W.

The XC6SLX150 FPGA is a member of the firm's Spartan-6 family of products, with each FPGA in the product line incorporating as many as six clock management tiles (CMTs), with each CMT consisting of two digital clock managers (DCMs) and one phase-locked loop (PLL), which can be used individually or cascaded. The model XC6SLX150 FPGA features 147,443 logic cells and more than 23,000 configurable logic slices. The integrated device makes use of more



5. This plot shows simulation errors of Doppler frequency shifts with different jerk rates applied.

$$\theta_{0}(n) = k_{0} + \sum_{j=1}^{n} \theta_{1}(j-1)/2^{c_{1}}$$

$$= k_{0} + \left[W\sum_{i=1}^{y} \theta_{1}(j-1) + (n-YW)\theta_{1}(Y)\right]/2^{c_{1}}$$

$$= k_{0} + \frac{YWk_{1}}{2^{c_{1}}} + \frac{k_{2}W(Y^{2}-Y)}{2 \times 2^{c_{1}+c_{2}}} + \frac{Wk_{3}(Y^{3}-3Y^{2}+2Y)}{6 \times 2^{c_{1}+c_{2}+c_{3}}}$$

$$+ \frac{(n-YW)k_{1}}{2^{c_{1}}} + \frac{(n-YW)Yk_{2}}{2 \times 2^{c_{1}+c_{2}}} + \frac{(n-YW)k_{3}(Y^{2}-Y)}{2 \times 2^{c_{1}+c_{2}+c_{3}}}$$

$$= k_{0} + \frac{nk_{1}}{2^{c_{1}}} + \frac{k_{2}(2Yn-WY-Y^{2}W)}{2 \times 2^{c_{1}+c_{2}}} + \frac{k_{3}W(Y^{3}-3Y^{2}+2Y) + k_{3}3(n-YW)(Y^{2}-Y)}{6 \times 2^{c_{1}+c_{2}+c_{3}}}$$

$$= k_{0} + \frac{nk_{1}}{2^{c_{1}}} + \frac{k_{2}(2Yn-WY-Y^{2}W)}{2 \times 2^{c_{1}+c_{2}}} + \frac{k_{3}(3nY^{2}-2Y^{3}W-3nY+2WY)}{6 \times 2^{c_{1}+c_{2}+c_{3}}}$$

$$(n \ge 0)$$

$$\begin{cases} k_{0} = \frac{f_{T}}{c}R \times 2^{N_{0}} \\ k_{1} = \frac{f_{T}}{c}\left(\frac{V}{f_{c}} + \frac{a}{2f_{c}^{2}}W + \frac{\hat{a}}{6f_{c}^{3}}W^{2}\right) \times 2^{N_{0}+c_{1}+c_{2}} \\ k_{3} = \frac{f_{T}\hat{a}}{cf_{c}^{3}}W^{2} \times 2^{N_{0}+c_{1}+c_{2}+c_{3}} \end{cases}$$

$$(6)$$

than 184,000 flip-flops and 1355 kb maximum distributed random access memory (RAM) to provide its performance with relatively low static power consumption and low dynamic power consumption. It was considered a good subject for investigation with the model, since it offers performance and capabilities that can be used across a wide range of DDS

applications, and would represent a good "typical" FPGA for modeling purposes.

This hybrid-clock third-order DDS model developed here is fairly straightforward and can be used under both same-clock and hybrid-clock DDS conditions, and can be used to predict the amount of power consumption under static as well as dynamic conditions. The simulation results for the BeiDou2 B1 carrier signal show that the signal Doppler simulation method achieves precision of 2 mHz. Compared with the same-clock condition, the third-order DDS under hybrid-clock conditions operates with less resource requirements and power consumption. The model offers an effective method for projecting the amount of power that will be required by a given FPGA product when employed as part of a DDS system. This simulation approach provides a means of precisely simulating Doppler signals, and is particularly useful for modeling portable high-dynamic-range satellite navigation equipment. mw

Editor's Note: For an expanded version of this article, including a full listing of equations, visit www.mwrf.com/systems/dds-model-tunes-doppler-simulation.

REFERENCES

1. D.U. Lee, W. Luk, and J.D. Villasenor, "A Gaussian noise generator for hardware-based simulations," IEEE Journal of Transactions on Computers, 2004, Vol. 53, No. 12, 2004, pp. 1523-1534.

 A. Brown and N. Gerein, "Modeling and simulation of GPS using software signal generation and digital signal reconstruction," Proceedings of the ION National Technical Meeting, 2000, pp. 646-652.

3. Bo Zhang, Guangbin Liu, and Wei Jiao, "Highorder DDFS Applied in Simulated High-dynamic GNSS signal synthesis," Proceeding of the 9th International Conference on Electronic Measurement and Instruments, Beijing, China, IEEE Computer Society, 2009, pp. 4102-4106.

4. Yuanyuan Song, Hui Zhou, Tao Zeng, and Lei Zhang," Algorithm and Realization of High Dynamic Satellite Signal Doppler Simulation Based on FPGA,"

Proceedings of the ION National Technical Meeting, 2010, pp. 1044-1050.

5. Xuejuan Zhou and Liqiao Dong, "A New Method for High-Precision Dynamic Clock in Navigation Simulator," Journal of Radio Engineering, Vol. 41, No. 11, 2011, pp. 37-39.

6. "BeiDou Navigaiton Satellite System Signal In Space Interface Control Doucment" China Satellite Navigation Office, 2012.

7. Mingjian Chen, Chunsheng Liu, and Xiu Wang, "Application of Phase Modeling Method and Smooth Phase Difference Method to Instantaneous Frequency Estimation," Shipboard Electronic Countermeasures, Vol. 31, No. 12, 2008, pp. 73-77.



Design Feature

YONG FANG | Researcher HAI ZHANG | Researcher

TIGUO GAN | Researcher

National Key Laboratory of Science and Technology on Vacuum Electronics,

of China, Chengdu (610054), People's Republic of China (PRC)

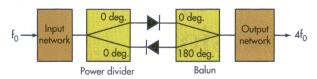
School of Physical Electronics, University of Electronic Science and Technology

YE YUAN | Researcher

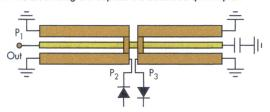
School of Electronic Engineering, University of Electronic Science and Technology of China, Chengdu (610054), People's Republic of China; e-mail: tiguogan@yahoo.com

Quadrupler Cuts Losses At W-Band

A unique design approach aids in the fabrication of a W-band quadrupler with low conversion loss that is capable of as much as +2 dBm output power from 80 to 100 GHz.



1. The block diagram depicts the balanced quadrupler.



2. This diagram shows the simple design of the CSDBQ structure.

chottky diode quadruplers provide practical means of generating signals at higher frequencies, especially when they can perform such functions with minimal conversion loss (CL). Lower loss generally means higher power levels at the output of the quadrupler and, fortunately, with the aid of a commercial computer-aided-engineering (CAE) software program, it has been possible to design a Schottky diode multiplier with low CL for applications requiring signals from 80 to 100 GHz. This monolithic frequency multiplier was fabricated with a 0.1-µm GaAs pseudomorphic-high-electron-mobility-transistor (pHEMT) process and provides as much as +2 dBm output power across its 20-GHz output bandwidth.

Due to their nonlinear characteristics, Schottky diodes are often the key elements in passive frequency multipliers. They are capable of producing stable, low-noise multiplied output signals when combined with an appropriate oscillator. Unfortunately, as the frequency increases, the dielectric circuit losses and roughness of the conductor surface can result in

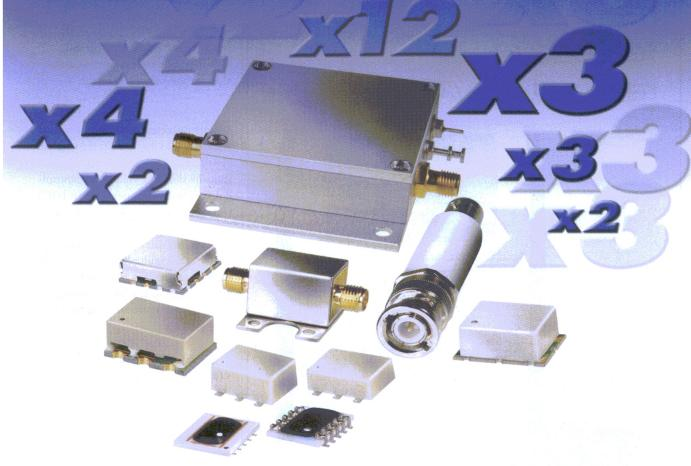
increases in the CL of a Schottky diode multiplier. As a result, one of the design goals when working with these components involves minimizing the CL.

A number of researchers have explored different approaches to passive multiplier designs, ²⁻⁴ with the importance of impedance matching for the source and load impedances of the Schottky diodes detailed in ref. 2, although an impedance-matching method or solution was not provided. A W-band frequency doubler was presented in ref. 3, with a quarter-wavelength short stub (at the fundamental frequency) used to provide a short circuit for the second-harmonic frequency at the input of the diode, and a quarter-wavelength open stub (at the fundamental frequency) used to short the fundamental frequency at the output of the diode.

This study did not present the effects of these stubs on CL performance, however. A similar design approach was presented in ref. 4.

Work in ref. 5 detailed a method for optimizing the input and output impedances to a high-gain active frequency multiplier with reflector networks. A similar approach was used in ref. 6 to optimize a frequency tripler. A W-band active frequency doubler was designed and fabricated with a 0.15-µm InGaAs/InAlAs/GaAs mHEMT process in ref. 7. These reports offered several different approaches for designing high-frequency multipliers, but with little description of CL optimization methods for the passive balanced multipliers. The present report examines the importance of impedance matching for the input and output multiplier ports, using input and output reflector networks to not only impedancematch to the impedances of the diodes, but to reduce the CL of the balanced multiplier.

One method of reducing the CL of a diode multiplier is to focus on the Schottky diode and its supporting circuitry. This can be done by examining the construction of a Schottky diode quadrupler, the design of the component's balun, opti-



Frequency Multipliers from 595 gty. 10-49

For your leading-edge synthesizers, local oscillators, and Satellite up/down converters, Mini-Circuits offers a large selection of broadband doublers, triplers, quadruplers, and x12 frequency multipliers.

Now generate output frequencies from 100 kHz to 20 GHz with excellent suppression of fundamental frequency and undesired harmonics, as well as spurious. All featuring low conversion loss and designed into a wide array of, off-the-shelf, rugged coaxial, and surface mount packages to meet your requirements.

Visit our website to choose and view comprehensive performance curves, data sheets, pcb layouts, and environmental specifications. And you can even order direct from our web store and have a unit in your hands as early as tomorrow!



mization of the input power network and the input/output reflector networks, optimization of the full quadrupler, and fabricating and testing the quadrupler to check how the modeled results compare with actual performance.

Figure 1 offers a block diagram of a generic balanced multiplier, with an antiparallel diode-pair structure used with a balanced-mixerconfiguration. In this configuration, only even-

harmonic frequencies are available at the output, with inherent rejection fundamental-frequency and odd-harmonic signals at the output.

As Eq. 1 shows, the nonlinear Schottky diode current-voltage (I-V) curves are closely related to the input signal amplitude. The input power can be optimized to obtain minimum CL from the multiplier by analysis of Eq. 1:



$$I = I_0[\exp(V_A/V_T) - 1]$$
 (1)

where:

 I_0 = the reverse saturation current; V_A = the diode external voltage; and V_T = the thermopower voltage;

Equations 2 and 3 show that the signals reflected by different reflector networks have different phase characteristics. Short-circuit (SC) transmission-line voltage is a sinusoidal function, but open-circuit (OC) transmission-line voltage is a cosine function. Changing the type of transmission line can optimize the performance of the multiplier. The voltage of an SC transmission line can be found by studying Eq. 2, while the voltage of an OC transmission line can be calculated by Eq. 3:

$$V(d) = 2jV^{+}sin(\beta d) \quad (2)$$

$$V(d) = 2V^{+}cos(\beta d) \quad (3)$$

where:

 V^+ = the voltage amplitude of the electromagnetic (EM) wave propagating along the positive direction;

 β = the phase constant of the transmission line; and

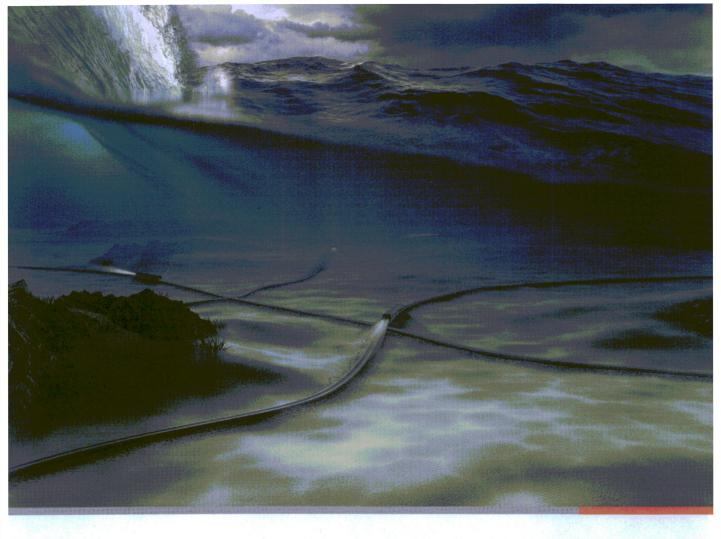
d = the length of the transmission line.

As a result, it is necessary to optimize the input-power network and the input/output reflection networks to minimize the CL of a high-frequency multiplier design.

A Marchand balun is often part of the design of balanced multipliers, mixers, and amplifiers. The balun can be designed in a number of different ways,

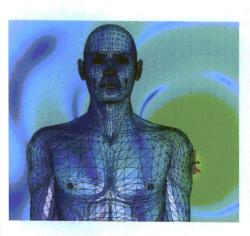
www.lpkfusa.com/pls • 1-800-345-LPKF

Laser & Electronics



Make the Connection

Find the simple way through complex EM systems with CST STUDIO SUITE



Components don't exist in electromagnetic isolation. They influence their neighbors' performance. They are affected by the enclosure or structure around them. They are susceptible to outside influences. With System Assembly and Modeling, CST STUDIO SUITE helps optimize component and system performance.

Involved in antenna development? You can read about how CST technology is used to simulate antenna performance at www.cst.com/antenna.

If you're more interested in filters, couplers, planar and multilayer structures, we've a wide variety of worked application examples live on our website at www.cst.com/apps.

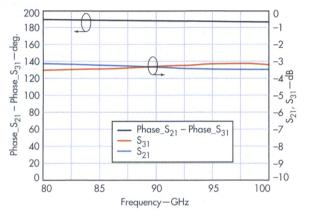
Get the big picture of what's really going on. Ensure your product and components perform in the toughest of environments.

Choose CST STUDIO SUITE –
Complete Technology for 3D EM.



with multiple planar balun structures proposed in ref. 9. The balun shown in *Fig.* 2 offers a similar design. From a study of *Fig.* 3, it is possible to learn that (a) the phase difference (P2 minus P3) is 185 to 190 deg. between 80 to 100 GHz and (b) the insertion loss (from P2 to P1 and from P3 to P1) is less than 3.6 dB from 80 to 100 GHz.

The input-power network and the input/output reflector networks can be optimized with the assistance of computer



3. The simulated phase and insertion loss for the balun are plotted versus frequency.

analysis using the Advanced Design System (ADS) software from Agilent Technologies (www.agilent.com) and load-pull technology for analysis. It is well known that the output port of a balanced frequency multiplier will only contain even-harmonic signals and, according to the nonlinear characteristics of the multiplier, the impact of CL is weak on the higher multiplied harmonic signals. So, analysis at the input port of the multiplier can focus on the input power, the fundamental-frequency signals, and the second- and fourth-harmonic signal impedance at the multiplier's input port. In addition, the second-, fourth-, and sixth-harmonic impedances at the output port of the multiplier should also be studied. The input and output reflector networks for the multiplier include SCs, OCs, and matching circuits (MCs).

Table 1 provides data for analysis of CL performance for different networks, with a number of conclusions possible by examining the table. For one thing, a change of CL impacted by the second- or fourth-harmonic reflector networks at the input port is about 0.1 dB, and this can be ignored. The appropriate input fundamental-frequency power reduces the VCL

For all graphics related to this article, visit www.mwrf.com, click on the Current Issue icon and the headline for this article.



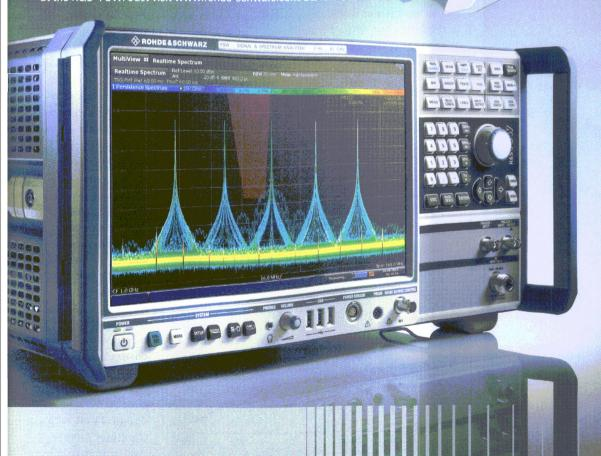
Why guess when you can know for sure?

The R&S®FSW signal and spectrum analyzer provides the insights you need Almost nothing happens in the frequency range up to 67 GHz that the R&S®FSW signal and spectrum analyzer won't tell you. Its unrivaled RF performance and analysis capabilities truly represent the high end of today's technology.

Now up to 67 GHz and 500 MHz BW

- Measure radar pulses and frequency-hopping or chirp signals automatically with a bandwidth of up to 500 MHz
- Analyze in realtime with 160 MHz bandwidth and 585 938 FFT/s to obtain 100% POI for signals as short as 1.87 μs
- I See pulses, spurious signals and modulation at the same time with MultiView
- ${\bf I} \ \ {\bf Detect\ all\ spurious\ signals\ up\ to\ 67\ GHz\ thanks\ to\ internal\ preamplifier}$
- Uncover details close to the carrier due to extremely low phase noise of –137 dBc/Hz at 1 GHz and 10 kHz offset

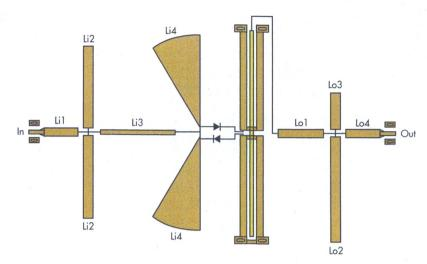
You'll be sure to find the key feature you need when you take a closer look at the R&S®FSW. Just visit www.rohde-schwarz.com/ad/fsw-ad.





BL Microwave Ltd. Discover the quality reliability and price advantage of BL Microwave of China LC filters(0.01-4GHz) Ceramic filters Cavity filters(0.3-40GHz) SSS filters Tubular filters Filter Banks/Duplexers Waveguide Filters Details of this offer are outlined on the form **BL** Microwave Ltd. Add:No.1, Huguang Rd., Shushan New Industry Zone, Hefei, Anhui Province, 230031 China Email:sales.chn@blmicrowave.com liyong@blmicrowave.com Web:www.blmicrowave.com

W-Band Quadrupler



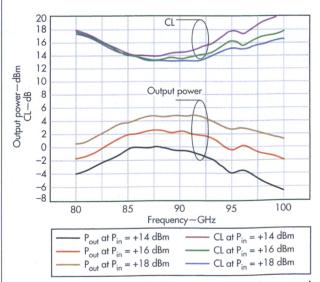
4. This diagram shows the optimized structure of the balanced quadrupler.

by about 1 dB, so the level of the fundamental input power should be a concern in the design of a frequency multiplier. When the second-harmonic reflector network is an open circuit at the output port, the CL is reduced by about 1 dB, which is an important consideration. Also, when the six-harmonic reflector network is an open circuit at the output port, the CL is reduced by about 0.2 to 0.4 dB, not a small amount of loss. According to these data, it is possible to optimize a Schottky diode multiplier for certain operating conditions. The spe-

cific structure is shown in Fig. 4.

As the studies show, a number of conclusions can be drawn. For one, the input reflector networks have been used to both impedance-match the fundamental-frequency signals and short-circuit the second- and fourth-harmonic signals. The output reflector networks are used to both impedance-match the fourth-harmonic signals and open-circuit the second- and sixth-harmonic signals. As shown in *Fig. 5* and *Table 2* (online only), the quadrupler's specific layout can be obtained by analysis

of these matching requirements. By using commercial analysis software such as ADS, it is also possible to determine the output power (based on an input-power level) and the CL curves for a frequency-multiplier design. From such computer simulation curves, the maximum output power point and minimum CL point for the quadrupler is found to be near

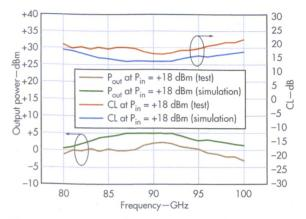


These curves show the quadrupler's simulated output power and conversion loss (CL).

87 GHz when the input power is around +20 dBm. The minimum CL is around 13 dB and the output power is around +7 dBm. This quadrupler design was realized with a 0.1-μm-gatelength GaAs pHEMT process (*Fig. 6*).

The device was testing in a Class 10,000 cleanroom, measured on wafer using a model M150 probe station from Cascade Microtech (www.cmicro.com), a model ACP110-S ground-signal-ground (GSG) W-band probe from Cascade Microtech, and a model W8486A W-band power probe from Agilent Technologies. Simulated and measured results are compared in *Fig. 7*, showing that the output frequency characteristics between modeled and measured results are somewhat offset. This is most likely because since the quadrupler works at W-band frequencies, the Schottky diode model may not be totally accurate.

Still, it was possible to simulate the performance of a Schottky diode multiplier from 80 to 100 GHz with results that were fairly close to the measurements of an actual fabricated quadrupler for that same range. The analysis showed that it is possible to reduce the multiplier's CL, provided that the input-power network and the input/output reflector networks are fully optimized. The monolithic quadrupler that was finally fabricated can produce output levels of about -3 to +2 dBm across the target frequency range of 80 to 100 GHz.



These curves compare the measured and simulated performance with frequency for the quadrupler.

"Design and optimization of large conversion gain active microwave frequency triplers," IEEE Microwave & Wireless Components Letters, Vol. 15, No. 7, July 2005, pp. 457-459.

7. Dong Min Kang, Ju Yeon Hong, Jae Yeob Shim, Jin-Hee Lee, Hyung-Sup Yoon, and Kyung Ho Lee, "A 77 GHz mHEMT MMIC Chip Set for Automotive Radar Systems," ETRI Journal, Vol. 27, No. 2, April 2005, pp.133-139.

8. Bong-Su Kim, Woo-Jin Byun, Min-Soo Kang, and Kwang Seon Kim, "E-Band Wideband MMIC Receiver Using 0.1 µm GaAs pHEMT Process," ETRI Journal, Vol. 34, No. 4, August 2012, pp.485-491.

9. W. M. Fathelbab, and M. B. Steer, "New classes of miniaturized planar marchand baluns," IEEE Transactions on Microwave Theory & Techniques, Vol. 53, No. 4, April 2005, pp. 1211-1220.

REFERENCES

1. Y. Campos-Roca, L. Verweyen, M. Fernández-Barciela, E. Sánchez, M. C. Currás-Francos, W. Bronner, A. Hälsmann, and M. Schlechtweg, "An optimized 25.5–76.5 GHz pHEMT-based coplanar frequency tripler," IEEE Microwave & Guided Wave Letters, Vol. 10, No. 6, June 2000, pp. 242–244.

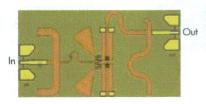
2. S. A. Maas and Y. Ryu, "A broadband, planar, monolithic resistive frequency doubler," IEEE Microwave and Millimeter-Wave Monolithic Circuits Symposium, 1994, pp.175-178.

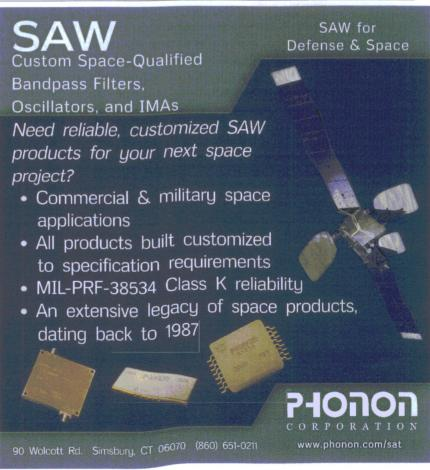
3. G. Hegazi, A. Ezzeddine, F. Phelleps, P. Mcnally, K. Pande, P. Rice, and P. Pages, "W-band monolithic frequency doubler using vertical GaAs varactor diode with n+ buried layer," Electronics Letters, Vol. 27, No. 3, January 1991, pp. 213-214.

4. S. Chen, T. C. Ho, K. Pande, and P. D. Rice, "Rigorous analysis and design of a high-performance 94 GHz MMIC doubler," IEEE Transactions on Microwave Theory & Techniques, Vol. 41, No. 12, December 1993, pp. 2317-2322.

5. D. G. Thomas, Jr. and G. R. Branner, "Single-ended HEMT multiplier design using reflector networks," IEEE Transactions on Microwave Theory & Techniques, Vol. 49, No. 5, May 2001, pp. 990-994.
6. J. E. Johnson, G. R. Branner, and J. P. Mima,

6. This microphotograph shows the fabricated quadrupler.





Design Feature

RAJ KUMAR | Senior Engineer TUHINA

TUHINA OLI | Engineer

NAGENDRA KUSHWAHA | Engineer

R.V.S. RAM KRISHNA | Engineer

Armament Research and Development Establishment (ARDE), Pashan, Pune-411 021, India
Defense Institute of Advanced Technology (DIAT), Deemed University, Girinagar, Pune-411 025, India; e-mail: raj34_shivani@yahoo.co.in

MICROSTRIP ANTENNA Boosts UWB Gain

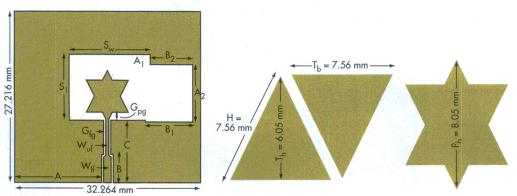
This compact, star-shaped slot antenna employs a frequency-selective surface as a reflector to help boost gain over a wide impedance bandwidth for UWB applications.

icrostrip antennas offer many benefits, including small size and light weight, along with ease of integration with microwave integrated circuit (MIC) and monolithic-microwave integrated circuit (MMIC) devices. They are well suited for transferring data, voice, and video as part of wireless communications applications, but they lack one important property for longer-distance communications: higher gain. Fortunately, it is possible to develop a microwave antenna with coplanarwaveguide (CPW) feed that offers radiation patterns with enough gain to serve ultrawideband (UWB) communications applications.

The antenna design features a star-shaped radiation patch with wide impedance bandwidth of 3.0 to

11.7 GHz. Through the use of a three-layer frequency-selective surface (FSS), the antenna can be fabricated with higher gain, enhancing the gain by 4 to 5 dB while maintaining the wide impedance bandwidth. The use of the FSS even helps reduce the antenna's backlobes.

The bandwidth of a patch antenna is limited if the patch is fabricated on a dielectric substrate that contributes to generation of surface waves, and in so doing reduces the bandwidth of the antenna.³ Numerous techniques are available to increase antenna bandwidth, such as incorporating different slot geometries in the ground planes, or the use of FSS screens, gapcoupled feeds⁴, and meandered ground planes.⁵ A UWB antenna with CPW feed can provide the good radiation patterns needed for broad bandwidth.



1. These diagrams show the geometry of the star-shaped UWB antenna.

Antennas for UWB communications can support a wide range of applications, including for microwave imaging, impulse radio communications, and biomedical applications. Increased antenna signal-to-noise ratio is needed

84 JUNE 2014 MICROWAVES & RF

PRECISION ATTENUATORS

2W to 100W



NOW from DC up to 40 GHz from \$2995 ea. (1-49)

Customers trust Mini-Circuits BW-family precision fixed attenuators for accuracy, reliability, and repeatability. Now, we've expanded your choices to cover DC-40 GHz! With accurate attenuation from 1 to 50 dB and power handling from 2 up to 100W, these attenuators now bring the same performance you've come to count on to even more applications!

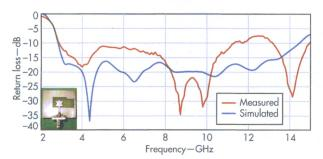
Visit minicircuits.com for free data, curves, quantity pricing, designer kits, and everything you need to find the BW attenuator for your needs. All models are available off-the-shelf for delivery as soon as tomorrow!



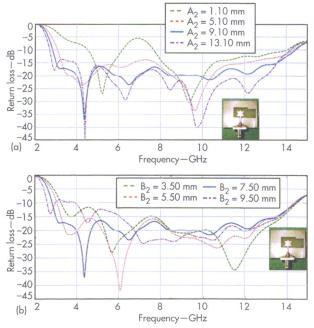
Increased antenna signal-to-noise ratio is needed for improved gain, and this can be achieved by designing antennas with unidirectional or semi-unidirectional radiation patterns."

for improved gain, and this can be achieved by designing antennas with unidirectional or semi-unidirectional radiation patterns. ^{6,7} The antenna gain can be improved in two ways: by increasing its efficiency or using a reflector surface. For increased efficiency, thinner substrates can be used to provide higher gain due to reduced surface-wave losses.

FSS surfaces are passive periodic structures of metallic or dielectric elements that can be used to control and manipulate the propagation of electromagnetic (EM) waves.⁸⁻¹⁰ FSS materials can be characterized by means of high surface impedance which retards the propagation of surface waves and supports



The plots show the measured and simulated reflection coefficients for the UWB antenna.



3. These plots show the effects of antenna parameters (a) ${\rm A}_2$ and (b) ${\rm B}_2$ on return loss.

in-phase reflections of waves striking the FSS surface, resulting in a high gain. ¹¹⁻¹⁵ For low-profile antennas, FSS designs should be compact, easy to fabricate, and commercially viable.

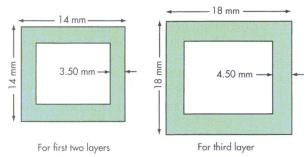
By using an FSS screen, it should be possible to improve antenna radiation pattern characteristics, directivity, polarization and, in many cases, bandwidth. FSS materials can be used as a filter, reflector, polarizer, propagation device, or as an artificial magnetic conductor (AMC).^{16,17}

Typical FSS structures already reported in technical literature include square, ring, loop, dipole, and fractal-based shapes. The characteristics and behaviors of these different FSS materials depend on the size, shape, periodicity, and geometric structure of each FSS unit cell.¹⁸

To demonstrate the effectiveness of FSS materials and shapes, a wideband FSS form consisting of a rectangular ring element was used to enhance the gain of a star-shaped patch antenna operating from 3.0 to 11.7 GHz. The antenna design was simulated with the help of the CST Microwave Studio computer-aided-engineering (CAE) simulation software from CST (www.cst.com), then fabricated and measured using commercial test equipment.

Figure 1 shows the structural details of the antenna. It was printed on one side of 1.58-mm-thick FR-4 circuit laminate with relative permittivity (ϵ_r) of 4.3 in the z-axis of the material and loss tangent (tan $\delta)$, or dissipation factor of 0.019 in the z-axis of the material. Initially, a simple symmetric rectangular-shaped slot was etched on the ground plane.

A double-stepped CPW feed line with widths of W_{lf} and W_{ub} and terminated on a star-shaped patch, was used to excite the slot. A double-stepped CPW feed was used for better impedance matching. Figure 1 also shows the formation of the star-shaped patch, which was formed by inverting and adding two isosceles triangles having base width T_b and height T_h , resulting in the star-shaped structure.



These are the unit-cell dimensions for the three layers of antenna FSS.



Speed your development with:

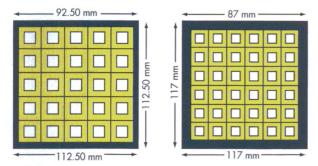
- ✓ Quick setup
- √ Runs directly from PC or front panel
- ✓ 1MHz–3GHz integrated signal generator
- ✓ Flexible pulse modulation, internal, external trigger
- Real-time display: VSWR, efficiency, temperature, DC power, voltage, current and more
- ✓ Easy system validation

Use with a range of Freescale reference designs.

Introducing the world's first integrated RF power development system—only from Freescale, the leader in RF power devices.

The global leader in RF power introduces another breakthrough—the Freescale RF power tool system, the industry's first fully integrated RF power application development system-in-a-box. Get all the components needed to design leading-edge RF power applications in a modular portable unit at a fraction of the cost of a traditional bench setup. Compatible with Freescale RF power evaluation boards and used by our own engineering teams, this innovative new tool simplifies your design process, reduces development time and costs, and gets you to market faster. Next time inspiration strikes, be ready. Visit freescale.com/RFpowertool





5. These are the overall screen dimensions for the different FSS layers.

To increase antenna bandwidth, the slot was made asymmetric by adding a rectangular section on one side (*Fig. 1*). The slot's asymmetric nature provides an inductive characteristic to counter the capacitive effects of the patch (produced by the fringing effect). The bandwidth can also be enhanced by changing the size and shape of the slot. The antenna was optimized further for miniaturization.

The return loss of the fabricated antenna was measured using a model R&S ZVA-40 vector network analyzer (VNA) from Rohde & Schwarz (www.rohde-schwarz.com). *Figure 2* compares measured and simulated return loss for the antenna. The measured impedance bandwidth of the antenna is 8.7 GHz (3.0 to 11.7 GHz).

From *Fig. 2*, it can be seen that measured and simulated results are in close agreement except at certain frequencies, where deviations may be due to substrate impurities or deviations because of SMA connectors.

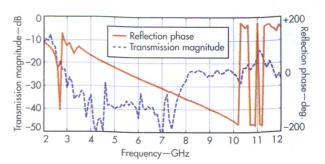
To study the effect of asymmetric slot on the return loss of the antenna, the two slot dimensions, A_2 and B_2 , were varied. *Figure 3* shows how return loss changes with variations in these slot dimensions. From *Fig. 3(a)*, it can be seen that as the value of A_2 increases, the return loss improves and frequency shifts downward.

As A_2 increases, the overall slot length increases, resulting in a shift towards lower frequencies. Also, the coupling between the ground and the radiating patch improves with

increasing value of A₂. This results in better impedance matching and improvement in return loss.

However, after a particular value of A_2 , the return loss deteriorates with increasing value of A_2 . So the value of A_2 must be optimized; the optimum value was found to be 9.10 mm. From $Fig.\ 3(b)$, it can be seen that B_2 has a similar effect on return loss as A_2 . The optimized value of B_2 was found to be 7.50 mm.

As opposed to the asymmetrical slot shown in *Fig. 1*, if the slot is extended on both sides, it again becomes symmetrical.



6. These plots show the reflection and transmission characteristics of the screen.

The effects of this extended symmetric slot on antenna return loss were studied, and found not ideally suited for UWB operation, even when the slot dimensions are optimized. These return-loss characteristics were studies by considering surface-current distribution for the antenna. High current distribution was found at 4.3 GHz, due to the star-shaped patch, with a resonance at 6.5 GHz due to second harmonics of 3.2-GHz fundamental signals.

By considering current distribution, the first resonance can be approximated as

$$f_1 = c/[SL(\epsilon_{eff})^{0.5}] \quad (1)$$

where:

 f_1 = the lowest resonance frequency (in Hz);

SL =the slot length (in m and equal to 0.065 m);

c =the speed of light (in m/s); and

 ϵ_{eff} is the effective relative permittivity which can be approximated by $(\epsilon_r+1)/2$.

The second resonance frequency can be approximated by con-

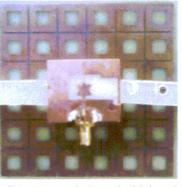
sidering the height of the patch to $\lambda/4$, and it is given by Eq. 2:

$$f_2 = c/[4L(\epsilon_{eff})^{0.5}]$$
 (2)

where:

L = the height of the star-shaped patch.

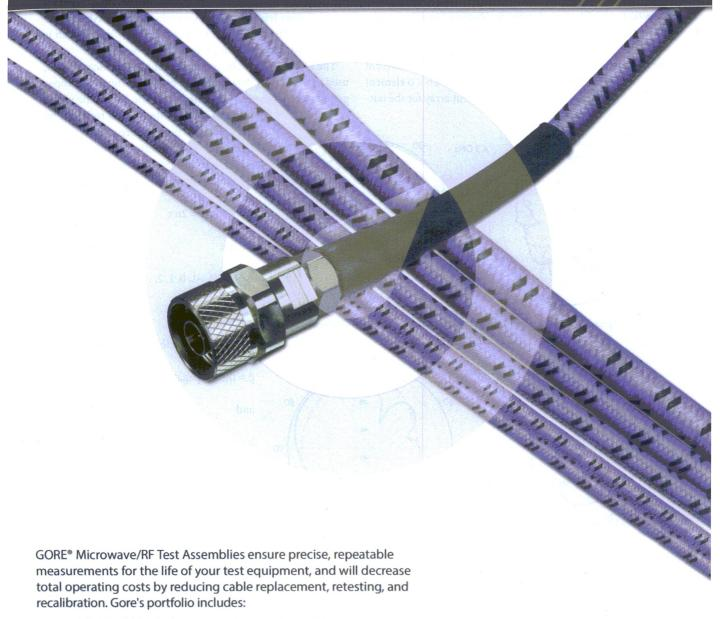
By using loop-type patches, the antenna FSS was successfully designed. Initially, a loop array was printed on one side of the substrate. Then, to increase the stopband bandwidth, different layers of FSS were



7. This photograph shows the fabricated UWB antenna with screen.

Performance Over Time

GORE® Microwave/RF Test Assemblies offer unmatched precision, repeatability and durability.



- GORE® PHASEFLEX® Microwave/RF Test Assemblies –
 Provide excellent phase and amplitude stability with flexure.
- 110 GHz Test Assemblies Engineered to be flexed, formed and repositioned while maintaining excellent electrical performance.
- VNA Microwave Test Assemblies Provide exceptional performance for precision test applications with frequencies through 67 GHz.
- General Purpose Test Assemblies Excellent electrical performance for everyday test applications.



gore.com/test





cascaded to form the final FSS. The FSS is a composite structure with two substrate layers sandwiched between three metallic layers. The 1.6-mm-thick substrate has relative permittivity, $\varepsilon_{\rm p}$ of 4.4. The unit element used for all three layers was a loop-type structure, with larger loop for the outermost layer. *Figure 4* shows the unit elements used in the different layers of the FSS. The FSS was fabricated with a 6 × 6 element array for two of the layers and 5 × 5 element array for the out-

ermost layer (Fig. 5). Figure 6 shows simulated magnitude of transmission and reflection phase for the FSS. The stopband (transmission less than $-20~\mathrm{dB}$) bandwidth is 8.3 GHz (2.6 to 10.9 GHz). The reflection phase of the FSS is linear which is desirable to increase the gain over a wider bandwidth.

The FSS is mounted below the antenna to enhance the gain, used as a reflector. Waves radiated by the antenna and propagating towards the FSS are reflected by the FSS. If the waves

radiated by the antenna and reflected by the FSS are in phase, antenna gain will be increased. The condition for the reflected waves from the FSS and the radiated waves from the antenna to be in phase is given by

$$\Phi_{FSS} - 2\beta h = 2n\pi$$

where:

$$n = ... -2, -1, 0, 1, 2, ...$$
 (3)

and

 Φ_{FSS} = the reflection phase of the FSS;

 β = the propagation constant in free space;

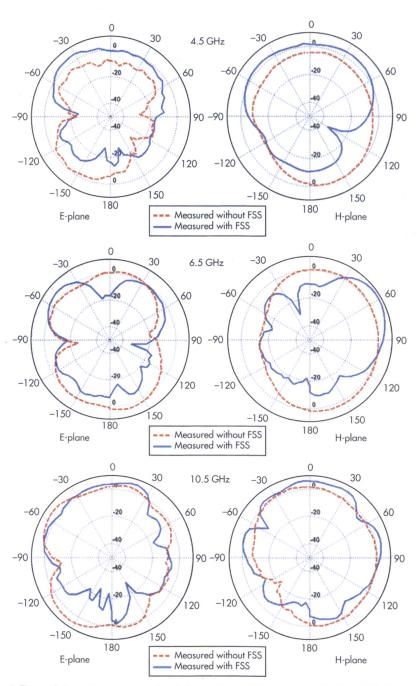
and

h = the height between the FSS and the antenna.

By using Eq. 1, h can be calculated as 26.13 mm.

Figure 7 shows the fabricated antenna prototype along with the FSS. The measured impedance bandwidths with and without the FSS are nearly same and equal to 8.7 GHz (from 3.0 to 11.7 GHz). The slight difference between the reflection coefficients (with and without FSS) is due to multiple reflections caused by the FSS.

The radiation patterns of the proposed antenna with and without the FSS were measured in an in-house anechoic chamber, with a double-ridged horn antenna used as the reference antenna. *Figure 8* compares measured E- and H-plane patterns with and without the FSS at three different frequencies: 4.5, 6.5, and 10.5 GHz. Radiation patterns without the FSS show a bidirectional nature in the E- plane and omnidirectional nature in the H-plane.



8. These plots compare measured radiation patterns of the antenna in the E- and H-planes with and without the FSS.

Low Phase Noise SAW VCO's

Model	Frequency (MHz)	Tuning Voltage(VDC)	DC Bias	Phase Noise @ 10 kHz (dBc/Hz) [Typ.]	
HFSO640-5	640	0.5 - 12	+5 @ 35 mA	-151	
HFSO745R84-5	745.84	0.5 - 12	+5 @ 35 mA	-147	
HFSO776R82-5	776.82	0.5 - 12	+5 @ 35 mA	-146	
HFSO800-5	800	0.5 - 12	+5 @ 30 mA	-146	
HFSO914R8-5	914.8	0.5 - 12	+5 @ 35 mA	-139	
HFSO1000-5	1000	0.5 - 12	+5 @ 35 mA	-141	
HFSO1600-5	1600	0.5 - 12	+5 @ 100 mA	-137	
HFSO2000-5	2000	0.5 - 12	+5 @ 100 mA	-137	

SAW VCO Features

- Small Size 0.5" x 0.5"
- Very Low Post Thermal Drift





Phone: (973) 881-8800 | Fax: (973) 881-8361

E-mail: sales@synergymwave.com Web: WWW.SYNERGYMWAVE.COM

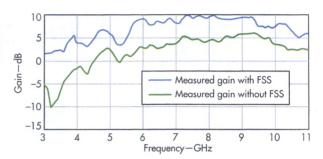
Mail: 201 McLean Boulevard, Paterson, NJ 07504

DIMENSIONS OF ANTENNA PARAMETERS (in mm)							
Parameter	G _{pg}	G _{fg}	W _{uf}	W _{lf}	А	В	С
Dimension	0.70	0.30	0.82	1.73	14.97	4.20	10.10
Parameter	A ₁	A ₂	B ₁	B ₂	Sı	S _w	
Dimension	1.50	9.10	8.20	7.50	10.50	14.30	

The radiation pattern becomes more directional with application of the FSS. The backlobes are reduced by around 10 dB (at 7.5 GHz) with the FSS. *Figure 9* shows the measured peak gain comparison of the antenna without and with the FSS. It reveals an improvement in the peak gain of around 4 to 5 dBi throughout the band after application of the FSS, with the gain under both conditions measured from 3 to 11 GHz.

In summary, a compact slot antenna with FSS provides high gain for UWB applications. The slot is asymmetrically placed in the ground plane to improve impedance matching. The antenna design offers a measured impedance bandwidth of 102% at a center frequency of 7.5 GHz. To boost gain, a three-metal-layer FSS is used as a reflector, providing improvement of 4 to 5 dBi in peak gain.





9. These plots show the peak gain for the prototype antenna with and without FSS across a frequency range of 3 to 11 GHz. The gain increased by about 4 to 5 dBi with application of the FSS .

REFERENCES

- C.A. Balanis, Antenna Theory Analysis and Design, Wiley-Interscience, New York, 2005.
- 2. G.Z. Rafi and L. Shafai, "Wideband V-Slotted Diamond- Shaped Microstrip Patch Antenna," Electronic Letters, Vol. 40, No. 19, 2004, pp. 1166-1167.
- 3. Hsing-Yi Chen and Yu Tao, "Antenna Gain and Bandwidth Enhancement Using Frequency Selective Surface With Double Rectangular Ring Elements," 9th International Symposium on Antennas Propagation and EM Theory (ISAPE), Guangzhou, PRC, November 29-December 2, 2010, pp. 271-273.
- 4. P.S. Hall, "Probe Compensation in Thick Microstrip Patches," Electronic Letter, Vol. 23, No. 11, 1987, pp. 606-607.
- 5. J.S. Kuo and K.L. Wong, "A Compact Microstrip Antenna with Meandering Slot in the Ground Plane," Microwave and Optical Technology Letters, Vol. 29, No. 2, April 2011, pp. 95-97.
- A. Pirhadi, H. Bahrami, and J. Nasri, "Wideband high directive aperture coupled microstrip antenna design by using a FSS superstrate layer," IEEE Transactions on Antennas and Propagation, Vol. 60, No. 4, April 2012, pp., 2101-2106.
- 7. N. Kushwaha and R.Kumar, "Design of slotted ground hexagonal microstrip patch antenna and gain improvement with FSS screen," Progress In Electromagnetics Research B, Vol. 51, 2013, pp. 177-199.
- 8. R. Ulrich, "Far-infrared properties of metallic mesh and its complementary structure," Infrared Physics, Vol. 7, No. 1, 1967, pp. 37-50.
- 9. T.K. Wu, Frequency Selective Surface and Grid Array, Wiley, New York, 1995.
- M.A. Hiranandani, A.B. Yakovlev, and A.A. Kishk, "Artificial magnetic conductors realized by frequency-selective surfaces on a grounded dielectric slab for antenna applications," IEE Pro.-Microwave Antennas Propagation, Vol. 153, No. 5, October 2006, pp. 487-493.
- 11. Liang and H.Y. David Yang, "Radiation characteristics of a microstrip patch over an electromagnetic bandgap surface," IEEE Transactions on Antennas & Propagation, Vol. 55, No. 6, June 2007, pp. 1691-1697.
- D. Sievenpiper, L. Zhang, R.F. Jimenez Broas, N.G. Alex'opolous, and E. Yablonovitch, "High-impedance electromagnetic surfaces with a forbidden frequency band," IEEE Transactions on Microwave Theory & Techniques, Vol. 47, No. 11, November 1999, pp. 2059-2074.
- 13. X.L. Bao, G. Ruvio, M.J. Ammann, and M. John, "A novel GPS patch antenna on a fractal hi-impedance surface substrate," IEEE Antennas & Wireless Propagation Letters, Vol. 5, 2006, pp. 323-326.
- 14, B.A. Munk, Frequency Selective Surfaces Theory and Design, Wiley, New York, 2000.
- 15. R. Dickie, R. Cahill, H. Gamble, V. Fusco, M. Henry, M. Oldfield, P. Huggard, P. Howard, N. Grant, Y. Munro, and P. de Maagt, "Submillimeter wave frequency selective surface with polarization independent spectral responses," IEEE Transactions on Antennas & Propagation, Vol. 57, No. 7, July 2009, pp. 1985-1994.
- 16. C.N. Chiu, C.H. Kuo, and M.S. Lin, "Bandpass shielding enclosure design using multipole-slot arrays for modem portable digital devices," IEEE Transactions on Electromagnetic Compatibility, Vol. 50, No. 4, November 2008, pp. 895-904.
- 17. B.A. Munk, P. Munk, and J. Pryor, "On designing Jaumann and circuit analog absorbers (CA absorbers) for oblique angle of incidence," IEEE Transactions on Antennas & Propagation, Vol. 55, No. 1, January 2007, pp. 186-193.
- 18. M. Xu, T.H. Hubing, I. Chen, T.P. Van Doren, I.L. Drewniak, and R.E. DuBroff, "Power-bus decoupling with embedded capacitance in printed circuit board design," IEEE Transactions on Electromagnetic Compatibility, Vol. 45, No. 1, February 2003, pp. 22-30.

EUROPEAN MICROWAVE WEEK 2014 FIERA DI ROMA, ROME, ITALY OCTOBER 5 - 10, 2014



EUROPE'S PREMIER MICROWAVE, RF, WIRELESS AND RADAR EVENT

The Exhibition (7th - 9th October 2014)

Pivotal to the week is the European Microwave Exhibition, which offers YOU the opportunity to see, first hand, the latest technological developments from global leaders in microwave technology, complemented by demonstrations and industrial workshops. Register as an Exhibition Visitor at www.eumweek.com, Entrance to the Exhibition is FREE.

The Conferences:

Don't miss Europe's premier microwave conference event. The 2014 week consists of three conferences and associated workshops:

- European Microwave Integrated Circuits Conference (EuMIC) 6th 7th October
- European Microwave Conference (EuMC) 6th 9th October
- European Radar Conference (EuRAD) 8th 10th October
- Plus, Workshops and Short Courses from 5th October
- In addition, EuMW 2014 will include the 'Defence, Security and Space Forum' Register for the conference online at: www. eumweek.com

Conference prices

There are TWO different rates available for the EuMW conferences:

- ADVANCE DISCOUNTED RATE for all registrations up to and including 5th September
- STANDARD RATE for all registrations made after 5th September



















ØIFFF







Register online now at www.eumweek.com

SIMULATION SOFTWARE OPTIMIZES MISSILE ANTENNAS

REMCOM,

315 South Allen St., Ste. 416, State College, PA 16801; (814) 861-1299,

www.remcom.com

NTENNA ARRAYS ARE making themselves useful in applications ranging from biomedical to radar. Such diverse applications place the arrays in environments that are far from their planar performance ideal.

To effectively predict and optimize the behavior of non-planar antenna arrays, powerful 3D simulators could be used in the

initial design stages. Remcom has released an application note investigating this option titled "Conformal Antenna Array Design on a Missile Platform."

The example in the application note is a 12-x-1 antenna array mounted on the side body of a theoretical missile. The design must overcome the challenging constraints of having a radiative body as an antenna-array mounting surface

while meeting airborne weaponry standards. The specifications of operation for this demonstration include a center frequency of 2.4 GHz, a main beam gain greater than 10 dBi, and side-lobe levels that are less than 20 dB below the peak

gain figures.

A planar conformal antenna is required to meet the surface requirements of the mis-

sile body. A parametric investigation is performed to optimize the patch antenna array for performance. The array is then bent to the missile's body shape for aerodynamics. Such bending shifts the operating frequency close to 2.45 GHz. After a slight patch diameter variation, however, the operating frequency again conforms to the specification. Scripts from Remcom's library are used to choose the

PTF,

50L Audubon Rd.,

Wakefield, MA 01880;

(781) 245-9090,

www.ptfinc.com

array amplitude and phase to meet the sidelobe and main gain figures.

The antenna array is then integrated into a 3D model of the missile body. Simulations are run using a variety of computer hardware permutations to demonstrate the time enhancements of using multicore graphical processing units (GPUs) for simulation. Using a single Intel Core i7, the simulation required 3 hrs. and 13 min. of simulation time. In contrast, using a single Nvidia Tesla C2070 GPU brought the simulation time down to 29 min, and 40 sec. Six Nvidia GPUs lowered the simulation time to 7 min. and 20 sec. This example demonstrates the simulation-time performance that can be acquired from GPU processing using 3D electromagnetic simulation software that can leverage the CUDA environment.

GNS SIGNALS ARE USED FOR FREQUENCY STANDARDS

THE PROLIFERATION OF global navigation satellite systems (GNSSs) could enable the implementation of a higher-quality frequency standard than the costly cesium atomic clock. This new system uses the base technology of the Global Positioning Satellite (GPS) systems to attain highly precise physical positions. In doing so, it provides frequency standards with accuracy better than 6E⁻¹³ over 24 hrs. Delving into the details of such a system, PTF provides an application note titled

"High Performance GNSS Disciplined Frequency Reference Standards."

To detect the precise position of a GNSS receiver, a connection is needed for a minimum of four satellites. This information also can be used

to derive accurate timing data, which can be used to control an oscillator's stability. There are two primary methods for generating the timing data: using the 1 pulse per second (1-PPS) signal or carrier-phase-disciplined-oscillator (CPDO) method. A hybrid of both methods would produce the highest accuracy. But the cost and complexity of a CPDO make it less viable than cleverly solving the accuracy issues associated with the 1-PPS method.

The 1-PPS method is highly stable over time. Depending on the resolution of the oscillator signal, however, it may shift each cycle relative to the oscillator's phase. Although an oven-controlled crystal oscillator (OCXO) has a very stable phase-

noise figure, the OCXO degrades over time in accuracy. If both a 1-PPS system and OCXO are combined effectively with a control loop, a highly accurate and stable frequency reference can be designed.

To align the 1-PPS signal with the oscillator's signal, one approach is to use the OCXO's base frequency and divide it down to a single cycle per second. But this method introduces inaccuracy based upon the phase noise of the oscillator. Even

with clever half-clock cycle techniques, a 5-ns error from a 100-MHz clock is not accurate for measuring 10-ns saw-tooth granularity errors. PTF claims to resolve this issue by using an interpolator charging capacitor technique, which re-

portedly enhances resolution on the quantization error by 1000 times. This would produce a phase measurement resolution of 0.1 ns, effectively synchronizing the two signals.

Using this technique and a simple controller, the company touts the potential for an RF signal with stability greater than $2E^{-11}$ phase noise beyond -125 dBc at 10-Hz offset from the carrier, and accuracy of greater than $1E^{-12}$ over 24 hrs. The quality of the RF-controlled signal could be degraded by other factors, such as poor power supplies, low-grade buffer amplifiers, poor analog/digital layout, and insufficient grounding. Thus, those factors also should be considered in the design.

9/



0.15-8000 MHz as low as 99¢ each (qty. 1000) O ROHS compliant.

Rugged, repeatable performance.

At Mini-Circuits, we're passionate about transformers. We even make own transmission line wire under tight manufacturing control, and utilize all-welded connections to maximize performance, reliability, and repeatability. And for signals up to 8 GHz, our rugged LTCC ceramic models feature wraparound terminations for your visual solder inspection, and they are even offered in packages as small as 0805!

Continued innovation: Top Hat.

A Mini-Circuits exclusive, this new feature is now available on every open-core transformer we sell. Top Hat speeds customer pick-and-place throughput in four distinct ways: (1) faster set-up times, (2) fewer missed components,

(3) better placement accuracy and consistency, and (4) high-visibility markings for quicker visual identification and inspection.

More models, to meet more needs

Mini-Circuits has over 250 different SMT models in stock. So for RF or microwave baluns and transformers, with or without center taps or DC isolation, you can probably find what you need at minicircuits.com. Enter your requirements, and Yoni2, our patented search engine, can identify a match in seconds. And new custom designs are just a phone call away, with surprisingly quick turnaround times gained from over 40 years of manufacturing and design experience!



International Microwave Symposium

IEEE 17-22 May 2015 · Phoenix, AZ MTT-S



IMS2015 MUST ATTEND!

The 2015 IEEE MTT-S International Microwave Symposium (IMS2015) is the premier conference for the Microwave and RF Industries! With over 9,000 attendees and over 600 industrial exhibits of the latest state-of-the-art microwave products, Microwave Week is the world's largest gathering of Radio Frequency (RF) and Microwave professionals and the most important forum for the latest and most advanced research in the area.

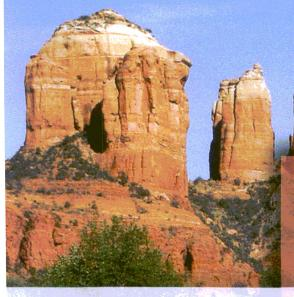
SUBMIT YOUR TECHNICAL PAPER TO IMS2015 TODAY!

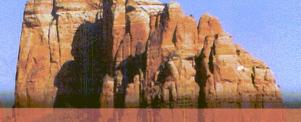
Technical Paper Submissions:

Authors are invited to submit technical papers describing original work on radio-frequency, microwave, millimeter-wave, and terahertz (THz) theory and techniques. The deadline for submission is 8 December 2014. Please refer to the IMS2015 website (www.ims2015.org) for detailed instructions concerning paper submission, as well as a complete list of technical areas.

EXPERIENCE ALL THE ADVANTAGES OF BECOMING AN EXHIBITOR AT IMS2015.

Become an Exhibitor: The 2015 IEEE MTT-S International Microwave Symposium is the world's premier microwave event. It features a large trade show, technical sessions, workshops and panel covering a wide range of topics. Attendee interests include wireless communication, RF technologies, high frequency semiconductors, electromagnetics, commercial and military RF, microwave and mm-wave electronics, applications, and much more.





IMS2015 EXHIBIT SPACE IS AVAILABLE.

For reservation questions or further information contact:

The Exhibits Department at MP Associates, Inc. tel: +303-530-4562

exhibits@mpassociates.com





FOR FULL CONFERENCE DETAILS VISIT WWW.IMS2015.ORG

JOIN THE CONVERSATION: #IMS2015





PIR Gain Broadband Power

These solid-state amplifiers offer distortion-free performance in coaxial and drop-in packages for design flexibility in broadband applications.

AMPLIFICATION IS ALMOST always needed in high-frequency systems, whether transmitting or receiving. When broadband amplification is needed, finding a solution can be most challenging, since a large number of simultaneous amplifier performance parameters, such as output power, gain, and even noise figure, must be satisfied over a wide frequency bandwidth.

Fortunately, the new model ZHL-5W-422+ coaxial amplifier

from Mini-Circuits (www.minicircuits.com) is an example of a broadband amplifier that not only delivers outstanding electrical performance with 5-W CW output power from 500 to 4200 MHz, but includes protective circuitry and numerous features to make its installation and use almost foolproof. The 50- Ω amplifier is well suited for military, commercial, test, and even amateur-radio applications, and can be supplied with or without

a heat sink.

Model ZHL-5W-422+ designates a coaxial amplifier with fan and heat sink, which is also available as model ZHL-5W-422X+ as the coaxial amplifier in its housing alone, without fan and heat sink (Fig. 1). The Class-A linear amplifier, which is based on GaAs FET active devices, provides adequate continuous output power for a variety of transmit operations. These include frequency-modulated (FM) radios, television transmitters, point-to-point radio transmitters, amateur radio, and laboratory use.

This is an amplifier with instrument-grade gain performance, with 20-dB minimum gain and 25-dB typical gain across its frequency range. Although these are not staggering gain numbers, what is impressive is the flatness of the gain with frequency, typically holding well within ±1 dB gain from 500 to 4200 MHz (Fig. 2). The amplifier is rated for worst-case gain flatness of ± 1.7 dB across its operating frequency range.

Perhaps not as apparent, this is an amplifier that also features directivity of better than 50 dB across its full operating frequency range (exceeding 60 dB at some frequencies). In addition, it is well matched for use in a wide range of applications, with a low input VSWR of no worse than 2.3:1 and typically at 1.70:1.

The low-input VSWR enables well-matched connections between signal sources, such as a feedline from an antenna,

> and the input port of the amplifier. Such "compatible impedances" help minimize mismatches and irregularities in amplitude and phase performance. As a result, with low-VSWR amplifier input ports that are well matched, the specified gain flatness can actually be

achieved. In addition, for applica-

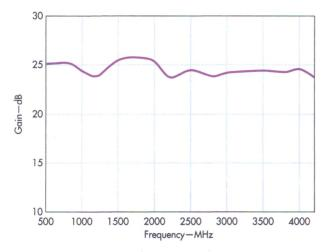
tions where phase irregularities due to impedance mismatches might be a problem—such when amplifying phase-modulated signals—these amplifiers help to minimize phase deviations across a wide bandwidth.

With or without the heat sink, the amplifier is rated for reasonable 5 W output power from 500 to 4200 MHz, with +35 dBm typical output power at 1-dB compression and +37 dBm typical output power at 3-dB compression. The linear amplifier boasts output third-order intercept point of at least +40 dBm and typically +45 dBm, and output second-order intercept point of at least +50 dBm and typically +55 dBm (Fig. 3). Two-tone output levels were measured with high-quality commercial test equipment, using two test tones set 1 MHz apart in frequency.

With its generous output-power levels, it also achieves high

1. Model ZHL-5W-422+ is a solid-state amplifier with fan and heatsink, while model ZHL-5W-422X+ is just the amplifier (right) for use from 500 to 4200 MHz.

GO TO MWRF.COM 97

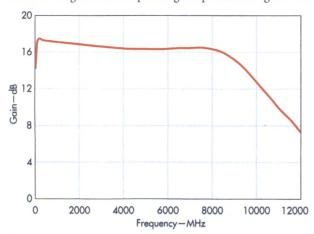


The small-signal gain of the model ZHL-5W-422+ amplifier remains flat through 4.5 GHz.

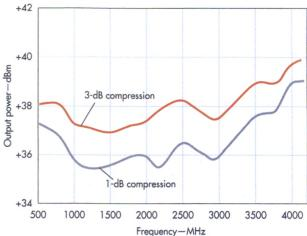
efficiency, boasting 30% typical operation under saturated output-power conditions and respectable noise figure across its frequency range (typically at 7 dB). The amplifier is designed for use from a 2-A supply at +28 VDC. It can handle input power levels as high as +20 dBm without damage. Models ZHL-5W-422+ and ZHL-5W-422X+ are RoHS compliant and supplied with SMA connectors.

Healthy output power in an amplifier can bring with it many risks; these come in the form of overheating, backup damage, and other potential problems as a result of short-circuit or open-circuit connections to a powered amplifier. No audio through RF/microwave amplifier is immune from damage due to faulty connections, but the model ZHL-5W-422+ has been designed to handle as many problems as possible.

The amplifier is unconditionally stable and features reverse polarity protection against "wrong-connection" hookups. The amplifier will not suffer damage when operated with an open or short output load under full CW output power. The amplifier, which is designed for an operating temperature range of -20



 Model GVA-123+ is a broadband amplifier in an SOT-89 package with gain within ±0.7 dB through 8 GHz.



 The upper trace shows output power at 1-dB compression and the lower trace is output power at 3-dB compression for the model ZHL-5W-422+ amplifier.

to +50°C, incorporates automatic shut-off protection when its base-plate temperature exceeds +85°C.

With the many challenges of broadband amplification at RF/microwave frequencies, perhaps the new model GVA-123+ amplifier from Mini-Circuits is even more impressive, packed into a tiny SOT-89 package for applications from 10 MHz to 12 GHz. Suitable for use in cellular base stations, in test equipment, in satellite-communications (satcom) equipment, and in avionics systems, this is an amplifier that practical defines gain flatness, with specified performance of ± 0.7 dB gain flatness from 0.05 to 8 GHz. While its gain does drop below 8 GHz (*Fig. 4*), this is a compact amplifier that offers 16.9 dB typical gain at 2 GHz, with typical return loss of 20 dB at that frequency and almost ruler-flat gain from 10 MHz to 8 GHz.

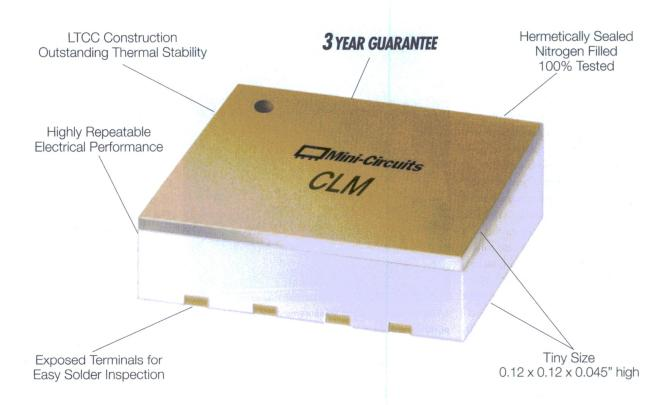
Of course, achieving desired results with RF/microwave amplifiers in broadband applications requires an understanding of amplifier distortion and noise behavior. Mini-Circuits has worked closely with leading test-and-measurement suppliers such as Agilent Technologies (www.agilent.com) to establish proven measurement techniques for characterizing its broadband amplifiers under a variety of operating conditions (see www.minicircuits.com/pages/pdfs/Advances_in_Ultra-High_Linearity_E-Mode_GaAs_PHEMT_MMIC_Amplifiers.pdf).

Broadband amplification was once primarily considered a requirement of measurement applications. Nevertheless, as more commercial and defense systems move to higher-order digital modulation schemes, wider signal bandwidths are needed—and amplifiers are needed to process those bandwidths. From Mini-Circuits, this is just a sampling of the latest crop of broadband solid-state amplifiers with good output power, reasonable gain, and excellent gain flatness.

MINI-CIRCUITS, P.O. Box 350166, Brooklyn, NY 11235-0003; (718) 934-4500, FAX: (718) 332-4661, www.minicircuits.com



Block High Level RF Interference... Protect Your Low Noise Receivers.



30 MHz to 8.2 GHz P_{MAX} 2 W

Our ultra wideband CLM-83-2W+ limiter cuts overpowered inputs, as high as 2W, down to +11.5 dBm in just 2 ns! Full throughput is restored 8 ns later, with an IL of 0.5 dB typical. It adds up to excellent protection against a wide range of spikes and power surges—even in the harshest environments, where unwanted signals prevail. And a tiny 3 x 3 x 1.14 mm footprint makes it easy to fit on crowded PCBs!

\$ **1995** from **1995** ea. qty. 10-49

The CLM has already qualified for tough MIL specs including gross and fine leak, acceleration, PIND, vibration, mechanical shock, and thermal shock, with an operating range from -55 to +100°C! For more details, go to minicircuits.com—it's even available on small-quantity reels! Order today, and you can get excellent protection for your sensitive applications in your hands as soon as tomorrow!



Test Chambers Analyze Mega-To Micro-Sized Antennas

To test today's complex antennas, test chambers and antenna test systems have rapidly evolved in terms of size, power, and capability.

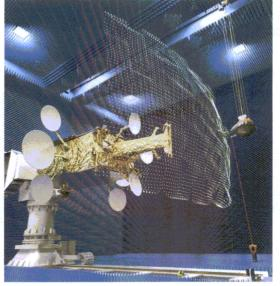
ANTENNA DESIGN IS quickly advancing as space-borne antennas grow bigger, millimeter-wave technology increases density, galliumnitride (GaN) technology widens bandwidth, and radar systems push the boundary on radiated power. The extremes of antenna size, power, bandwidth, and complexity are clearly expanding. These advancements are placing a serious burden on antenna test systems. As technology evolves to allow more complex and higher-bandwidth electronics, test and measurement equipment is able to better scale with the devices.

But these advancements do not aid the test-chamber and testplanning engineers. As a result, test antenna companies that offer anechoic, near-field, far-field, highpower, and wide-bandwidth test

chambers have to take more creative approaches. This need is underscored by the fact that the environments and platforms in which these antennas operate are becoming more diverse and electrically populated.

From space-borne to airborne and automotive platforms, multiband antennas and multi-antenna systems are finding their way into every human-populated environment. This makes highly accurate radiation tests critical and often necessary for licensing purposes. Yet it is usually difficult to test larger antenna structures, as the cost of shipping and assembly is prohibitive. A creative solution to this problem is currently being prototyped by Astrium GmbH (www.astrium.eads.net) in conjunction with the European Space Agency as part of the Advanced Research in Telecommunications Systems (ARTES) program.

The Portable Antenna Measurement System (PAMS) is being designed to handle cases where it is difficult and expensive



1. The Portable Antenna Measurement System (PAMS) can perform near-field probing along a planar or tilted surface using laser trackers for precision measurements. (Courtesy of Astrium GmbH)

to build a dedicated test site or ship large antennas to test sites (Fig. 1). The system comprises a multi-sensor node that can be suspended and supported using the existing crane infrastructure of a satellite or antenna assembly facility. Modular anechoic shielding can be placed around the antenna under test (AUT) for accurate antenna measurements. The AUT also can be placed in an echoic environment for diagnostic antenna measurements. The current PAMS prototype is being demonstrated in a facility at the Astrium Antenna Test Centre in Munich, Germany.

The PAMS performs near-field (NF) testing by probing with a technique called the Fast Irregular Antenna Field Transforma-

tion Algorithm (FIAFTA). This algorithm uses the concept of plane-wave expansion. Its speed is enhanced with the Multilevel Fast Multipole Method (MLFMM). With this approach, the PAMS isn't bound by precise geometric scan profiles and contours. As a result, it doesn't have to go through a whole matrix of a measurement grid to maintain accuracy. The system can work in a free-form NF probing scheme with the exact position of the probe actively tracked by commercially available laser trackers.

Because the PAMS uses the assembly infrastructure for the large antenna, measurement volume isn't limited by test-site dimensions. As a result, the PAMS can be used to test a satellite during assembly, in an integrated test facility, or even at the launch site after the satellite has been transported. The PAMS probe also can be modularly equipped with probes designed for the specific frequency range desired for testing. The current



2. The Spherical Near-Field Antenna Test Facility (SNFTF) can test an antenna's behavior in the near-field and extrapolate far-field behavior using this data. (Courtesy of European Space Agency)

prototype is designed to test in the L-band and 33-GHz area of the K-band for performance verifications this summer.

Astrium also offers traditional antenna test facilities, which are capable of performing measurements for gain, swept frequency, multi-frequency, equivalent isotropically radiated power (EIRP), multi-beam, polarimetric radar-cross section (RCS), and radar pulse modes. Among these solutions are the Compact

.

Antenna Test Range CCR 75/60, Cylindrical Near-field Test Range CNTF-8, and Feed Calibration Test Chamber. The CCR 75/60, which measures $5 \times 5 \times 6$ m, covers frequency ranges from 1.5 to 200 GHz with optional 500-GHz capability. It is well suited for multi-beam and multi-frequency antenna-pattern measurements of dual linear or circular polarizations (Fig. 2).

In contrast, the CNTF-8 offers a planar test area of 10×8 m or a cylindrical test area of 6×8 m. The CNTF-8 covers 400 MHz to 100 GHz with a temperature capability of -60° to +80° C. It is primarily designed for the acceptance and qualification of lightweight and high-gain spacecraft antennas.

The Feed Calibration Test Chamber is designed for calibration measurements of various feed systems and NF probes for spacecraft antennas. The test zone area is $0.8 \times 0.8 \times 0.8$ m. The chamber can test systems to 40 GHz sunder the same temperature conditions as the CNTF-8. For those looking to extend test power, environmental conditions, and security, another option is Raytheon's Antenna Test Facility (ATF) in El Segundo, Calif. The ATF is designed for testing prototype antenna technologies for space, advanced radar, communications, and airborne systems.

Sporting a six-floor and 17,000-square-foot facility, the ATF's indoor anechoic chambers and compact ranges are protected against environmental conditions and exterior RF interference. The chambers' exterior RF interference attenuation is greater than 100 dB to 100 GHz. There are four chambers within the ATF that can be used simultaneously. Chambers 1 and 2 feature compact ranges integrated within the anechoic chamber. Each chamber is equipped with positioners for rotating antennas, analysis software equipment, control-room instrumentation, and processing equipment.

An anechoic tapered chamber provides NF and far-field (FF) measurement capability with cylindrical, spherical, or planar methods. This chamber can be equipped with instruments that enable testing from 0.2 to 34 GHz, 0.1 to 110 GHz, and even to 140 GHz. The planar-near-field (PNF) range has a 10-×-10ft. chamber that can house antennas to 8 ft. for 6-to-18-GHz testing using Nearfield Systems' PC-driven data-acquisition software. Additional equipment can enhance this chamber for analysis to 110 GHz. For antenna heavy lifting, the Georgia Tech Research Institute (GTRI) offers a variety of test chambers and ranges to support the largest loads.

In fact, the GTRI also boasts electromagnetic test and evaluation facilities spanning 200 MHz to 110 GHz in the NF and FF ranges. The GTRI features a planar/cylindrical NF range, a spherical NF range, an anechoic chamber, an outdoor

FF range, and a turntable range. The turntable range

can support a load in excess of 200,000 lbs. and can elevate approximately 90 ft. above the tower base. This elevation capability enables the range to test tank-sized targets to 32 deg. of elevation at different angles. It also can support vehicle-mounted antennas. On the outdoor FF range, a three-axis positioner can support 30-ft.-diameter antennas to 30,000 lbs. while providing high mechanical precision.

> For those engineers looking to test high frequencies in small spaces, the Microwave Vision Group offers the μ-Lab (Fig. 3). This portable millimeter-wave test chamber measures 7 × 5×5 ft. It is mounted on caster wheels

with a folding tabletop side for an attached peripheral computer. The test chamber can support devices to laptop size. It boasts an offset column for chip measurements that can support devices to 5×5 cm.

The frequency capability of the μ -Lab is 50 to 110 GHz with add-ons that can drop the frequency range to 18 GHz. To specifically test NF and FF chips, miniature connectorized antennas, and portable electronics, the µ-Lab has highly refined elevation and azimuth-axis control assemblies.

3. Using a compact anechoic chamber with integrated far-field and spherical near-field testing could enable faster development times for millimeter-wave devices. (Courtesy of Orbit FR)

GO TO MWRF.COM 101

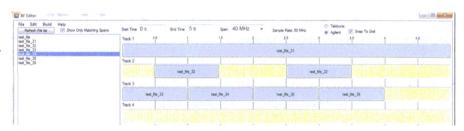
Product Feature

JAMES TABER | Director of Marketing & Sales X-COM Systems, 12345-B Sunrise Valley Dr., Reston, VA

Signal Editing Software Creates Custom Waveforms

This PC-based software permits modifications to be made to captured signal files, creating new files and signal formats with a single mouse click.

CAPTURED SIGNALS THAT can be digitized, stored, and modified to create different signal sequences of interest are in demand for a wide range of applications, from electronic warfare to laboratory and field testing of communications and radar systems. Assisting the process substantially is the latest version of the RF Editor software



RF Editor boasts 10 independent tracks into which waveforms or waveform sequences can be moved and then reconnected to form a single file.

from X-COM Systems (www.xcomsystems.com). This offering allows flexible modifications on signal files of any length, whether captured over the air, offloaded from a signal analyzer, or created in software tools such as MATLAB from The MathWorks (www.mathworks.com). Using as many as 10 independent tracks (see figure), it allows users to trim, join, repeat, lengthen, delay, filter, or shift signals in frequency.

The digital files resulting from monitoring small or even very large swaths of spectrum can be long and occupy terabytes of memory. Consequently, it is necessary to reduce these files to include only those waveforms considered to be signals of interest, which is complicated by the fact that they may occur intermittently or randomly over a long period of time. This task is one of many that can be performed by X-COM's Spectro-X signal analysis software, which uses four different types of search engines to find the files and then create a new file containing only the desired sections.

Since the RF Editor and Spectro-X software are seamlessly integrated, a user need only transfer a file from Spectro-X to RF Editor; it is then modified to the desired degree and can be saved with a single mouse click to create a new, custom waveform file. The file can then be sent back to Spectro-X where it can be used for testing as a stimulus, in EW systems, or in signal-intelligence (SIGINT) systems.

RF Editor allows functions to be performed both sequentially and automatically, such as frequency shifting, file decimation, and bandpass filtering with bandwidths as narrow

as 10% of a waveform segment's span. Other features include presets for fast frequency shifting and span adjustment, power adjustment with 0.1-dB resolution, and the capability to apply frequency offsets, interference, and noise.

Version 3.0 of RF Editor adds new features to earlier versions of the software while also being faster and easier to use. Perhaps the most important of these features, stitching, allows unwanted portions of spectrum-capture files identified in Spectro-X to be eliminated or replaced with data from a different file. The files are then reconnected, producing versions that are much smaller in memory size.

The new "group modify" function significantly reduces the time required to modify the attributes of large numbers of signal-capture files. The user now simply selects a group of files to be modified, indicates the desired modifications from the many choices provided by RF Editor, and the software will make the modifications without operator intervention.

The new software also now supports the .xdat file format used by X-COM's VSG5000A multichannel signal generator and IQC5000A RF capture, recording, and playback system. These files contain much more information than standard .dat files. RF Editor 3.0 and Spectro-X software, as well as trial versions of each, are available from X-COM.

X-COM SYSTEMS, 12345-B Sunrise Valley Dr., Reston, VA 2019; (571) 612-5490, e-mail: sales@xcomsystems.com, www. xcomsystems.com

PXI SYNTHESIZERS RUN TO 4.1 GHz

CLOCK GENERATORS are now available in the modular PXI format, for applications through 4.1 GHz with low phase noise. Model BI401 is a frequency-synthesized square-wave clock generator module from Brilliant Instruments (www.b-i-inc.com) that fits within a single PXI instrument slot. It is available in two basic models, with frequency ranges of 1 µHz to 2.1 GHz (model BI401-2G) and 1z to 4.1 GHz (model BI401-4G), with both models capable of producing DC outputs. The phase noise is only -102 dBc/Hz offset 10 kHz from a 1-GHz carrier with outstanding performance in the time domain, with less than 0.5 ps jitter. The square-wave synthesizer achieves frequency switching speed of better than 250 µs.

The model BI401 square-wave synthesizer provides single-ended and differential output ports. The single-ended port

is capable of 6-V peak-to-peak output amplitude; the differential port offers 1-V peak-to-peak maximum amplitude with 65-ps risetime. The PXI frequency synthesizers include a standard timebase of a 2-ppm temperature-compensated crystal oscillator (TCXO), with an option for an oven-controlled-crystal-oscillator (OCXO) timebase with 0.02-ppm accuracy.

These frequency synthesizers incorporate Practically Perfect frequency resolution to provide 20 digits of frequency resolution with less than 1 ps of accumulated drift per year. At 4 GHz, the frequency resolution is 0.1 nHz. The frequency synthesizers, which are ideal for a variety of applications in both test and measurement and radar systems, con-

ment and radar systems, consume only 14 W power. They are shipped with operating software that is compatible with MS Windows and Linux operat-

Model BI401 is a synthesized square-wave clock generator that fits within a single 32-b PXI slot.

ing systems and written in plain C++ language for ease of porting to other software environments. Each model BI401 frequency synthesizer is supplied in a 3U PXI module measuring 5.1×7.3 in. and weighing 6.4 oz. (180 g).

BRILLIANT INSTRUMENTS, INC., 1600 West Campbell Ave., Ste. 206, Campbell, CA 95008; (408) 866-0426, FAX: (408) 866-0431, e-mail: sales_inquiry@b-i-inc.com, www. b-i-inc.com

AMPS TRIM NOISE FROM 9 kHz TO 18 GHz

LOW-NOISE AMPLIFIERS (LNAs) that maintain spectral purity under a wide range of conditions will usually find a place in many different systems, and a new family of LNAs from Pasternack Enterprises (www.pasternack.com) prom-

ises excellent performance from 9 kHz to 18 GHz. Based on GaAs pseudomorphic-high-electronmobility-transistor (pHEMT) device technology, the amplifiers are supplied in compact modules with SMA coaxial They are available with noise figures from 0.8 to 3.0 dB



connectors. A line of packaged LNAs with coaxial conare available nectors covers a total frequency range of 9 noise figures kHz to 18 GHz.

and gain levels from 25 to 50 dB, depending upon model and frequency range. The output-power levels extend from +10 to +18 dBm.

As an example, model PE15A1001 offers a noise figure of 2 dB from 2 to 4 GHz with 38-dB small-signal gain and ± 1 -dB gain flatness. It provides minimum saturated output power of ± 13 dBm across its octave bandwidth and draws 200 mA supply current from a ± 12 -VDC supply.

At higher frequencies, model PE15A1004 operates from 12 to 18 GHz with noise figure of 3 dB and 38-dB small-signal gain with ± 1 dB gain flatness. It also offers +13-dBm saturated output power across its frequency range. For lower noise figure, model PE15A1010 works from 2 to 6 GHz with 0.9-dB noise figure and small-signal gain of 40 dB with ± 1 -dB gain flatness. It delivers +14-dBm output power at 1-dB compression and draws 90 mA current from a +12-VDC supply.

Hermetic and nonhermetic versions are available; all of the amplifiers are unconditionally stable with built-in voltage regulation, automatic bias sequencing, and reverse-bias protection. for ease of installation in a wide range of circuits and systems They are fully internally impedance matched for use at 50 Ω , eliminating the need for external impedance-tuning components. The amplifiers are designed for a broad operating temperature range of –40 to +85°C. The new LNA family features a total of 14 amplifiers ready for shipment from stock.

PASTERNACK ENTERPRISES, 17802 Fitch, Irvine, CA 92614; (949) 261-1920, www.pasternack.com

103

InfoCenter

ADVERTISER	PAGE ADVERTISER	PAGE
A		
AEROFLEX / INMET, INC		v.e-MECA.com, sales@e-MECA.com
EROFLEX / WEINSCHEL, INC	57 MINI CIRCUITS /SCI COMPONENTS 12 14	
ETHERCOMM www.aeroflex	51, 55, 65,77, 85, 95, 99, 107 www.mini	circuits.com; sales@minicircuits.com
:IHERCOMM	, MITEG	71, 73, 75
SILENT TECHNOLOGIES		www.miteq.com
www.agilent.com/fi	www.mfi-	·milliren.com; sales@mti-milliren.com
www.	.atceramics.com	,
TSU CORPORATION	c2 NARDA DIV OF L-3 COMMUNICATIONS	
\ INC		www.nardamicrowave.com
CORPORATION www.arra.com;	sales@arra.com	www.ni.com/redefine
DRPORATIONwww.awrcorp.cc		
B	NOISECOM	exyn.com, emaii: saies@nexyn.com
WAVE LTD.		www.noisecom.com
w.blmicrowave.com; email:sales.chn@blmicrowave.com, liyon		
	NXP SEMICONDUCTORS	
RELESS INC	17	www.nxp.com/rf
www.ciaowireless.com; sales@c	92	
	www.cml.com OMNITIG INC	
r		iyig.com; Omniyig@ix.netcome.com
ROSPACE & ELECTRONIC	10	
www.cra	nege com/mw6	
ERICA INC	PHASE MATRIX INC	22
www.c	st.com/antenna www.ni-m	icrowavecomponents.com/quicksyn
www.cttinc.com: s	sales@cttinc.com	www.nhonon.com/sat
D		
	w.dbmcorp.com PULSAR MICROWAVE CORP	www.pmi-rf.com; sales@pmi-rf.com
	w.dbmcorp.com PULSAR MICROWAVE CORP	e.com; sales@pulsarmicrowave.com
CA 2014	108	
tnovak@munic	h-tradetairs com DEMINITED	
4	93 www.rfmw.	com/Rosenberger: sales@rfmw.com
	w.eumweek.com RIGOL USA	
ALE SEMICONDUCTOR(AUSTIN)	ROHDE&SCHWARZ GMBH&CO KG	81
www.freescale.c	om/Rfpowertool	vww.rohde-schwarz.com/ad/fsw-ad
и		
www.herotek.com; ini	13	
NICROWAVE CORPORATION	60	
www.hittite.com;	ads@hittite.com www.skywc	orksinc.com; sales@skyworksinc.com
		63
ww	96 w.IMS2015.org	www.thinkSRS.com
	SYNERGY MICROWAVE	45, 61, 91
TRIES INC	80	ave.com; sales@synergymwave.com
www.jfwindustries.com; sales@jt	Windustries.com	ave.com, salesesynergymwave.com
₩		
www.krytar.com, s	ales@krytar.com	
	www.rrmmicrowave.com	n, email: infohp@trmmicrowave.com
R TECHNOLOGY CORPORATION www.linear.com/pr	19 W	
SER & ELECTRONICSwww.linear.com/pi	voduct/LTC5551 W.L. GORE & ASSOCIATES INC	
www.	lpkfusa.com/pls	www.gore.com/test
OM TECHNOLOGY SOLUTIONS, INC	This index is provided as an additional service by the presponsibility for errors or omissions.	oublisher, who assumes no
	nacom.com/gan responsibility for errors or omissions.	

(ISSN 0745-2993)

Microwaves & RF is published monthly. Microwaves & RF is sent free to individuals actively engaged in high-frequency electronics engineering. In addition, paid subscriptions are available. Subscription rates for U.S. are \$95 for 1 year (\$120 in Canada, \$150 for International). Published by Penton Media, Inc., 9800 Metcalfe Ave., Overland Park, KS 66212-2216. Periodicals Postage Paid at Shawnee Mission, KS and at additional mailing offices.

POSTMASTER: Send change of address to Microwaves & RF, Penton Media Inc., P.O. Box 2095, Skokie, IL 60076-7995. For paid subscription requests, please contact: Penton Media Inc., P.O. Box 2100, Skokie, IL 60076-7800. Canadian Post Publications Mail agreement No. 40612608. Canadian GST# R126431964. Canada return address: IMEX Global Solutions, P.O Box 25542, London, ON N6C6B2.

Back issues of MicroWaves and Microwaves & RF are available on microfilm and can be purchased from National Archive Publishing Company (NAPC). For more information, call NAPC at 734-302-6500 or 800-420-NAPC (6272) x 6578. Copying: Permission is granted to users registered with the Copyright Clearance Center, Inc. (CCC) to photocopy any article, with the exception of those for which separate copyright ownership is indicated on the first page of the article, provided that a base fee of \$1.25 per copy of the article plus 60 cents per page is paid directly to the CCC, 222 Rosewood Dr., Danvers, MA 01923. (Code 0745-2993/02 \$1.25 +.60) Copying done for other than personal or internal reference use without the expressed permission of Penton Media, Inc., is prohibited. Requests for special permission or bulk orders should be addressed in writing to the publisher.

Copyright 2014 • Penton • All rights reserved. Printed in the U.S.

Device Switching Time Testers from AVTECH

Avtech offers a full line of ultra fast pulsers for switching time testing of diodes, transistors, optoisolators and phototriacs. Some of our standard models include:

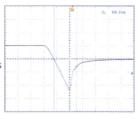
AVR-EB5-B: +2A / -4A pulser for PIN diode t_{RR} tests AVR-CD1-B 100 to 200 A/us pulser for diode dI/dt t_{RR} tests AVR-EBF6-B: +50 mA to +1A pulser for diode t_{FR} tests

AVR-EBF6-B: +50 mA to +1A pulser for **diode t**_{FR} tests
AVR-D2-B: MIL-S-19500 **transistor** switching time tests
AVR-DV2-B: ±2 kV pulser for **dV/dt** transient immunity tests



Pricing, manuals, datasheets, test results:

www.avtechpulse.com/semiconductor Tel: 888-670-8729 Fax: 800-561-1970 info@avtechpulse.com



Model AVR-CD1-B output waveform 2 A / DIV 40 ns / DIV



Attention Advertisers:

For digital ad specifications and requirements, please visit the Ad Production web site:

www.pentondigitalads.com



The Original Electronics Parts Search & Procurement Tool

Search Parts

Part #

Manufacturer

Q

SEARCH PARTS FAST

Your Trusted Source

www.SourceESB.com

GO TO MWRECOM 105

New Products

BAW Filters Screen 2.4 GHz

A PAIR of bulk-acoustic-wave (BAW) filters developed by

TriQuint for wireless applications at 2.4 GHz—such as Bluetooth and wireless-local-area-network (WLAN) systems—that must coexist with Fourth-Generation (4G) networks is now available from the firm's stocking distributor, RFMW, Ltd. Models 885062 and 885071 pass desired WiFi

signals and provide high rejection in adjacent 4G Long-Term-Evolution (LTE) cellular bands while fitting into compact housings measuring just $1.4 \times 1.2 \times 0.46$ mm. Model 885062 exhibits maximum insertion loss of 1.7 dB

in the WiFi passband, with out-of-band rejection of 53 dB from 2300 to 2365 MHz and 58 dB from 2365 to 2370 MHz. Model 885071 has maximum WiFi passband insertion loss of 1.9 dB, with out-of-band rejection of 53 dB

from 2300 to 2370 MHz and 55 dB from 2496 to 2501 MHz. Both filters are rated for average power-handling capability to +28 dBm, and both are AEC-Q200 qualified for automotive applications.

RFMW, LTD. (stocking distributor for Tri-Quint), 188 Martinvale Lane, San Jose, CA

95119; (408) 414-1450, e-mail: info@rfmw.com, www.rfmw.com

Caps Extended For COTS Applications

THE APS series of multilayer ceramic capacitors (MLCCs) for commercial off-the-shelf (COTS) applications has been extended with the addition of high-temperature

models. The APS series MLCCs are available in six case sizes from 0603 to 2220; in six voltage ranges span-



TriQuint 885062

ning 16 to 500 V; and with capacitance values from 10 pF to 22 µF. They are available with four different dielectric materials (NPO, X7R, X8R, and X8L), three capacitance tolerances (±5%, ±10%, and ±20%), and a number of

different termination choices. When tested to military-standard (MIL-STD) requirements, the capacitors exhibit

a low failure rate of less than 1 ppb. They are suitable for applications in military, aviation, and telecommunications circuits.

AVX CORP., One AVX Blvd., Fountain Inn, SC 29644; (864) 967-2150, www.avx.com

Mixers Convert 2 To 18 GHz

THE MICROLITHIC line of in-phase/ quadrature (IQ) frequency mixers covers bands of 4 to 16 GHz and 2 to 18 GHz in compact housings. These mixers, with as much as 30-dB typical unturned sideband suppression, include the 2-to-18-GHz model MLIQ-0218, with a 3.5-GHz-wide intermediate-frequency (IF) band and 18-dB sideband suppression. The mixer also provides 40-dB typical isolation between the local-oscillator (LO) and RF ports. Suitable for radar, electronicwarfare (EW), and test-and-measurement applications, the mixer line also includes the 4-to-16-GHz model MLIQ-0416, with IF range of DC to 3.5 GHz and typical conversion loss of 5.5 dB for RF/LO input levels to +8 dBm. MARKI MICROWAVE, INC., 215 Vine-

yard Ct., Morgan Hill, CA 95037; (408) 778-4200, FAX: (408) 778-4300, e-mail: info@markimicrowave.com, www. markimicrowave.com

Plastic-Pack GaN Powers 3.8 GHz

BOOSTING SIGNAL levels at high frequencies often requires efficient transistor power, and a line of gallium-nitride (GaN) high-electron-mobility-transistor (HEMT) devices from Cree helps cut costs with economical packaging. Supplied in plastic dual-flat no-leads (DFN) surface mount packages, these affordable transistors are meant to compete with silicon and gallium-arsenide

(GaAs) devices for applications from 0.7 to 3.8 GHz. The product line includes 15- and 30-W output-

power transistors for use at +28 and +50 VDC, in such systems as Long-Term Evolution (LTE) cellular networks. In one reference design, the devices are capable of approximately 50% drain efficiency at 10-W average output power and 16-dB linear

gain from 2.5 to 2.7 GHz. Samples and reference designs are available for the 30-W model CGH27030S, the 15-W model CGHV27015S, and the 30-W model CGHV27030S GaN HEMT transistors.

CREE, INC., 4600 Silicon Dr., Durham, NC 27703; (866) 924-3645, (919) 287-7888, www.cree.com



Mini-Circuits programmable attenuators give you more options and more freedom with both USB and Ethernet control. Available in versions with maximum attenuation of 30, 60, and 90 dB with 0.25 dB attenuation steps, all models provide precise level control with accurate, repeatable performance for a wide range of test applications. Our unique designs

maintain linear attenuation change per dB over the entire range of attenuation settings. Supplied with user-friendly GUI control software and everything you need for immediate use out-of-the-box, Mini-Circuits programmable attenuators offer a range of solutions to meet your needs and fit your budget. Visit minicircuits.com for detailed performance specs, great prices, and off-the-shelf availability!

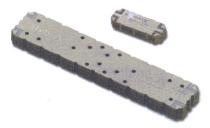
RoHS compliant

	Models	Attenuation Range	Attenuation Accuracy	Step Size	USB Control	Ethernet Control	RS232 Control	Price \$ ea.
	RUDAT-6000-30	0 - 30 dB	±0.75 dB	0.25 dB	/	-	1	\$395
NEW	RCDAT-6000-30	0 - 30 dB	±0.75 dB	0.25 dB	1	1	5-13	\$495
	RUDAT-6000-60	0 - 60 dB	±1.00 dB	0.25 dB	1	-	1	\$625
	RUDAT-6000-90	0 - 90 dB	±1.70 dB	0.25 dB	/	_ 1	/	\$695
NEW	RCDAT-6000-60	0 - 60 dB	±0.30 dB	0.25 dB	/	/	-	\$725
NEW	RCDAT-6000-90	0 - 90 dB	±0.40 dB	0.25 dB	1	1	-	\$795



Hybrid Couplers Cut Losses To 3.4 GHz

A SERIES of low-loss, wideband hybrid couplers is represented by the models WH0530TF and WH1727F, which are part of the HybriX signal-distribution family of products. Model WH0530TF is a hybrid coupler optimized for use



from 0.5 to 3.4 GHz and ideal for use in switch networks, in antenna feeds, and with power amplifiers. It provides at least 20-dB isolation from 500 to 3400 MHz, with maximum insertion loss of 0.5 dB. The maximum voltage standing-wave ratio (VSWR) over that frequency range is 1.20:1. The model

WH1727F hybrid coupler is well suited for 4G Long-Term Evolution (LTE) applications from 1700 to 2700 MHz. Over that range, it achieves low typical insertion loss of 0.1 dB with 30-dB typical isolation between ports. Both couplers are designed for operating temperatures from –55 to +85°C. **EMC TECHNOLOGY**, 8851 SW Old Kansas Ave., Stuart, FL 34997; (772) 600-1608; www.emc-rflabs.com

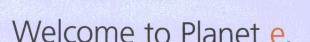
SAPPHIRE TRIMMER capacitors in the V9000 series are miniature components that offer tunable capacitances from 1 to 12 pF in compact housings. In spite of being only 0.64 in. across at the minimum capacitance value, these components are rated for working voltages to 2 kV and can handle voltages as high as 3 kV at frequencies as high as 10 GHz. The sapphire trimmers maintain



stable performance with time and temperature and are mechanically strong and moisture resistant. They feature high quality factor (Q) of 3000 minimum at 100 MHz, and they are compatible with SAC 305 reflow solder processing. These nonmagnetic trimmers are well suited for applications in magnetic-resonance-imaging (MRI) circuits and systems according to the firm's strict traceability and testing regimes.

KNOWLES CAPACITORS, Old Stoke Rd., Arminghall, Norwich, Norwalk NR14 8SQ, United Kingdom; +44 (0) 1603 723310, FA: +44 (0) 1603 723301, www.knowlescapacitors.com



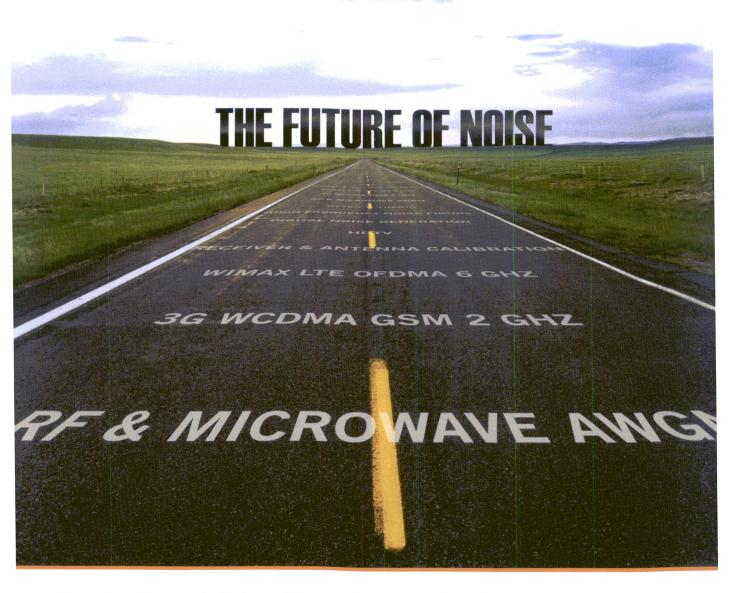


26th International Trade Fair for Electronic Components, Systems and Applications Messe München, November 11–14, 2014 www.electronica.de

Contact U.S. Office: Francesca Novak Phone: 646.437.1016 | fnovak@munich-tradefairs.com 50 years electronica







Noisecom's cutting edge technology will lead you down the road to success with our innovative and high-speed solutions.

As a global provider of noise generators, modules, diodes and specialized test solutions we are ready to meet your present needs, as well as address your future applications.

For more information visit: www.noisecom.com or call +1 973-386-9696.

- RF & Microwave AWGN
- Digital Noise Generation
- Satellite Communications (BER, Eb/No)
- Wireless (WiMAX & LTE)
- >60 GHz Noise Figure
- Serial Data Compliance (Jitter, Rj)
- Wireless HD Testing
- Receiver & Antenna Calibration









